A REDUCED COMPLEXITY - CENTRALIZED POWER CONTROL SCHEME FOR DS/CDMA CELLULAR COMMUNICATION

by

Ruby Rong Zhang

B.A.Sc. The University of British Columbia, 1993

A THESIS SUBMITTED IN PARTIAL FULFILLMENT
OF THE REQUIREMENTS FOR THE DEGREE OF
MASTER OF APPLIED SCIENCE
in the School
of
Engineering Science

SIMON FRASER UNIVERSITY

June 1996

APPROVAL

Name: Ruby Rong Zhang

Degree: Master of Applied Science

Title of thesis: A Reduced Complexity - Centralized Power Control Scheme for DS/CDMA Cellular Communication

Examining Committee:

Dr. P. Ho
Associate Professor, Engineering Science, SFU
Senior Supervisor

Dr. J. Vaisey
Assistant Professor, Engineering Science, SFU
Internal Supervisor

Dr. S. Hardy
Professor, Engineering Science, SFU
Examiner

Date Approval: June 28, 1996

PARTIAL COPYRIGHT LICENSE

Title of Thesis/Project/Extended Essay

"A Reduced Complexity - Centralized Power Control Scheme for DS/CDMA Cellular Communication"

Author:

(signature)

Ruby ZHANG
(name)

June 28, 1996
(Date)

ABSTRACT

The goal of power control in cellular Code Division Multiple Access (CDMA) is to deliver a desired Carrier-to-Interference ratio (CIR) to the users in the network, irrespective of their locations and channel conditions. As shown in [7-9], effective power control algorithms are essential to reduce the co-channel interference and increase the capacity in both the uplink and downlink. At present, only a distributed power control strategy had been considered for the fast power control process [5,36]. Since the same frequency band is reused in every cell of the DS/CDMA cellular system, intuitively, power control should be done on a more global scale in order to achieve better system efficiency. In this thesis, we present an improved centralized power control methodology called Reduced Complexity Centralized Power Control (RC-CPC). This algorithm improves not only the downlink capacity compared with the distributed power control algorithm but also the feasibility of the centralized power control in the DS/CDMA system. The RC-CPC technique requires each mobile to monitor the links between itself and its home base as well as its neighboring bases. The conditions in the various links are prescreened and processed at the home base and then reported to the central power controller. Upon receiving the pre-processed link conditions from all the bases, the central controller assigns transmitter power levels to the different bases in such a way that all active links will have an acceptable CIR. We considered both cases of fast and slow power control and compare the performance of the RC-CPC with three other algorithms: fully centralized power control (upper bound), fixed transmitter power (i.e., no power control at all), and fully distributed power control. As a performance measure, the outage probabilities with different system protection ratios are used. In addition, the CIR statistics and system capacities are examined. The overall results indicate that the proposed power control methodology has the potential for better performance than the fixed step distributed power control.

To

God

for His loving kindness

Acknowledgments

I would like to thank Dr. Paul Ho for suggesting the research subject and supervising me helpfully and patiently throughout my studies. I also would like to thank Dr. J. Vaisey and Dr. S. Hardy who spent their time in reading and revising my thesis. Financial supports from the National Science and Engineering Research Council of Canada and Canadian Institute for Telecommunications Research are gratefully acknowledged.

Above all, I thank God for his grace and blessings upon my family.

Contents

List of Figures

List Of Abbreviations

CDMA	Code Division Multiple Access
TDMA	Time Division Multiple Access
FDMA	Frequency Division Multiple Access
FM	Frequency Modulation
PN	Pseudorandom Noise
DS	Direct Sequence
SIR	Signal to Interference Ratio
CIR	Carrier to Interference Ratio
SNR	Signal to Noise Ratio
SINR	Signal to Interference and Noise Ratio
AWGN	Additive White Gaussian Noise
BPSK	Binary Phase Shift Keying
FEC	Forward Error Correction
MAI	Mutual Accessing Interference
BER	Bit Error Rate
bps	bits per second
Hz	Hertz
kHz	kilo-Hertz
MHz	Mega-Hertz
dB	Decibel
rms	root mean square
PCA	Power Control Algorithm

CPCA	Centralized Power Control Algorithm
DBPCA	Distributed Balancing Power Control Algorithm
DPCA	Distributed Power Control Algorithm
SRA	Stepwise Removal Algorithm
SMIRA	Stepwise Maximum Interference Removal Algorithm
LI-SRA	Limited Information - Stepwise Removal Algorithm
RC-CPC	Reduced Complexity - Centralized Power Control
DR	Dynamic Range

List of Notations

W	Frequency Bandwidth
R	Information bit rate
G	Processing gain or bandwidth expansion factor
T_c	Chip duration of a PN code
T_b	Bit duration of the data signal
C	Carrier power
I	Interference power
N	Total number of users in the system at an instant
E_b	Bit energy
I_0	Interference bit energy
N_0	Noise power spectral density
U_i	Number of users in cell i
K	Number of cells
M	Number dominant interfering cells monitored by the mobiles
g_{ji}	The link gain from the base assigned to the i-th user to the j-th user
P_i	The transmitted power for the i-th user from its assigned base
γ_i	The CIR seen at the i-th user
λ_{max}	Maximum eigenvalue of the **H** and **F** matrix
γ^*	The achieved balanced CIR

γ_0	The system protection ratio
H	The full size Link gain matrix
F	Reduced size link gain matrix
$\|.\|$	Matrix norm
P	Power allocation vector for users with a size of $1\times N$
S	Power allocation vector for cells with a size of $1\times K$
σ	Standard derivation of the log-normal function
m	Path loss exponent
f_c	Carrier frequency
f_D	Doppler frequency
β	Scaling factor for CIR balancing power control
α_i	Attenuation factor in the i-th path
v	Traveling speed of the portable user
c	Speed of light
ϕ_c	Autocorrelation function
J_0	Zeroth-order Bessel function of the first kind
χ	Prescreening threshold
μ	Scaling factor for χ

Chapter 1

Introduction

Cellular radio is the earliest form of modern wireless "personal communication." It has experienced a tremendous growth since a decade ago. This growth poses the need for technology that can increase cellular system capacity and improve its performance. Comparing with the two widely used narrow-band multiple access schemes, Frequency Division Multiple Access (FDMA) and Time Division Multiple Access (TDMA), the less widely used wide-band multiple access scheme, Code Division Multiple Access (CDMA), has shown to be a viable alternative to satisfy the above requirement for the next generation of cellular systems [1]. Currently, the use of spread spectrum techniques (upon which CDMA is designed) in wireless communication applications has become a very active area of research and development [1,2,3].

Spread spectrum signal is distinguished by the characteristic that its bandwidth W is much greater than the information bit rate R. The bandwidth expansion factor, $G = W/R$, also called the processing gain, is much greater than unity. This unique feature of spread spectrum signal makes CDMA most capable of mitigating effectively multipath fading and interference in the cellular radio environment [4]. In addition, this large

processing gain underlies other important multiple access features such as frequency reuse, soft hand-off, fast and accurate power control, and space and time diversity. In this thesis, we will concentrate on the topic of power control algorithms. To lay a background for our study, the first chapter of this essay begins with the CDMA concept and some of its attractive features.

1.1 CDMA Concept and Attributes

The naming of Code Division Multiple Access (CDMA) suggests that this multiple access scheme separates users based on the different spreading *code* each user uses. With their own codes as identities, all users share the same frequency bandwidth W ($W>>R$). This is the basic difference between CDMA and other multiple access schemes such as FDMA and TDMA. With FDMA and TDMA, different users are separated in terms of different *frequency* domains and *time* slots that each user occupies. Figure 1-1 illustrates the resources sharing of CDMA, FDMA and TDMA.

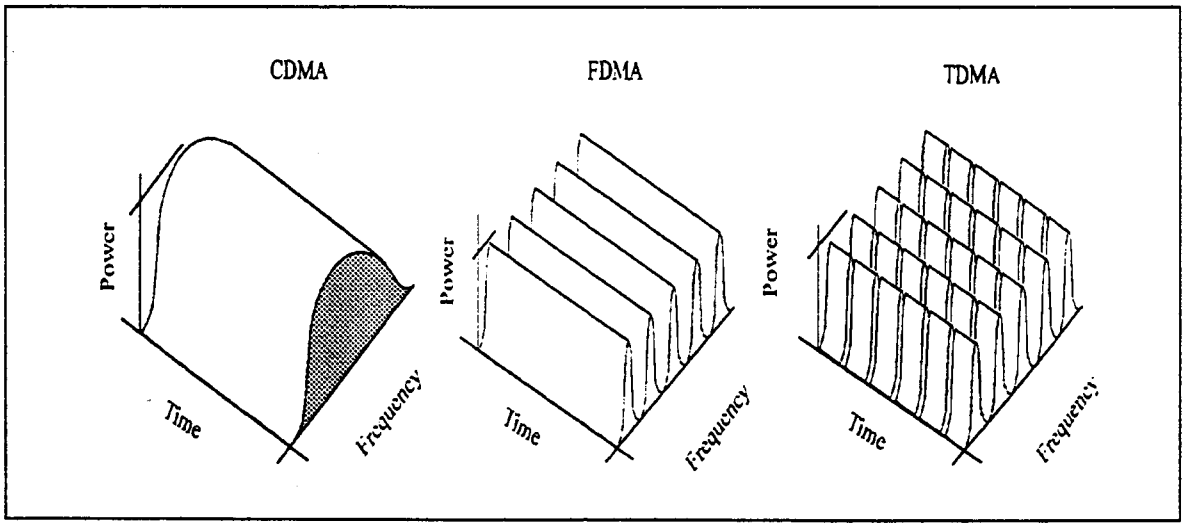

Figure 1-1. Frequency and Time Domain Representations of CDMA, FDMA and TDMA [5].

CDMA can be viewed in either the frequency or time domain [5]. The multiple access signals appear to be on top of each other like addition of wide-band noise. They all share the same frequency spectrum without frequency assignments or frame schedules as required in the other two multiple access schemes.

Direct Sequence (DS) is one of the modulation and spreading techniques used in CDMA that attracts the most interest. The DS modulation uses the binary pseudonoise (PN) sequence to modulate the carrier. The PN sequence is first added in modulo 2 to the binary message (data signal), and the sum is then used to modulate the carrier. For instance, when the modulation uses Binary Phase Shift Keying (BPSK), then the phase of the carrier is shifted pseudo-randomly according to the pattern of the PN code at a rate of W times/s, where W is also known as the spread spectrum bandwidth.

Figure 1-2 illustrates the relationship between the data signal and the PN code sequence.

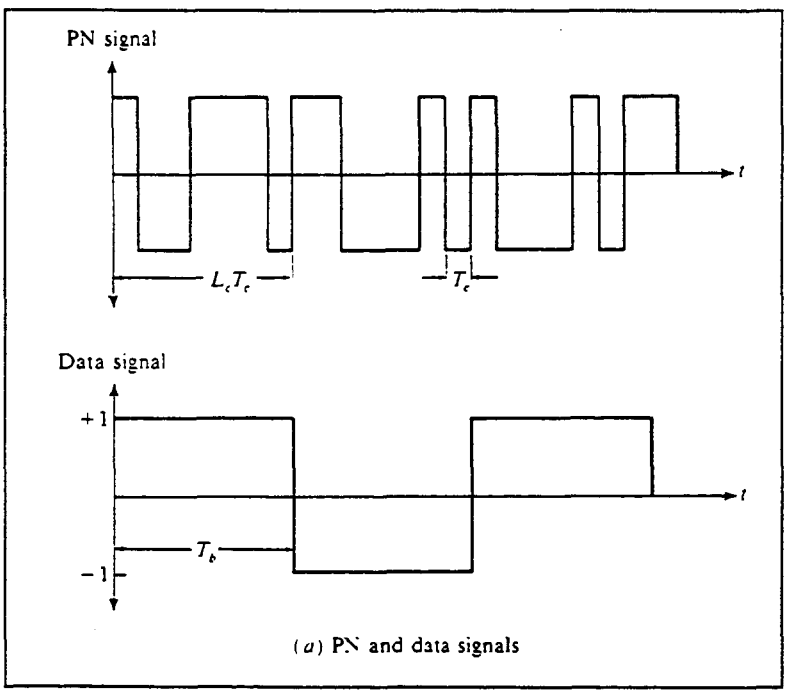

Figure 1-2. The PN code and Data Signal [6]

Each PN sequence consists of many rectangular pulses called the chips [6]. The chip interval is measured by $T_c = 1/W$ seconds. If the data bit duration is $T_b = 1/R$ seconds, where R is the information bit rate, then the processing gain, G, as mentioned previously may again be expressed by

$$G = \frac{W}{R} = \frac{T_b}{T_c}. \tag{1.1}$$

As a result of the DS modulation and spreading process, each transmitted signal consists of a different PN code in the same spread spectrum. A complete schematic of the current DS/CDMA transceiver is shown in Figure 1-3. It explicitly illustrates how the DS spreading is done and how noise and interferences are suppressed by the correlation process with PN codes.

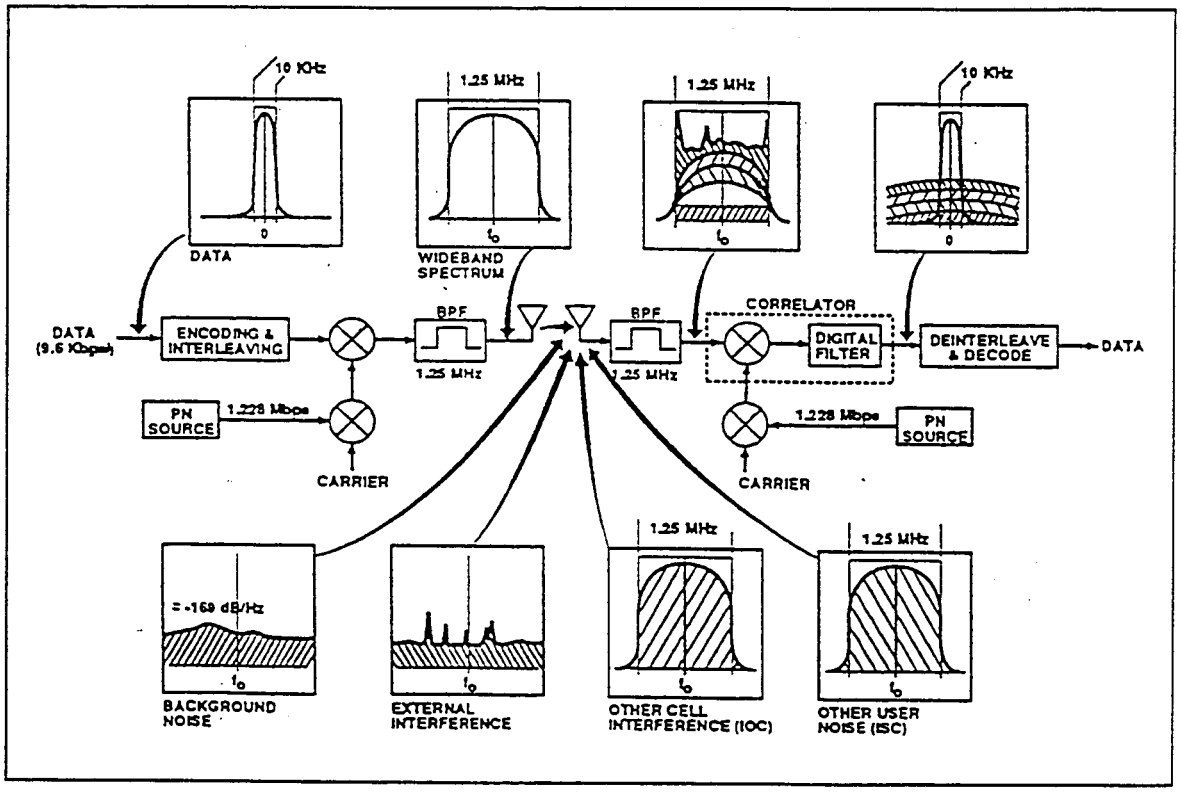

Figure 1-3. A View of DS/CDMA System [5].

As shown in Figure 1-3, the DS modulation and spreading process in the transmitter spreads the data in 10 kHz bandwidth to 1.25 MHz wide-band spectrum. The modulated wide-band signal, along with the background noise and interference from other sources (spread to the same bandwidth), are transmitted and detected at multiple receivers. Only the corresponding receiver can recover the transmitted information intended for it by identifying the pseudo-random pattern, the PN code used by the particular transmitter. With the correlation process, where the received signal is multiplied by a reference with the same PN code, the wide-band carrier is despread, and the resulting base-band signal is obtained after filtering. In addition, as graphically shown in Figure 1-3, the added interference and noise are not despread at the receiver but remain as wide-band signals. These wide-band interference and noise are rejected by a filter which only passes the desired base-band signal. As a result, the received base-band Signal-to-Interference-plus-Noise Ratio (SINR) and the system capacity are enhanced with the system processing gain $G = W/R$. The following sections will explain the CDMA capacity and various techniques specially used in CDMA design to improve the system capacity.

1.1.1 Capacity

CDMA system capacity is closely related to the processing gain G and the Carrier-to-Interference Ratio (CIR). A coarse estimate of capacity in an ideal case can be obtained with the following argument. Suppose each user's transmitted power is controlled so that all signals are received at the base station at equal power levels. If C represents the received carrier power of each user, and N denotes the number of users transmitting in the band, and if the background noise is negligible, then the total interference, I, seen at the base is

$$I = (N-1)C. \tag{1.2}$$

Assuming a single cell system, then the CIR is

$$C/I = 1/(N-1). \tag{1.3}$$

Obviously, for a meaningful system with $N > 1$, the above received CIR is less than one. That means, in a spread spectrum CDMA system, the CIR is negative in decibel (dB) before despreading. Whereas in a narrow-band system, without spreading or despreading, the standard CIR is much higher and always greater than one. For example, the analog FM cellular, which is a narrow-band system, requires a CIR > 18 dB in its demodulation process [7].

Expanding equation (1.3), the received signal power C also equals to the transmission bit rate R multiplied by the received signal bit energy E_b. The total interference I also equals to the system bandwidth W in Hz multiplied by the interference power spectral density I_0. The CIR is therefore:

$$\frac{C}{I} = \left(\frac{E_b}{I_0}\right)\left(\frac{R}{W}\right) = \left(\frac{E_b}{I_0}\right) \Big/ \left(\frac{W}{R}\right). \tag{1.4}$$

The Signal-to-Interference Ratio (SIR), or E_b/I_0, is the bit energy to interference spectral density ratio obtained after despreading. It is the figure of merit of a digital modem. The SIR required varies typically between 3 and 9 dB, depending on its implementation, use of error correction coding, channel impairments such as fading, power control techniques as well as error rate requirements. Other than the SIR, the processing gain G, or W/R, is important as well. This parameter is much greater than unity as stated previously. Hence, equation (1.4) implies that the E_b/I_0 can be raised from a negative CIR in dB to a much higher positive value by a large processing gain W/R. This

relation also applies to the capacity. By combining equation (1.3) and (1.4), we have the following relationship for the capacity N:

$$N - 1 = \frac{W}{R} \Big/ \frac{E_b}{I_0}. \tag{1.5}$$

1.1.2 Frequency Reuse

Given the fact that the available spectrum for cellular systems is limited, the concept of frequency reuse is applied to improve the capacity. In the narrow-band systems such as FDMA and FDMA/TDMA, the available frequency spectrum is divided into many sets of frequencies. One cell can only use one set of these frequencies. The cells immediately adjacent to this cell can not use the same frequency set; otherwise, the mutual interference, called co-channel interference, among neighboring cells is too high to permit useful transmission. In order to increase the spectrum efficiency and capacity, the same set of frequencies may be reused in a distant cell. Since band-pass filters cannot completely reject the co-channel interference, adequate physical isolation is required between two channels using the same frequency in order to achieve the CIR requirement. In other words, the performance has to rely on the spatial separation provided by the cell structure and directive base station antennas.

For a narrow-band cellular system using 30 kHz channel bandwidth such as the AMPS, the frequency reuse plan employs a 7-group cluster to meet the requirement keeping CIR $\geq$ 18 dB [7]. Figure 1-4 illustrates the allocation of cellular channels with a cluster of 7 cells replicating over a large area. The frequency reuse factor of such a system is 1/7. Since the same frequency slot is reused once every seventh cell, the cell

capacity is only one-seventh of the total available channels. For example, in a FM cellular system where the channel bandwidth is 30 kHz, in the 1.25 MHz allocated spectrum the total number of channels is 1.25 MHz/ 30 kHz = 41.67. Since the cell reuse pattern is 7-cell clusters, i.e., reuse factor = 1/7, then, the radio capacity m is 41.67/ 7 = 6 channels per cell.

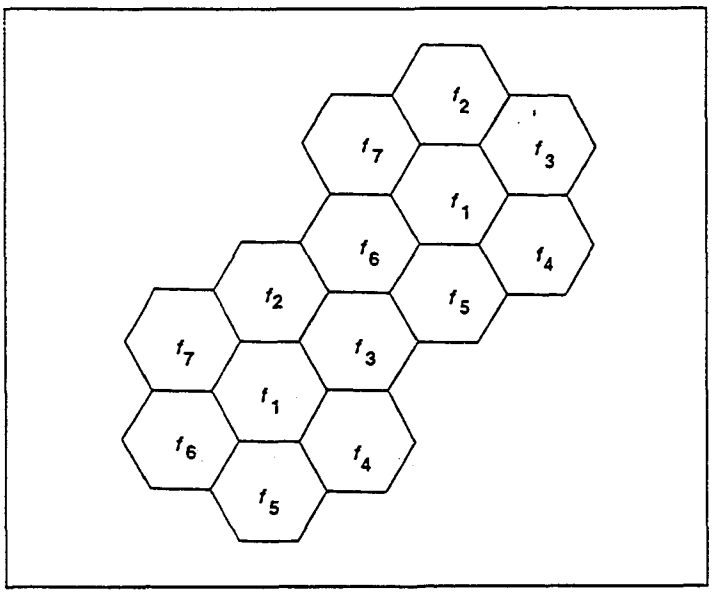

Figure 1-4. Frequency Reuse Clusters [7]

On the other hand, in CDMA cellular systems, all users in the system share the same available spread spectrum. Frequency reuse is universal. In this case, the use of effective power control and interference cancellation techniques helps to minimize the co-channel interference contributed by all users. In fact, CDMA signal is inherently capable of combating and suppressing the detrimental effects of interference arising from other users of the same channel and self-interference due to multipath propagation [6]. Ideally, because the same frequency is reused in every cell in the whole system, the frequency reuse factor is 1; but practically, the energy in each cell spills out and interferes with one another. The resulting frequency reuse factor is less than 1, about 65% with the use of

omni-directional antennas [5]. Nevertheless, comparing with the reuse factor of only 1/7 in the analog FM cellular, CDMA has a much higher frequency reuse efficiency which can result in a significant greater capacity. Furthermore, because of the universal frequency reuse in CDMA, insertion of users and new cells does not require a revision of the frequency plans of existing cells. It is easier to increase user intensity and introduce new features as well.

1.1.3 Power Control

Universal frequency reuse demands effective power control of each user in both the uplink and downlink directions. In the uplink direction, the total interference to the signal from a given mobile received at its home base station is comprised of interference from all other mobiles in the same cell plus the interference from mobiles in all neighboring cells. In other words, each mobile station's signal competes with all other mobile stations' signals. Similarly, in the opposite direction, the signal from a base station that arrives at a given mobile station has to compete with signals from all other base stations. This kind of co-channel interference significantly limits the capacity. To effectively control the interference with the goal of increasing system capacity, power control is essential in the CDMA design.

In the uplink direction, both closed and open loop power control are used to combat fading effect and reduce the near-far ratio interference, in which case a strong signal received from a near-in mobile masks the weak signal received from a far-end mobile at the base. The closed loop scheme consists of a feedback mechanism that allows the estimation of the uplink channel quality at the base and transmitting this information back to the portable. The portable then adjusts its transmitter power according to the measurement made at the base station. This is necessary because the frequency band is

separated for the uplink and downlink directions, and the fading characteristic is frequency dependent. On the other hand, the open loop scheme does not have the feedback loop. Each portable simply adjusts its transmitted power level based on the downlink received power. The higher the received power is, the lower its transmitted power is assumed, and vice versa. While the closed loop scheme provide more accurate power adjustment, the open loop scheme provides faster response to the channel variation.

In the downlink direction, portables near their home base stations receive stronger signals from their bases and less interferences from other cells. By reducing the power transmitted to these portables and increasing the power transmitted to those near the cell boundaries or those experiencing deep fades, the overall capacity can be increased. Thus, the basic idea is to control the transmitter power at the base station so that its signal arrives at each portable unit with the minimum required SIR [5]. As in the uplink, downlink power control can be open or closed loop. The focus of this thesis is on the downlink.

1.1.4 Soft Hand-off

In cellular systems, a hand-off mechanism is needed to continue a call when a portable unit crosses the boundary between two cells. In analog cellular systems, the cell site handling a call notices that the received signal strength from a portable has fallen below a predetermined threshold value. It assumes the portable is near the cell boundary, so it tells the system controller to send out the hand-off request. If one of the neighboring cell sites detects and reports an adequate signal level from the portable, then an idle channel from the channel set used at this new cell site is selected, and a control message to switch to this new channel is sent to the portable. At the same time, the system controller switches the call from the first cell site to the appropriate radio at the second cell site. This kind of hand-off is called hard hand-off with the break-before-make switching function [5].

The same control structure is used in the digital FDMA/TDMA-based system. Because disjoint slots are assigned to each user in each cell, an idle channel from the new cell's channel set must be selected to continue the transmission between the new base and the portable. If an idle channel is not available, or the portable fails to hear the command to switch channels, the hand-off fails. And quite often, when a portable is near the border between the two cells, the signal levels tend to fluctuate at both cell sites. The results is a ping-pong effect which causes the call to drop easily [5].

In a CDMA system, every cell uses the same CDMA channel. This makes it possible for a portable unit to receive and send the same call simultaneously to and from two different base stations as shown in Figure 1-5.

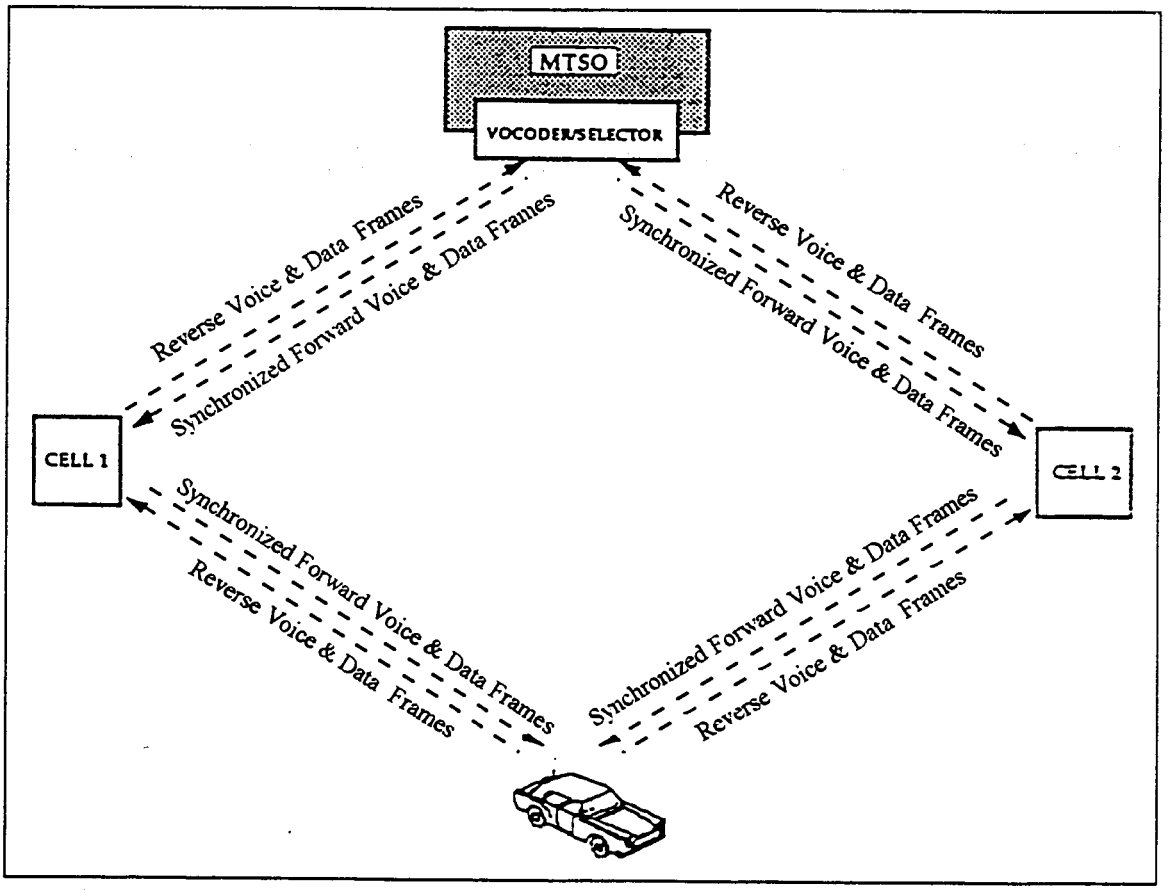

Figure 1-5. Multiple Links during Hand-off [5]

Furthermore, the forward links employ pilot signals which all have the same maximum length PN sequences but cell-specific time-offsets. It can be easily used to identify the signals from adjacent cells. The relative time-offsets of pilots from neighboring cells are either known as a piori or broadcast to all users [8]. This makes it feasible for a portable to continually track all available pilots from both its original cell and neighboring cells. In the mean time, each portable maintains a list of all pilots whose signals are above a certain threshold. Once a new pilot is detected and found to be comparable with the signal strength from the original cell, it signals its home base station and the switching office. This enables the second cell's base station to both send and receive signal to and from the corresponding portable.

As shown in Figure 1-5, the portable unit uses diversity combining of the two signals carrying the same data to enhance the overall received signal. This process is called soft hand-off. It is a form of path diversity that can be easily provided with CDMA because the wide-band frequency is reused in every cell. Whereas, in TDMA, channels from adjacent cells are disjoint and orthogonal to each other, it requires a more complicated transmitting and receiving structure in order to benefit from the diversity combining effect.

In summary, soft hand-off provides a make-before-break switching function. The link from the original cell is dropped only when its signal is too weak to be decoded correctly, whereas the link with the second cell is brought in gradually. Consequently, the hand-off process is smoother, more robust and reliable than hard hand-off in the conventional system.

1.1.5 Space and Time Diversity

In a mobile radio environment, reflections and scattering of the radio wave produce multiple propagation paths between the base station and the portable unit. With narrow-band transmissions, the existence of multiple paths causes severe fading and inter-symbol interference. However, with wide-band CDMA modulation, the different paths, which have delays longer than several chips duration, may be independently detected and combined through the use of a Rake receiver [6]. The Rake receiver consists of L parallel correlators for L propagation paths. By properly combining the signals from the different paths, not only is multipath fading being mitigated, the modem's performance also improves because of the diversity effect. Soft hand-off is one example of exploiting space (path) diversity with simultaneous links from multiple cell sites. Space diversity can also be provided by multiple cell site antennas.

Another advantage of the DS/CDMA systems over narrow-band systems is its capability to achieve a higher order of time diversity. This is because the inherent excess redundancy due to the DS spreading in a CDMA system can be exploited by using low-rate, high redundancy Forward Error Correction (FEC) coding. In practice, code rates of 1/2 and 1/3 are used in the downlink and uplink respectively. It provides a high order of time diversity to lower the required E_b/I_0 for an acceptable error rate performance.

1.1.6 Voice Activity Cycle

Voice activity detection is one of the processing features that can be easily incorporated into the spread spectrum multiple access system but not to the other conventional systems. In a typical full duplex two-way voice conversation, the duty cycle of each voice signal is usually less than 50% [5,8]. Consequently, by stopping the transmission during the

"silent" periods, we can reduce the average transmitter power of all users and hence the interference received by each user. This means the capacity is increased in proportion to the overall rate reduction by a factor of 2 [5]. It should be pointed out that because of the time delay associated with reassigning the channel resource during the speech pauses, it is not cost effective to exploit the voice activity factor in either FDMA or TDMA system.

1.1.7 Unequal Cell Loading and Soft capacity

In FDMA and TDMA systems, the number of available channels is fixed, and they are divided and parceled out to each cluster of cells (usually 7 cells) according to a fixed and inflexible plan. When the demand for service is at a peak, it is impossible to add even one more signal to a fully occupied system. On the other hand, the capacity of CDMA is only interference limited. Transmissions in the surrounding cells contribute to the most interference in the center cell. The number of channels available in this center cell depends upon the loading of the surrounding cells. If these surrounding cells are less than fully loaded, then the capacity of the center cell can be easily increased. Even if this center cell is already heavily loaded, the system can allow a small degradation in the bit error rate and increase the number of available channels. It allows a soft capability relationship between the number of users and the grade of service. This soft capability is especially important for avoiding dropped calls at hand-off because of a lack of channels [5].

1.2 The Power Control Issue

We have demonstrated that in cellular CDMA, the same frequency is reused in every cell at all time. Therefore, the mutual accessing interference (MAI) is the most restraining

factor on the system capacity of the current DS/CDMA design. To alleviate the severe reduction of multiple-access capability caused by the MAI, a stringent power management is essential. The focus in this thesis is on the downlink power control design in a cellular CDMA system. Most earlier work on power control emphasizes on algorithms that aim at keeping the received power of the desired signal at some constant level [7,16,37]. This is favorable as the receiver dynamic range can be quite small. However, it is the SIR that directly determines the system performance, and hence controlling the SIR rather than the signal strength is more desirable from the radio link performance perspective [38].

Basically, two different approaches are available in SIR based power control. One is the fully distributed SIR-based power control scheme in which power is adjusted independently according to the received SIR on each individual link [36-40]. In such a scenario, the power adjustment made by any individual user to maintain its acceptable SIR will in turn affect the interference seen by all other users. This interaction creates some degree of positive feedback among the individual power control processes. As a result, system stability becomes crucial in the design of such algorithms.

The other approach is the centralized power control schemes presented in [22-25]. In these schemes, there is a hypothetical central controller controlling all transmitter power to achieve a balance SIR in a global scale. SIR balancing can improve the capacity of a spread spectrum cellular mobile radio system [20-21]. However, the existing design is based upon the assumptions of perfect estimation of the static channel qualities, in which the fading effect in a radio propagation channel is ignored and mobiles are assumed stationary at all time. In addition, these centralized power control schemes require an enormous amount of information exchange among the users, base stations and the controller, which is difficult to implement in practice. More details on these existing power control algorithms will be reviewed in the next chapter.

1.3 Contribution of the Thesis

The objective of the thesis is to design a feasible centralized power control algorithm for improving the downlink capacity of a CDMA system. Since the existing centralized power control schemes require an enormous amount of information exchange in the system, its implementation is not practically feasible. We introduce in this thesis an improved centralized power control scheme based on pilot signal monitoring and estimation. By monitoring and tracking the pilot signals from the home base and neighboring bases which are already required for system synchronization and the soft hand-off process (see section 1.1.4), each mobile attains the limited available link gain information. The mobile reports these link gain measurements to its home base. The home base then does some preprocessing before transmitting the necessary information to a central controller through a high speed backbone network. Based on this available pilot information, the central controller allocates the power to different bases in a fashion to minimize the outage probability. In result, the complexity of centralized power control should be greatly reduced.

As for the downlink capacity performance, we simulated both the instantaneous and average power control processes in a multi-user CDMA cellular system. Rather than testing on some particular portables in the center cell, all portable's SIRs in every cell are measured in order to observe the interaction among different cell users in the system. A detail signal propagation model was used in the study which included both the fast-varied Rayleigh fading and the shadowing effects, which have not been considered before in any of the centralized power control studies. The downlink capacity was estimated under various SIR thresholds. The result indicates that the improved centralized power control scheme not only achieved higher capacity compared with the fixed step distributed power control scheme but also had reasonable implementation complexities.

1.4 Outline of the Thesis

Chapter 2 reviews the existing power control techniques in existing cellular system designs, which include the centralized power control, the distributed balancing power control and the fully distributed power control techniques. The centralized power control and the fully distributed power control algorithms are the main focuses of the review.

Chapter 3 starts with the description of the mobile radio environment, propagation channel model and system model. Then the existing fully centralized and fully distributed power control schemes are applied in the multi-cell, multi-user DS/CDMA system model. Simulation results are presented with the performance comparisons on the outage probability between the two power control schemes. The trade-off between simplicity and performance of the two designs leads us to find an improved centralized power control algorithm that provides both good outage performance and reasonable implementation complexity.

Chapter 4 introduces the new improved centralized power control algorithm, called the reduced complexity centralized power control (RC-CPC). The chapter describes how the algorithm simplifies the original centralized control scheme with distributed computation and the limited channel information. The distributed processing at each base includes link-gain computation, user prescreening and admission control procedures.

Simulation results on the outage probability, the system capacity and the CIR statistics are presented in Chapter 5. Various fast power control techniques are compared as well. In addition to fast power control, we also examine the system performance under average power control.

Chapter 6 concludes the study and takes a look at future research directions.

Chapter 2

Literature Overview

The application of power control in cellular radio systems have been studied by many researchers in the literature [16-42]. The goal of our study is to improve the performance of the power control schemes in terms of system capacity and implementation complexity. This chapter gives a review of 3 classes of existing power control techniques:

1. Centralized Power Control (CPC) -- a central controller gathers all the link gain information and controls the transmitter power for all users in all cells [22-28].

2. Distributed Balancing Power Control (DBPC) -- each cell controls the transmitter power levels individually, but some information are exchanged among different cells to stabilize the system and balance the CIR on each link [29-35].

3. Distributed Power Control (DPC) -- transmitter power is controlled in a fully distributed fashion, i.e., power adjustment by a user is based solely on individual received information, and it can be open loop [16-19] or closed loop [36-42] power control.

Before reviewing these algorithms, we first introduce some of the terms and performance criteria used in our study.

2.1 Concepts and Definitions

Frequency reuse as explained before is the core concept in cellular communication systems because it can significantly increase the system capacity. Yet the interference due to common use of the same channel, known as the co-channel interference, in turn limits the efficiency of spectrum utilization. Power control is an effective technique in reducing co-channel interference in CDMA and allowing as many users as possible to obtain satisfactory reception. Reception is said to be satisfactory if the receiver's CIR is greater than the system protection ratio γ_0, which is the minimum required CIR for an acceptable bit error rate (BER) performance. Thus, the lower the required CIR is, the higher is the capacity potential. Equation (1.4) shows the relationships among the CIR, the processing gain G (W/R) and the base-band SIR (E_b/I_0). A lower required CIR is also mapped to a lower base-band required SIR with a given processing gain G.

The processing gain plays an important role in determining the efficiency of the system. The larger the processing gain, the better is the ability of the system to mitigate the multipath (e.g., using a RAKE receiver to resolve the delayed spread) [8]. Also, more users can share the same frequency band since the number of users N increases with the processing gain G as described by equation (1.5). Typical values for G range from 100 to

1,000. In the IS-95 standard for DS/CDMA cellular systems, the chip rate is about 1.228 Mchips/s, and the spread spectrum bandwidth is 1.25 MHz [15]. It gives a bandwidth expansion factor of 128. In addition, with various coding techniques and sectorization used, the required base-band SIR is normally in the range of 4 ~ 9 dB for a BER of 10^{-3} [11,15,36]. These parameter values will be assumed in our following studies.

2.1.1 The CIR Model

Consider a system that has a finite number of cells and consists of M number of independent channel pairs (uplink and downlink channels). M >1 corresponds to a F/TDMA system [22]-[27], and M =1 corresponds to a DS/CDMA system [28]. A channel can be a frequency band or a time slot. In a F/TDMA system, the channels are reused in other cells according to some (quasi-) fixed channel assignment scheme (e.g., the pattern of 7-cell clusters shown in Figure 1-5); whereas in a CDMA system, all users in all cells use the same wide-band channel. The actual implementation of the channel is not of importance to our review here. It can be any one of them, FDMA, TDMA or CDMA. In most of the studies [22]-[27], the adjacent channel interference, which is the interference from the nearby channels used in the same cell (e.g., different carrier frequencies or time slots), is neglected for simplicity. In addition, each channel pair is assumed to be used only once in each cell. That means there is no intracell interference neither, because intracell interference is due only to the common use of same channel within the same cell. The thermal noise sources are also neglected. However, the co-channel interference due to the reuse of the same channels in other cells exists. This is a major limitation in maximizing the system capacity [10]. The main objective here is to reduce the co-channel interference and to maintain the signal quality (i.e., the CIR). Without any loss in generality, the following analysis will be restricted to the downlink. It can also be applied to the uplink by changing the notation [23-24]. Moreover, with the above simplified assumptions, the analysis in [24] shows that the following centralized power control

algorithm can theoretically achieve the same CIR in the uplink and downlink directions at every instant.

To derive the CIR seen at a user, we adopt the link gain model shown in Figure 2-1. Assume there are K cells in the system. At some instant, the total number of users is $N = U_1+U_2+...+U_K$, where the first set of U_1 users are assigned to base 1, the next set of U_2 users are assigned to base 2, and so on.

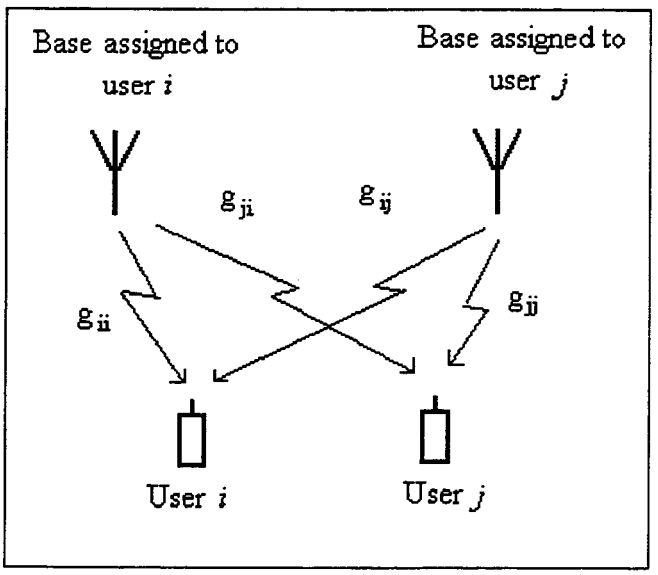

Figure 2-1. A link gain model

In the above link gain model, g_{ji} is the link gain from the base station of the i-th user to the j-th user. Each g_{ji}, where $i, j = 1..N$, varies with the distance and shadowing loss between the base station and the portable user. More details on the propagation model will be presented in the next chapter.

The co-channel interference seen at the i-th user is modeled as the sum of the received powers from all active interferers. Thus, the measured CIR at the i-th user

denoted by γ_i is the desired received power divided by the total interference. It is written as

$$\gamma_i = \frac{g_{ii} p_i}{\sum_{j=1}^{N} g_{ij} p_j - g_{ii} p_i}, \qquad \forall j \tag{2.1}$$

where p_i is the signal power transmitted by the base station of the i-th user intended for the i-th user, and N is total number of users using the same channel known as the co-channel set. To simplify the above equation, we define the normalized link gain matrix as $\mathbf{H} = [h_{ij}]$, where

$$h_{ij} = g_{ij} / g_{ii} \tag{2.2}$$

is the individual normalized link gain.

For all user i, $1 \le i \le N$, γ_i in equation (2.1) is desired to be greater than or equal to the system protection ratio γ_0. Rewriting equation (2.1) with the expression of normalized link gains and the requirement that $\gamma_i \ge \gamma_0$ for all i yields

$$\gamma_i = \frac{p_i}{\sum_{j=1}^{N} h_{ij} p_j - p_i} \ge \gamma_0 \qquad \forall i. \tag{2.3}$$

Similar to the analysis done in [22], we can rewrite the above equation again in the form of

$$(1+\gamma_0^{-1}) p_j \ge \sum_{i=1}^{N} h_{ji} p_j, \tag{2.4}$$

or in a matrix form of

$$\frac{1+\gamma_0}{\gamma_0}\mathbf{P} \geq \mathbf{HP}, \tag{2.5}$$

where the power allocation vector $\mathbf{P}$ contains the following structure:

$$\mathbf{P} = (p_1^1, p_2^1, \cdots p_{U_1}^1, \cdots, p_i^v, \cdots, p_1^K, \cdots, p_{U_k}^K), \tag{2.6}$$

with the element p_i^v as the power allocation for the i-th user assigned to cell v. There are total of N elements for N users in K cells. Similarly, the link gain matrix $\mathbf{H}$ can be partitioned according to the users assigned to different cells:

$$\mathbf{H} = \begin{bmatrix} \mathbf{I}_1 & \mathbf{H}_{1,2} & \cdots & \mathbf{H}_{1,K} \\ \mathbf{H}_{2,1} & \mathbf{I}_2 & \cdots & \mathbf{H}_{2,K} \\ \vdots & \vdots & \ddots & \vdots \\ \mathbf{H}_{K,1} & \mathbf{H}_{K,2} & \cdots & \mathbf{I}_K \end{bmatrix}, \tag{2.7}$$

where $\mathbf{I}_k$ is an identity matrix of size U_k. and

$$\mathbf{H}_{k,i} = \begin{bmatrix} \cdots h_{1,i} \cdots \\ \cdots h_{2,i} \cdots \\ \vdots \\ \cdots h_{U_k,i} \cdots \end{bmatrix}_{U_k \times U_i}, \tag{2.8}$$

is a matrix of size $U_k \times U_i$. Note that all the columns in $\mathbf{H}_{k,i}$ are identical, and each column consists of U_k number of different entries. The l-th entry in a column represents the link gain $h_{l,i}$, $l=1...U_k$, from the i-th base to the l-th user in cell k.

Since each channel 's link quality is independent among different bases and users, the link gain matrix **H** has N independent rows and columns. Moreover, the matrix **H** is non-negative. According to Perron-Frobenius Theorem in Matrix Theory [47], if **A** is a non-negative $N \times N$ irreducible matrix, then the spectral radius $\rho(\mathbf{A})$ is a simple eigenvalue of **A**, and all other eigenvalues are less than $\rho(\mathbf{A})$ in modules. Moreover, an eigenvector associated with $\rho(\mathbf{A})$ may be taken to be positive [47]. This means for the nonnegative link gain matrix **H** in (2.5), we can find a real positive $\rho(\mathbf{H})$, denoted by λ_{max}, such that

$$\lambda_{\max} \mathbf{P} = \mathbf{HP}, \tag{2.9}$$

where **P** is one of the positive eigenvectors (i.e., all entries have the same sign) associated with λ_{max}.

From equations (2.5) and (2.9), it can be concluded that if **H** has a maximum eigenvalue λ_{max} satisfying

$$\lambda_{\max} \le \frac{1+\gamma_0}{\gamma_0}, \tag{2.10}$$

and the corresponding eigenvector **P** in equation (2.9) is used as the transmitter power allocation, then all users will experience a CIR of

$$\gamma^* = \frac{1}{\lambda_{\max} - 1} \ge \gamma_0. \tag{2.11}$$

2.1.2 The Outage Probability

Based on the system protection ratio γ_0, we define the outage probability as the probability that a randomly chosen link is subject to excessive interference [22]. For the j-th user, the cumulative probability distribution function (CDF) of γ_j is denoted by $F_j(x)$. When $x = \gamma_0$, we have

$$F_j(\gamma_0) = \text{Prob}\left[\gamma_j \leq \gamma_0\right]. \tag{2.12}$$

This probability is evaluated by calculating the fraction of time (over the entire call duration) the j-th user experiences a CIR lower than γ_0. Averaging the results over all N co-channel users will provide the outage probability of the system. Minimizing the outage probability is one of the performance criteria for the power control algorithms.

2.2 The Centralized Power Control Algorithms (CPCA)

In the ideal case, a CPCA is an algorithm that can have access to all link gain measurements and can control all transmitter power instantaneously. Its main tribute in cellular system designs is globally reducing the co-channel interference due to frequency reuse and ensuring the signal quality (CIR) is above γ_0. The idea of CIR-based centralized power control was dated back in the early 70's when Aein [20] investigated co-channel interference management in satellite networks. In his work [20], Aein proposed controlling the transmitter power in order to achieve a balanced CIR, i.e., attain the same

CIR on each link between a user and the user's home base. Later when spread spectrum was still a favorite communication technology in the military, Nettleton and Alavi [21] applied and extended the concept of balancing CIR to spread spectrum cellular radio systems. Their result further showed that CIR balancing could improve the capacity of a spread spectrum cellular radio system. Using the basic ideas in [20-21], Zander derived an optimum CPCA which minimized the outage probability [22]. This CPCA was further analyzed by Grandhi *et al.* in [23], and it again was shown to have an optimal power solution in achieving a balanced CIR at all receivers.

With the balancing scheme in centralized power control [22]-[24], all receivers share the same CIR, i.e., $CIR = \gamma^*$, for all users. Unfortunately, it is possible that the balanced CIR is lower than the system protection ratio γ_0, and consequently the reception may be unsatisfactory for all receivers. To achieve satisfactory reception, some transmitters may be prohibited from transmitting, and this leads to a so called user removal procedure [22]. An ideal user removal process is one that can achieve $\gamma^* \geq \gamma_0$ by removing as few users as possible. Obviously, such process requires substantial computational complexity. For this reason, Zander proposed in [22] a simpler sequential procedure, called Stepwise Removal Algorithm (SRA), which can be implemented practically. This procedure is again slightly improved by the Stepwise Maximum-Interference Removal Algorithm (SMIRA) proposed by Lin *et al.* in [25]. In the following sections, we will review the CPCA combined with different removal procedures [22]-[26].

A Brute Force Algorithm (BFA) was first considered in implementing the optimum removal procedure [22]. The algorithm would first calculate the γ^* corresponding to the original link gain matrix **H** and see if it is above the system protection ratio or not. If not, it would try to remove all combinations of at most *N-2* links, and computing the eigenvalue of each reduced system until the condition as described in equation (2.10) is met. Clearly, such an algorithm would find an optimal solution in a finite number of steps, since by removing combinations of *N-1* links, no interference would remain. When

implementing the BFA to remove unusable links, the total number of eigenvalue computations that has to be performed in the worst case is equal to 2^N-N-2 [22], that is, it grows exponentially with N. To overcome this practical problem, the SRA [18] and SMIRA [21] sequential procedures were proposed. These two algorithms operate as follows.

Stepwise Removal Algorithm (SRA) [18]:

Step 1: Determine γ^* corresponding to the matrix **H**. If $\gamma^* \geq \gamma_0$, then use the corresponding eigenvector $\mathbf{P}^*$ and stop; otherwise set $N'=N$ and perform Step 2.

Step 2: Remove user k which has the maximum of row sums R_k or column sums R_k^T in the matrix **H**, where

$$R_k = \sum_{j=1}^{N'} h_{kj}, \quad \text{and } R_k^T = \sum_{j=1}^{N'} h_{jk}, \tag{2.13}$$

and form the $(N'-1)\times(N'-1)$ matrix **H'**. Determine γ^* corresponding to **H'**, If $\gamma^* \geq \gamma_0$, then use the corresponding eigenvector $\mathbf{P}^*$ and stop; otherwise, set $N'=N'-1$ and repeat Step 2.

Because the row and column sums provide bounds on the dominant (i.e., the largest) eigenvalue of the matrix **H** (i.e., $1 < \lambda^* \leq \|\mathbf{H}\|$) [48], the user removal criterion, therefore, seeks to maximize the lower bound for γ^* of the next matrix **H'**. With the sequential removal procedure, the "unusable" links are removed stepwise until the achievable CIR in the remaining links are above the system protection ratio. For this SRA algorithm, to remove one user, the link gain matrix's eigenvalue and eigenvector pair must be found. This means, in the worst case, one needs to solve the eigen system only N-2 times, which is far less than the 2^N-N-2 times required for the BFA algorithm.

Equation (2.13) suggests that the SRA algorithm removes the potential interferers only based on their link gain information. The power levels of different users are not considered in the removal scheme. An improved version of the SRA, called the Stepwise Maximum-Interference Removal Algorithm (SMIRA) works as follows:

Stepwise Maximum-Interference Removal Algorithm (SMIRA) [25]:

Step 1: Determine γ^* corresponding to the matrix **H**. If $\gamma^* \geq \gamma_0$, then use the corresponding eigenvector $\mathbf{P}^*$ and stop; otherwise, set $N'=N$ and perform Step 2.

Step 2: Compute

$$R_l = \sum_{j=1, j\neq l}^{N'} h_{lj} * p_j, \tag{2.14}$$

$$R_l^T = p_l * (\sum_{j=1, j\neq l}^{N'} h_{jl}), \tag{2.15}$$

and $R_{\max,l} = \max(R_l, R_l^T)$ for all l, $1 \leq l \leq N'$. Remove user k for which $R_{\max,k} = \max_l (R_{\max,l})$ and form the $(N'-1)\times(N'-1)$ matrix **G'**. Determine γ^* corresponding to **G'**. If $\gamma^* \geq \gamma_0$, then use the corresponding eigenvector $\mathbf{P}^*$ and stop; otherwise set $N'=N'-1$ and repeat Step 2.

The term "maximum interference" is used because R_l represents the total interference received by the mobile in cell l and R_l^T represents the total interference to other mobiles caused by base station l. Clearly, the SMIRA algorithm requires N^2 more multiplication that the SRA algorithm each time a link is removed. However, the computational complexity is dominated by solving the eigenvalue and eigenvectors, thus the additional N^2 multiplications are negligible [26]. Moreover, the SMIRA considers transmitting power to be an important factor in removing users. The idea is that the larger

the transmitting power, the greater the interference it causes to mobiles in the other cells. Therefore, if a user which uses a high transmitting power is removed, then it is likely that the remaining users can achieve CIR$\geq\gamma_0$. The results in [26,28] show that the CPCA with SMIRA indeed provides a better outage probability than the CPCA with SRA.

In [28], the SRA and SMIRA procedures are studied in a DS/CDMA system with interference due to lack of orthogonality in the uplink direction. The result shows that large capacity gains can be obtained potentially by using the SRA or SMIRA in order to achieve a balanced CIR system, and the capacity gains increase with the number of removed links in both SRA and SMIRA. Note that the system capacity is evaluated as the maximum number of users the system can support without exceeding a certain outage probability. In [28], an outage probability of 10% with a fixed γ_0 at -15 dB is used for the capacity evaluation in the DS/CDMA system.

In all the above mentioned studies [22-28], users are assumed stationary and uniformly distributed over the entire area. The motion induced fast Rayleigh fading is not considered in the link gain model. Thus, all entries in the link gain matrix **H** varies slowly with only the long-term fading effect. As will be described in the next two chapters, the channel model for our power control study will include the slow fading process as well as the fast fading process. Moreover, rather than acquiring and processing all the link gains in the system, the proposed improved centralized power control algorithm is based on limited available link gain information only.

2.3 The Distributed Balancing Power Control Algorithms (DBPCA)

The application of the previously reviewed centralized power control algorithms would require reliable measurements of all link gains in the system. These may not be possible in a practical system. Therefore, these CPCAs serve mainly as tools to derive upper bounds on the performance of transmitter power control algorithms rather than being suited for practical implementation. In this section, we will review a class of Distributed Balancing Power Control Algorithms (DBPCAs) [29]-[35] which approximate the behavior of the centralized SRA by using only limited path gain information. Under such DBPCAs, the CIRs in all active links evolve and reach a common CIR after a number of steps.

First, let us summarize a class of DBPCAs as follows:

$$\begin{aligned} &\mathbf{P}^{(0)} = \mathbf{P}_0, \quad \mathbf{P}_0 > 0 \\ &P_i^{(k+1)} = \beta^{(k)} P_i^{(k)} \left[(1-\alpha) + \frac{1}{\gamma_i^{(k)}} \right], \\ &\beta > 0 \text{ and } -\infty < \alpha \le 1, \end{aligned} \tag{2.16}$$

where $\mathbf{P}_0$ is an arbitrary positive vector, $P_i^{(k)}$ denotes the transmitting power of the base station in cell i in the k-th discrete time, $\gamma_i^{(k)}$ denotes the CIR at the mobile in cell i in the k-th discrete time; and $\beta^{(k)}$ denotes the weighting factor in the k-th discrete time. The parameter α is normally chosen between 0 and 1 [31-32]. The common performance criterion for this class of power control algorithms is whether all CIRs, γ_i for all i, can be balanced or not and how fast the $\gamma_i^{(k)}$ for all i can converge. The iterative steps in equation (2.16) can be expressed as

$$P_i^{(k+1)} = \beta(\sum_{j=1}^{N} P_j^{(k)} h_{ij} - \alpha P_i^{(k)}), \tag{2.17}$$

which when written in matrix form is given by

$$\mathbf{P}^{(k+1)} = \beta^{(k)}(\mathbf{H} - \alpha\mathbf{I})\mathbf{P}^{(k)} = \beta\mathbf{Z}\mathbf{P}^{(k)}. \tag{2.18}$$

As all the link gains in **H** are positive real numbers, $\mathbf{Z} = \mathbf{H}\text{-}\alpha\mathbf{I}$ ($\alpha \leq 1$) is an irreducible non-negative matrix. With the Perron-Frobenius theorem [48], the above class of algorithms can achieve CIR balancing with probability one. The detailed description is presented in [31-32]. In brief, equation (2.18) represents the power method for finding the eigenvector **P** corresponding to the largest eigenvalue λ_{max} of the **H** or **Z** matrix. The CIR obtained by this power method converges to a balanced solution, i.e., all CIR = γ^* as in the centralized power control scheme. Therefore, they are considered as distributed balancing algorithms. Here, $\beta^{(k)}$ needs to be properly chosen to prevent the transmitter powers from becoming too large or too small. A possible choice for $\beta^{(k)}$ could be $1/\|\mathbf{P}^{(k)}\|$. This would ensure a constant average power level but at the expense of additional communications among the base stations [26].

Note that equation (2.18) indicates an iteration approach for reaching the desirable CIR balancing. However, even ignoring the fast fading effect [22-35], the normalized link gain matrix **H** is still constantly changing with the slow fading gain. Consequently, the maximum number of iterations allowed for balancing can be a critical parameter for the distributed balancing procedure. Theoretically, the speed of convergence of the power method (2.18) depends on how much larger is the largest eigenvalue compared to the others [32]. Experimentally, choosing different values for the parameter α in equation (2.18) results in various speed of convergence [26].

Similar to the SRA in CPCAs, in a DBPCA, a user removal procedure is necessary to remove some unusable links so that CIR $\geq \gamma_0$ in the remaining links. Thus, the Limited Information Stepwise Removal Algorithm (LI-SRA) proposed by Zander in [32] is adopted in the numerical evaluation in [26]. Simulation results in [26] show that $\alpha=1$ provides the best outage probability among this class of algorithms, and it also converges faster than the case with $\alpha=0$. The LI-SRA algorithm works as follows:

LI-SRA Algorithm [32]:

Step 1: Initialize $\mathbf{P}_0=1$. Measure and store the CIR vector $\gamma^{(0)}$.

Step 2: If $\gamma_i^{(0)} \geq \gamma_0$ for all i, then stop; otherwise, perform Step 3.

Step 3: Operate the distributed balancing algorithm for at most L steps. If at some step k ($k<L$), $\gamma_i^{(k)} > \gamma_0$ for all i, then stop; otherwise, perform Step 4.

Step 4: Remove the link that has the smallest initial CIR, $\gamma_i^{(0)}$. Go to Step 1.

The above user removal algorithm can be also applied with the SMIRA used in the centralized power control algorithms. In the power control system just stated, if a link is removed based on the highest transmitter power criterion rather than the smallest initial CIR as in Step 4 above, then this algorithm is called Distributed Balancing Stepwise Maximum Interference Removal Algorithm (DB-SMIRA) [28]. As stated before, the larger the transmitting power, the greater the interference it causes to other users in the system. Therefore, by removing the link corresponding the largest transmitter power, the remaining user may be more likely to achieve γ_0. In short, both the LI-SRA and the DB-SMIRA are considered as effective user removal algorithms used in the distributed balancing power control system to achieve capacity gain.

The simulations in the studies [22-35] assumed that in a static channel the link gain matrix is roughly constant during the balancing phase of the algorithm. The result shows

that with only the slow-varying shadowing effect, the DBPCA can achieve outage probabilities that are comparable to the CPCA [26]. Although the performance is slightly worst compared with the "full-information" centralized control algorithms, the implementation for the DBPCA is simpler and more feasible as it only requires the local CIR measurements.

It should be pointed out that the removal procedure (LI-SRA or DB-SMIRA) in the DBPCAs still requires the comparison of the minimum CIR or the maximum transmitter power in all the cells in the system. It could, in a sense, be argued as a centralized power control algorithm. Nevertheless, the balancing procedure, which is computationally the most intensive one, is almost completely distributed. Only the weighting factor β needs rescaling in order to maintain a reasonable dynamic range requirement for the transmitter power control. As a result, such additional amount of information exchange helps the system to become stable, which is crucial for the practical implementation.

In the following sections, we will review another class of the power control algorithms in which the transmitter power is controlled in a totally distributed fashion, and they are the simplest power control schemes in terms of practical implementation.

2.4 The Fully Distributed Power Control Algorithms (DPCA)

Eliminating any form of information exchange among different cells, the fully distributed power control algorithms are considered the simplest algorithms in which power

adjustment is made based on the information provided by each individual link only. Currently, both open loop and closed loop distributed power control are employed in cellular CDMA communication systems.

2.4.1 Open Loop Distributed Power Control

In a cellular CDMA system, each cell site transmits a pilot signal for initial acquisition and synchronization. Based on the detection of the pilot signal from the corresponding base station, the portable unit attempts to estimate the path loss from the base transmitter to itself. If the physical channel is completely symmetrical, measuring the power level of the signal received from the base station would determine the transmitter power level required for that user to be received by the base station. This ideal situation is almost never the case, since the forward and reverse links are centered at two widely separated frequencies [15]. Nevertheless, these measurements of base station signals provide a rough estimation of the average propagation loss to each user. Consequently, the mobile station can then adjust its own transmitter power according to the strength of the received signal. It is a function normally performed in receivers by the automatic gain control (AGC) circuits [8]. The stronger the received signal is from its corresponding base station, the lower is its transmitter signal, and vice versa. Such a scheme is able to compensate for large scale variations in the channel, including the loss due to range and shadowing which is the same for both directions.

As one kind of open loop distributed power control, studies in [16-18, 42-44] focus on reducing the near-far ratio interference and obtaining the absolute power setting as a function of mobile-to-base distance. The objective of these proposed power control laws is to equalize the performance within the cells, since otherwise the users near the boundary of the cell would experience a transmission quality much poorer than those close to the base station. Nevertheless, it is assumed that the base station knows its own

distance from each mobile instantaneously (with the measurements on the opposite link) and is able to control its power according to a known power control law. Neglecting fading, Lee in [16] proposed a simple power control law:

$$P_j = P_R\left(\frac{r_j}{R}\right)^n, \tag{2.19}$$

where P_j is the transmitter power at the cell site for the j-th mobile unit, r_j is the distance between the cell site and the j-th mobile unit, and P_R is the power required to reach those mobile units at the cell boundary R. The value for the exponent n depends on the channel conditions, $n = 2$ is assumed in a non-fading environment [16]. In a Rayleigh fading environment, $n = 4$ leads to a higher capacity than $n = 2$ [18]. More elaborate approaches are presented in [42-44]; nevertheless, degradation in the system performance is found in the presence of multipath effects and shadow fading.

2.4.2 Close Loop Distributed Power Control

As already noted, propagation loss, specially short term fading, is not symmetric in the reverse and forward links. This is because fading depends strongly on the carrier frequency, which may differ considerably in the two directions. To compensate for the short term fading, a closed loop power control mechanism can be used. The basic idea is to adjust the transmit power based on measurements made at the corresponding receiver. In [37-40], Ariyavistitakul and Chang studied the signal and interference statistics with feedback power control based on two conventional models: one based on absolute received power and the other on received CIR. The latter was shown to be a more practical technique, since it is CIR, not the received signal strength, that determines the received bit error probability. Figure 2-2 shows the feedback loop model for the CIR

based power control algorithm, which applies equally well to both the uplink and the downlink directions.

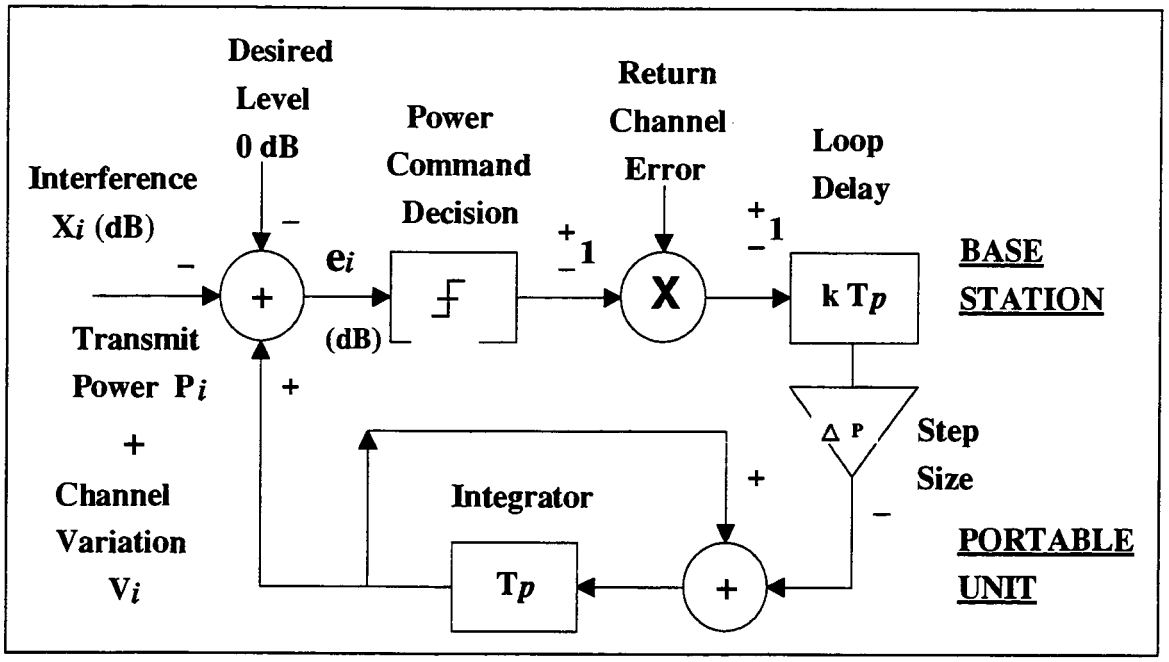

Figure 2-2. Distributed CIR based feedback power control model

In the feedback loop, a receiver compares its received CIR with the desired threshold. If the received CIR is below the threshold, the receiver will generate a power up command, and vice versa. The transmitter responds to the power command bit by adjusting the power up and down by a fixed step, say Δp dB. This power adjustment procedure is repeated every T_p second, where T_p is called the power sampling period and $1/T_p$ is the power adjustment rate. As shown in [37-40], the power control rate must be many times that of the channel's fade rate to permit tracking of the fast Rayleigh fading (e.g., one command every 1.25 msec proved adequate in the field tests [5]). Note that the model considered in [37] also includes the possibility of return channel errors and the extra

loop delay kT_p due to the two-way signal propagation delay as well as the time delay involved in generating, transmitting, and executing a power command. This power updating command is generated after despreading and based on the base-band SIR required. Moreover, the power command bit is assumed to be unprotected since the usual long delay due to coding/interleaving is inconsistent with the need for fast power control.

The main findings in [37] are the following: for a very slow fade rate (e.g., up to 5 Hz for an 8 kbps information bit rate), the increase in average required base-band SIR to achieve 10^{-3} BER is not very sensitive to the increase in the power control delay kT_p, but this sensitivity increases when the fade rate increases. Under the same slow fading condition, power control with 1 dB step size corrects most of the channel fading because the required SIR at this fading rate is within 1 dB of the static channel performance. In addition, SIR based closed loop power control is more practical, and it gives better CIR performance compared with the other algorithm which tries to equalize the absolute received power on each link.

The authors in [39-40] also specifically address the stability issue in the systems with CIR based distributed power control. The stability issue is important in this case because power adjustment is made based on individual information only. Since a power change of any user can affect the total interference seen by all other users, it creates some degree of positive feedback to the individual control processes. Thus, various mechanisms must be incorporated in the design to stabilize the individual power control processes. First, a maximum transmitter power level can be used to stabilize the system when the load is reaching the maximum. Second, a minimum power can be used when the system is very lightly loaded, in which case thermal noise dominates the total interference. In addition, the presence of external interference from other coverage areas helps to stabilize systems with CIR-based power control. In fact, the stability is demonstrated [39] in the case which the number of active users is large (e.g., several tens of simultaneous users) in

the system so that the interference variation due to individual power changes is negligible, i.e., the total interference always remains nearly constant.

Mermelstein and Jalali [36] also studied the effects of power control on the capacity of microcellular CDMA systems. The feedback model is the same as described above. Rather than studying the complicated interactions between individual power control processes in the entire system, the investigations focused on the base-band SIR (CIR divided by the processing gain G) seen at the center cell (in the uplink) or at the portables that are in communication with the center cell (in the downlink). The commutative distribution function (CDF) of these SIR measurements is used to determine the system capacity. Note that the capacity in [36] is defined as the maximum number of users in the system such that the outage probability (2.1) is less than 1%. In their simulation studies, a Doppler frequency of 2 Hz was assumed for a carrier frequency of 2 GHz and the power sampling period is 1.25 msec. The achievable capacity was assessed as a function of path diversity, feedback power control, and other factors. For example, with three-sectored antennas, the simulation result showed the cell's capacity is almost three times that of a cell with an omni-directional antenna at the base station. As for the effect of power control, the studies showed that the fast feedback power control mechanism can reduce the required SIR by 4~10 dB when compared with slow power control. Such differences in SIR requirement also depend on the number of transmit antennas used and can be as large as 10.2 dB with 2 antennas used at the base. The research [36] also concluded that the downlink capacity is lower than that of the uplink even if fast power control is employed in both directions.

In summary, fully distributed power control is much simpler in terms of practical implementation. It does not require information exchange as in both the CPCA and the DBPCA. Moreover, the feedback control mechanism tracks the fast Rayleigh fading process with an oversampling rate for power command. Such fast tracking of fading gains may not be realizable in the DBPCA because of the limitation of rate of CIR convergence.

The fast changing link gain matrix does not permit the completion of CIR balancing phase. Nevertheless, both CPCA and DBPCA have the advantages of global management and balanced CIR performance. The global management ensures the system is stable. Whereas in fully distributed power control systems, the system stability issue is crucial because of the positive feedback effect created by individual power control processes and the lack of information exchange among bases and users.

2.5 Research Direction

From the above review, it is concluded that with the advantage of having full knowledge of the link gain information, the fully centralized power control scheme should achieve better performance in terms of minimizing the system's outage probability [22]. On the other hand, the distributed power control scheme requires much less in terms of information measurement and exchange, and is simpler to be implemented in practice. We will apply both centralized and distributed power control in a multi-cell, multi-user DS/CDMA environment and compare their outage performances under fast fading conditions. After that, we will present in Chapter 4 an improved centralized power control scheme which has both advantage of global power management and implementation feasibility.

Chapter 3

Performance Comparison of Centralized and Distributed Power Control

In a cellular CDMA system, each communication link between a base station and a user is time-variant and distinctive because of the fast and independent fading process. This chapter first presents the microcellular system model upon which our study is based. Then it investigates the outage performance of both the centralized and distributed power control techniques. Both techniques have been thoroughly reviewed in the last chapter. Here, we will present the simulation results which will compare their outage performances in the multi-cell, multi-user system model.

3.1 DS-CDMA Microcell System Model

Understanding the mobile communication environment is essential prior to our simulation study of power control techniques. The following sections describe a typical radio propagation channel model, followed by the DS/CDMA system layout and the traffic model.

3.1.1 Channel Model

A transmitted signal propagating through the air experiences path loss, multipath fading and interference from other sources. The operating frequency of the CDMA spread spectrum signal centers within the UHF (Ultra High Frequency) band (e.g., 0.3~3 GHz in current systems). In a mobile radio environment, the UHF signal propagation can be characterized by two terms: slow fading and fast fading [7]. Slow fading, also called long-term fading, is the average path loss mainly due to the range and terrain configuration (e.g., flat terrain, hilly terrain or mountain area) between the base station and the mobile user. On the other hand, fast fading, also known as the short-term fading, is mostly caused by man-made environment (e.g., in rural, suburban or urban area).

Generally, the average path loss experienced by a CDMA signal is formulated as the product of the m-th power of distance and a log-normal component representing shadowing losses; see [7] for a detail analysis. For a user at distance r from the base station, the average attenuation is $\rho(r)$, which is defined as

$$\rho(r) = r^{-m} 10^{\xi/10}, \tag{3.1}$$

where ξ, in decibels, has a normal distribution with a zero mean and a standard deviation of σ. The parameter σ ranges from 6-12 dB with a typical value of 8 dB. On the other hand, the parameter m ranges from 2.7-4.0 [9]. This model represents the slowly varying path losses, and it applies equally well to both the reverse and the forward links. The log-normal component in (3.1) is the envelope of the fading signal strength, as shown by the dotted curve in Figure 3-1. It is also called a local mean (i.e., each value corresponds to an average of the field strength at each local point) or the long-term fading gain. This long-term fading gain varies very slowly as the mobile travels and the radio medium changes.

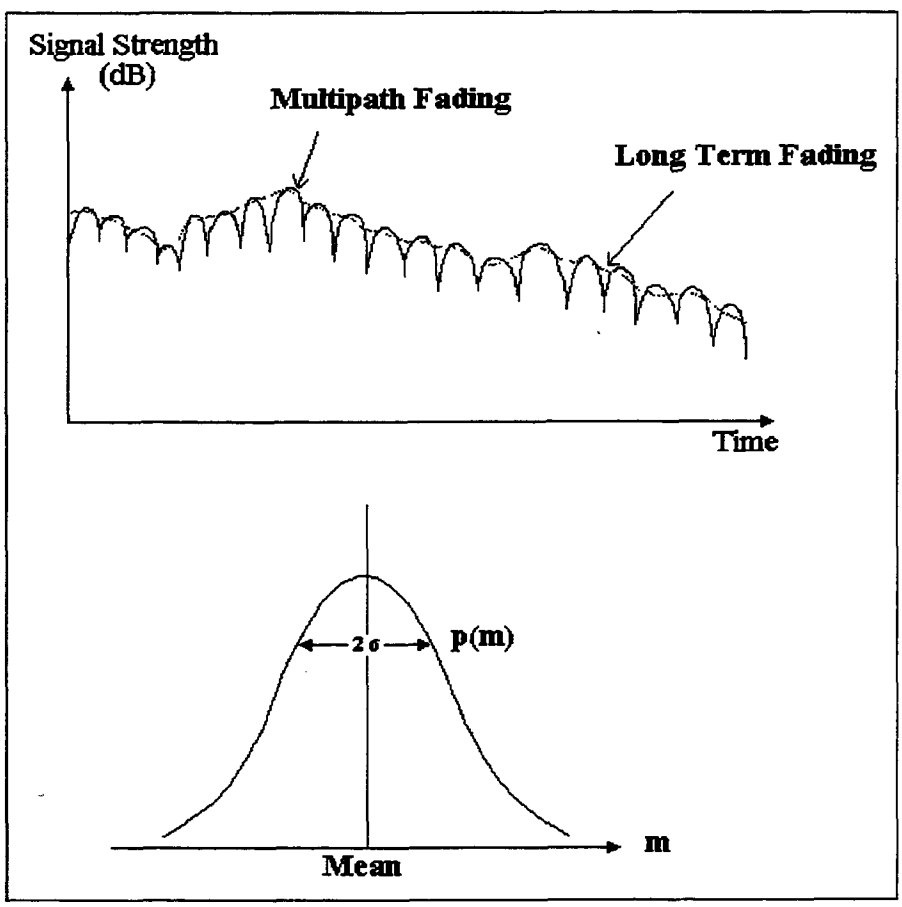

Figure 3-1. Long-term fading and log-normal distribution [7]

Short-term fading is mainly caused by multiple reflections of a transmitted wave by local scatterers such as houses, buildings and other human built structures, or by natural obstacles such as forests surrounding a mobile unit. It results in the radio waves going through different paths before reaching the receiver unit. Figure 3-2 illustrates an indoor communication environment where multiple propagation paths exist.

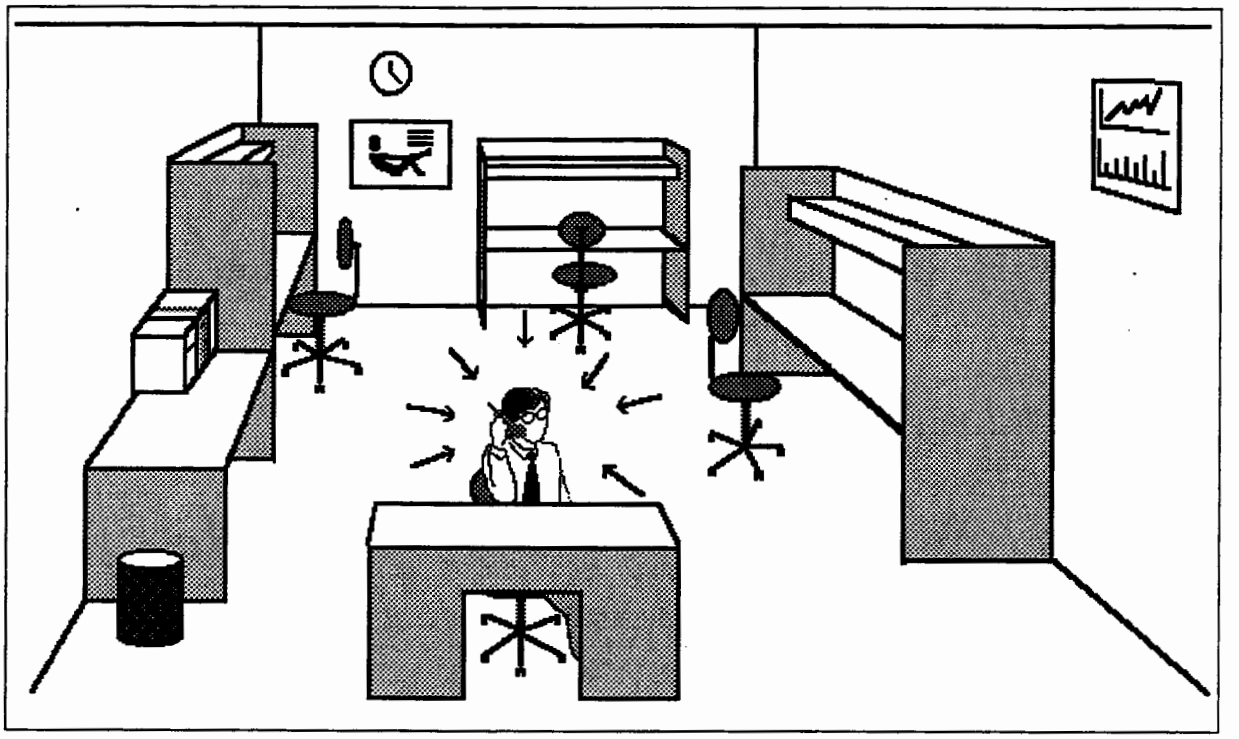

Figure 3-2. Indoor multipath propagation

Consider the following scenario: A base station transmits a signal $s(t)$ to a mobile unit which itself is moving at a velocity v and surrounded by moving objects and stationary reflectors. The signal $s(t)$, can be written as

$$s(t) = \mathrm{Re}\left(u(t)e^{j2\pi f_c t}\right), \tag{3.2}$$

where $u(t)$ is the base-band signal, f_c is the carrier frequency, and Re(·) denotes the real part of a signal. The transmitted signal is reflected and refracted by a variety of surfaces before it reaches the intended listener, i.e., there exists multiple propagation paths between the transmitter and the receiver. Associated with each path is a propagation delay and an attenuation factor [6]. As a result, the received signal $x(t)$ is of the form:

$$\begin{aligned} x(t) &= \sum_i \alpha_i(t)s[t-\tau_i(t)] \\ &= \mathrm{Re}(\{\sum_i \alpha_i(t)e^{-j2\pi f_c\tau_i(t)}u[t-\tau_i(t)]\}e^{j2\pi f_c t}), \end{aligned} \tag{3.3}$$

where $\alpha_i(t)$ is the attenuation factor associated with the i-th path and $\tau_i(t)$ is the corresponding propagation delay. The channel represented by (3.3) is a time variant fading channel, and the equivalent low-pass received signal $r(t)$ is

$$r(t) = \sum_i \alpha_i(t)e^{-j2\pi f_c\tau_i(t)}u[t-\tau_i(t)]. \tag{3.4}$$

By writing $r(t)$ in the form of

$$r(t) = \int_{\tau=-\infty}^{\infty} u(t-\tau)c(\tau,t)d\tau, \tag{3.5}$$

this means the time varying impulse response of the channel is

$$c(\tau,t) = \sum_i \alpha_i(t)e^{-j2\pi f_c\tau_i(t)}\delta[\tau-\tau_i(t)]. \tag{3.6}$$

As shown in [6], $c(\tau,t)$ is usually modeled as a wide sense stationary complex Gaussian process with uncorrelated scattering at different delays. This means

$$\begin{aligned}\phi_c(\tau_1,\tau_2,\Delta t) &= \frac{1}{2}\overline{c^*(\tau_1,t)c(\tau_2,t+\Delta t)} \\ &= \sigma_1^2 J_0(2\pi f_D \Delta t)\delta(\tau_1-\tau_2),\end{aligned} \tag{3.7}$$

where σ_1^2 is the power associated with the path delay τ_1 (a discrete multipath model is assumed here), $J_0(\cdot)$ is the zeroth-order Bessel function of the first kind, and f_D is the maximum Doppler frequency (also known as the fade rate), given by

$$f_D = \frac{v \cdot f_c}{c}, \tag{3.8}$$

where c is the speed of light. It should be pointed out that the above equation (3.7) implies a isotropic scattering model and is commonly termed the Jake's model [49].

The fast fading channel can be further characterized by the delay-power profile. The delay-power profile of the channel is defined as

$$G(\tau) = \sum_i \sigma_i^2 \delta(\tau - \tau_i). \tag{3.9}$$

If $G(\tau)=\sigma_1^2\,\delta(\tau)$, then the channel is a flat fading channel, and the received signal becomes

$$r(t) = c(t)u(t), \tag{3.10}$$

where $c(t)$ is a complex Gaussian process with an autocorrelation of $\sigma_1^2 J_0(2\pi f_D \tau)$. On the other hand, if $G(\tau)$ consists of more than one "impulses", then the channel becomes a

frequency selective fading channel. This means the different frequencies of the transmitted signal are attenuated differently and these attenuation factors also change with time.

In the context of CDMA transmissions, where the chip rate is much higher than the actual data rate, the following tap-delay line model shown in Figure 3-3 is usually adopted for the frequency selective fading channel:

$$c(\tau,t) = \sum_{n=1}^{L} c_n(t)\delta(t - nT_c), \tag{3.11}$$

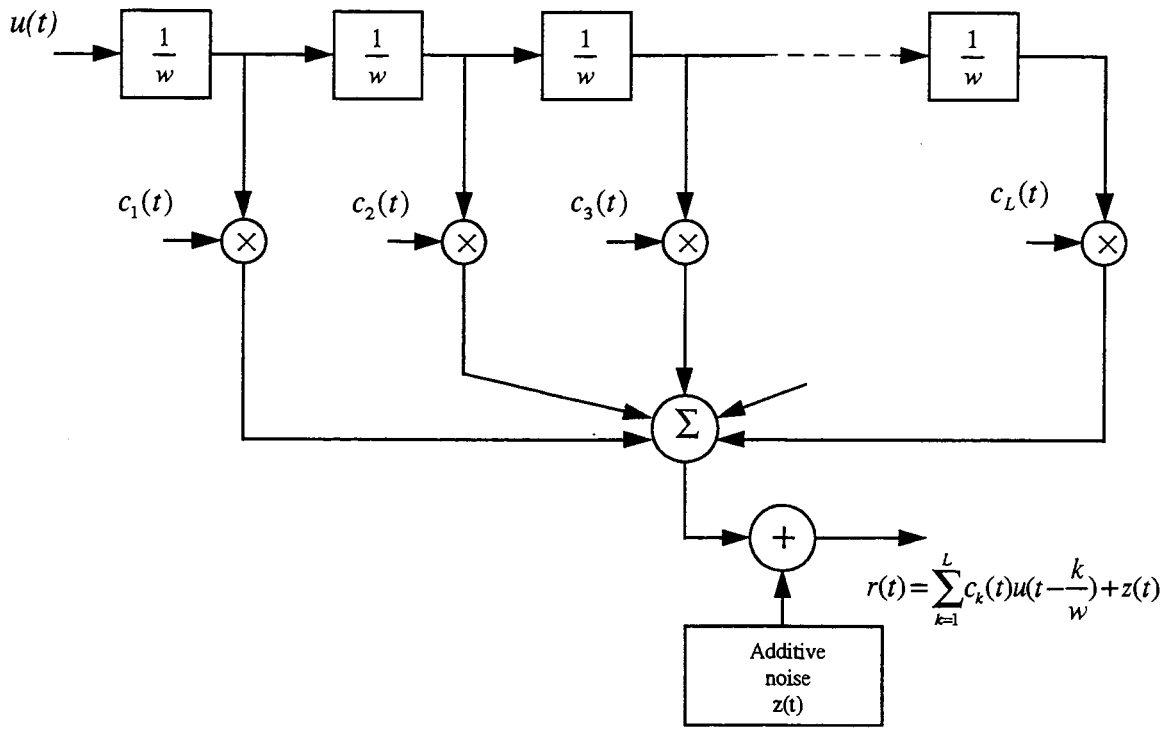

Figure 3-3. Tapped-delay Line for a Frequency Selective Channel [6].

where LT_c is the total delay spread in the channel, the $c_i(t)$ $(i=1...L)$ are independent Rayleigh fading processes, and T_c is the chip duration. Noted that L is also known as the

diversity order of the channel. With proper receiver processing, specifically with the use of the so-called RAKE receiver [6], the performance of a CDMA system will be much better in a frequency selective fading channel than in a flat fading channel, as long as the rms delay spread is less than one data symbol duration. The RAKE receiver which consists of a bank of L parallel correlators (or matched filters) can collect the signal energy from all the received signal paths that fall within the span of the delay line [8]. As mentioned earlier, we can create an artificial multipath channel by transmitting replicas of the same signal at different delays in order to make use of the diversity combining reception.

For convenience in our study, we consider a flat fading channel. The main reason is simplicity since generating multiple fading processes is very time consuming. In addition, the effect of a multipath environment can be simply translated into a different detection threshold requirement [36], and this can be easily handled by generating results for different CIR thresholds.

In addition to adopting a flat fading model, we also assume the fading process itself can be represented accurately by a third order autoregressive model. Specifically,

$$x(n) = a_1 x(n-1) + a_2 x(n-1) + a_3 x(n-1) + e(n), \tag{3.12}$$

where

$$x(n) = c(t)\Big|_{t=nT_p}, \tag{3.13}$$

is a sample of the flat fading process, $e(n)$ is a zero mean complex Gaussian random process, T_p is the power sampling period, and the coefficients a_1, a_2, a_3 are chosen in such a way that

$$\begin{aligned}\phi(n) &= \frac{1}{2}\overline{x(m+n)x^*(m)} \\ &= \sigma^2 J_0(2\pi n f_D T_p), \qquad (n = 0,1,2,3).\end{aligned} \tag{3.14}$$

The a_i's can be solved by invoking the Yule-Walker equation [48]

$$\begin{bmatrix} a_1 \\ a_2 \\ a_3 \end{bmatrix} = \begin{bmatrix} \phi(0) & \phi_{xx}(1) & \phi_{xx}(2) \\ \phi_{xx}(1) & \phi(0) & \phi_{xx}(1) \\ \phi_{xx}(2) & \phi_{xx}(1) & \phi(0) \end{bmatrix}^{-1} \begin{bmatrix} \phi_{xx}(1) \\ \phi_{xx}(2) \\ \phi_{xx}(3) \end{bmatrix}. \tag{3.15}$$

It should be pointed out that although the Jake's model (equation 3.7) is a more commonly used model for fading processes, it is time consuming as far as simulation is concerned. Our third order autoregressive model, on the other hand, is simpler, and for a given fade rate f_D, it provides a slightly faster fading effect than the Jake's model.

3.1.2 System Layout and Traffic Model

Besides the channel model, other important models in our study are the models for system layout and traffics. For the former, we assume there are K cells in the system on a square grid layout. Each cell has its own base station located at the center of the cell with an omni-directional antenna. Portable users are uniformly distributed over the entire area, and each communicates with the closest base station. Hand-off operation is based on the rule of the nearest neighbour. When a portable user moves across the cell boundary and enters into a new cell, it immediately belongs to the new cell and communicates with the new base station. Soft hand-off with path diversity reception may lower the intercell interference and further improve the capacity performance, but it is not implemented in our simulation study.

As for the traffic model, we model the user arrival process as a Poisson process with a mean arrival rate of λ users/minute. The calling duration is assumed exponentially distributed with a mean equal to l minutes. At the beginning of the simulation, the system is assumed empty. Then after a period of time, the number of users in the system reaches a steady state, since the arrival rate and average call duration are kept constant. The steady state period is used to evaluate the system performance for each individual link.

The downlink (base to mobile) and the uplink (mobile to base) operate at separate frequency bands, so that the mobiles only experience interference from other bases and the bases only experience interference from the mobiles. We concentrate on the downlink performance because as stated earlier, the capacity of the system is assumed limited by the downlink capacity [5, 36].

Since the frequency is reused in every cell, each user not only receives signals from its home base station, but also interfering signals from all other base stations. These mutual interference among users limits the frequency reuse efficiency in a CDMA system, and the aim of this chapter is to report the performance of both the centralized and distributed power control algorithms under the channel and system models stated earlier. The practicality of the centralized power control technique will not be addressed in this chapter, but will be considered in chapter 4 when we present our improved centralized power control algorithm.

To evaluate the system performance, we use the outage probability based on the required CIR threshold. As mentioned before, with an acceptable bit error rate, e.g., BER $=10^{-3}$, the required base band SIR (E_b/I_0) ranges from 4 to 10 dB in the downlink [15]. With a processing gain of 128, we choose the CIR threshold in the range of [-17 ~ -11] dB .

3.2 Capacity Gain for Centralized Power Control

Having presented the signal propagation channel model and the multi-cell, multi-user system model, we now apply the centralized power control algorithm reviewed in chapter 2 to the above mentioned DS/CDMA system. As stated before, the centralized power control scheme [22] requires full knowledge of the link conditions between all base stations and all users in the system. Upon receiving the link conditions from all bases, the central controller assigns transmitter power levels to the different users in each cell in such a way that all active links will have an acceptable CIR. Note that in the previous studies of centralized power control [22-26] only an orthogonal channel model and a slow fading condition have been considered. Here we consider fast power control in a multi-user and multi-cell CDMA system under fast fading condition. Before proceeding to the simulations, we will briefly restate the purpose and implication of the user removal algorithm which is used in the centralized power control system.

Recall in equations (2.5) and (2.10), the largest eigenvalue λ_{max} for a given link gain matrix **H** determines the CIR experienced by all users. This leads to a bi-modal behavior -- either all the users experience an CIR above the threshold, or all below the threshold. To avoid the latter disastrous situation and increase the system capacity, we adopt the Stepwise Removal Algorithm (SRA) reviewed in chapter 2. That is, in the event of $\gamma^* < \gamma_0$, the central controller will assign zero power to a subset of the users so that the rest of the users will have a common CIR = γ^* that is above γ_0. Such a user removal algorithm aims to maximize the γ^* corresponding to the link gain matrix **H** by removing some of the links whose CIRs are below the system protection ratio.

The removal procedure may appear as a strange way to achieve high system capacity. However, we should consider those links which cannot achieve the system

protection ratio as useless. Using a nonzero transmitter power in such a link will only cause more interference to other users. Moreover, a user experiencing poor transmission quality should be considered handed over to another base station (communicating with another cell site) in order to improve the performance locally. As a result of using the removal procedure, the capacity gain of the global system is maximized.

Based on the removal procedure, if a new user needs to be removed immediately after powered up, then the system simply rejects this new user. The user being rejected can try to enter the system later with a random delay. This leads to a process known as the call admission control process. The centralized power control algorithm (CPCA) studied here incorporated both the admission control when a new user arrived and the stepwise removal algorithm (SRA) at each power updating instant.

3.3 Simulations

As just stated, the centralized power control scheme incorporates stepwise removal in conjunction with the call admission control to achieve the capacity gain. In particular, the SRA is adopted because it had less computational complexity than the SMIRA (Stepwise Maximum Interference Removal Algorithm) proposed in [25]. In the following sections, we first present the simulation results for the CIR performance of the fully centralized power control schemes. Second, we compare the outage probabilities between two fast power controlled systems: one with fully centralized power control, and the other with fully distributed power control.

The simulation model is based on a 16-cell system on a square grid layout. Different from the link gain model used in [22], in our simulation studies, a white Gaussian noise component is added to the link gain measurements, g_{ji} in each link, with an average

SNR = 20 dB at the vertices of the cells. Other numerical settings are the following: The radio propagation attenuation model uses a path loss exponent of m = 4 with a standard deviation σ = 8 dB. The maximum Doppler frequency, f_D, is set to 10 Hz, and the power sampling rate is set to 100 Hz, so the normalized fade rate $f_D T_p$ is 0.1. The observation period is about 10 minutes long. Users arrived in this period follow the Poisson distribution at an average arrival rate of 40 calls per minute, and the call duration is exponentially distributed with a mean of 3 minutes. Initially, the system is assumed empty without active users. After two to three minutes, it enters into a steady state period as the average number of active users in the entire system becomes steady. During this period, we evaluate the CIR performance of all active links and the outage probabilities of the power controlled system.

3.3.1 CIR Performance of the Centralized Power Control

First, we want to show numerically how important the user removal process is for the fully centralized power control algorithm. We chose a fixed CIR threshold equal γ_0, say at -14 dB, and simulated all the active links between every base station and every randomly distributed user in the system. At each sampling time, the central controller knows the instantaneous link gain matrix **H** and calculate the maximum achievable γ^* accordingly. As explained earlier, with CIR balancing in the centralized control scheme, all users will received the same CIR equal γ^*. Figure 3-4 shows the CIR distributions of the two fully centralized power control schemes in a log-scale (logarithm of 10): one with user removal, and the other without user removal. Note that by setting the CIR threshold at -14 dB, we have the corresponding base-band SIR equal 7 dB given that the processing gain is 128. In addition, the CDF of CIR distribution is expressed in the form of

$$F(x) = Prob(\text{CIR}<x). \tag{3.16}$$

When $x=\gamma_0$, $F(\gamma_0)$ becomes the outage probability as defined in Chapter 2.

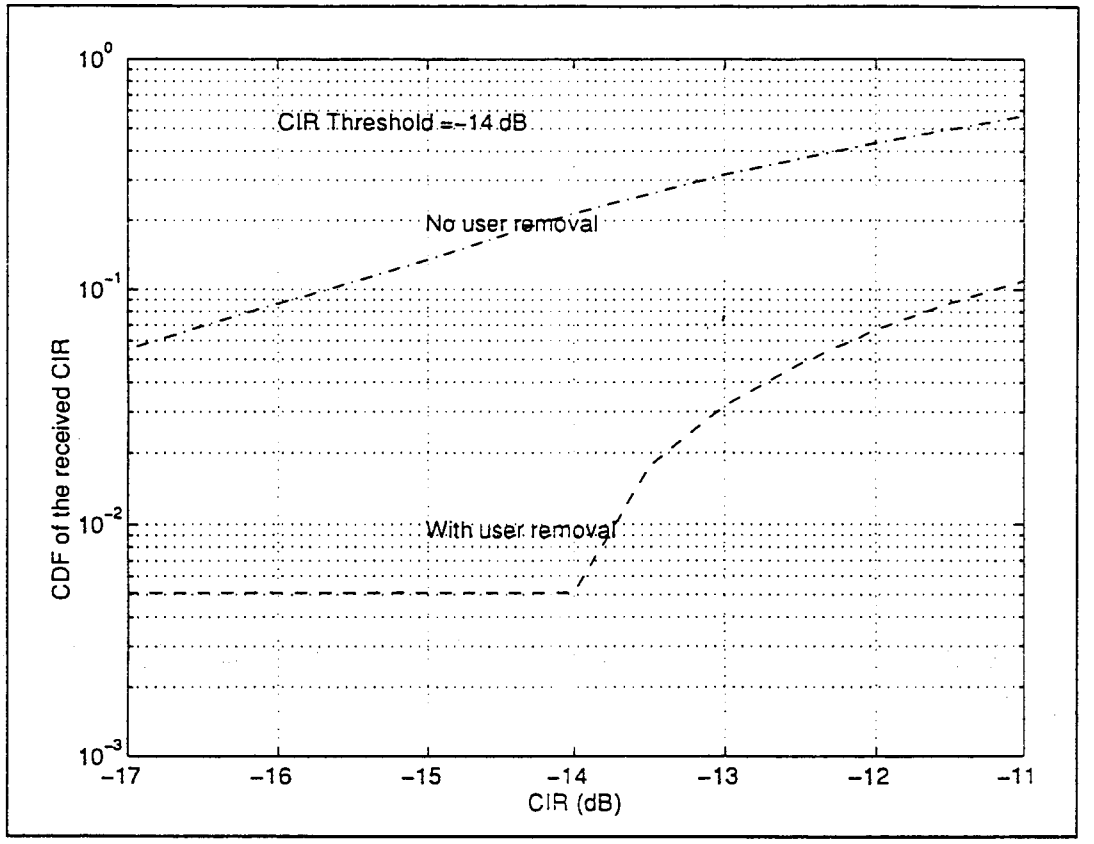

Figure 3-4. CIR Distribution with Fully Centralized Power Control

From the above figure, we can see that the centralized power control scheme with user removal performs much better than the one without user removal. The former yields an outage probability equal 0.5%, whereas the latter yields an outage probability equal 25%. The total outage improvement for the former is 24.5%. The lower the outage is, the better chance users have their CIRs greater than the required threshold. The above result confirms the importance of the user removal process for achieving high capacity gains.

Next, we want to show how the centralized power control scheme performs with varied CIR thresholds. So with the same numerical settings as mentioned above, except the CIR threshold is varied between -17 dB and -11 dB, we simulated the received CIR distribution. Figure 3-5 shows a set of CDF curves each corresponds to a different CIR threshold. These CIR thresholds in the range of -17 ~ -11 dB are match to 4 ~ 10 dB in the base-band SIR with a processing gain of 128. Note that from now on, the fully centralized power control scheme will incorporate SRA as the user removal algorithm.

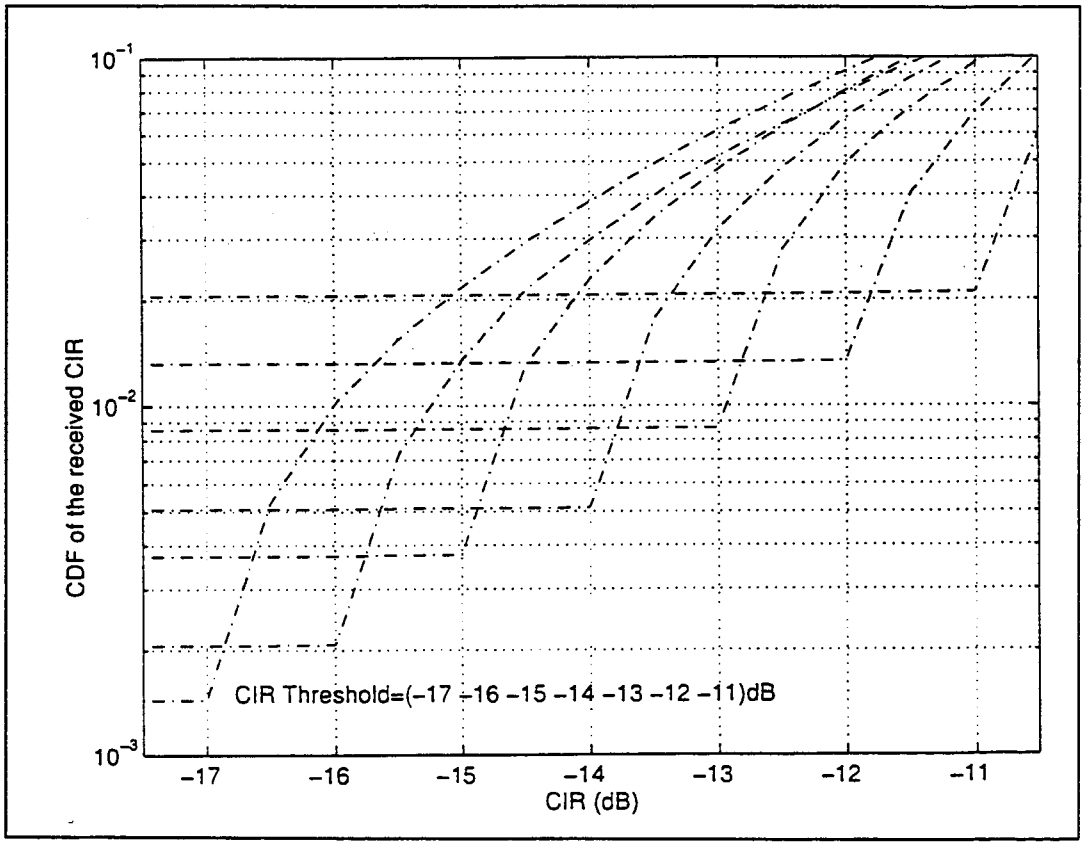

Figure 3-5. CIR Distribution for Fully Centralized Power Control with varied CIR thresholds

From Figure 3-5, we see that when the CIR threshold varies, the probability curve shifts towards the new threshold. As the threshold increases from -17 dB to -11 dB, the CDF of the CIR at the threshold point, i.e., $F(x = \gamma_0)$, changes from 0.13% to 2.1%. This more than 10 times change in outage probability indicates the performance of the centralized power control depends strongly on the CIR threshold γ_0. Nevertheless, the 2.1% outage at the threshold of -11 dB is still relatively low compared with the performance of fully distributed power control which we will show in the next section.

Figure 3-5 also shows that all CDF curves rise abruptly beyond the threshold points. The reason for this is because of the user removal procedure. After removal, all active users have the same CIR equal γ^*, which is always above or equal to γ_0 except those being removed. The percentage of the users being removed is represented by the level portion of the CDF curve to the left of the threshold point. As the CIR threshold increases, the level portion of each CDF curve moves up and the rising portion gets steeper. That means more users need to be removed in order to achieve the higher required threshold. Finally, from these set of CDF curves, we concluded that fully centralized power control can effectively adjust the transmitted power to obtain just the minimum required CIR $\geq \gamma_0$. As the result, the total transmitted power and the interference level in the entire system can be both reduced.

3.3.2 Comparison of the Power Control Algorithms

As stated before, we want to compare the outage performance between the two DS/CDMA systems: one with centralized power control and the other with distributed

power control. Therefore, we simulated both systems based on the same system models described earlier. In addition, the distributed power control scheme that we simulated for the downlink uses the feedback mechanism [37] that we reviewed in chapter 2. A mobile station measures the CIR at its receiver, and compares it with the CIR threshold. If the measured CIR is lower than the threshold, the power command bit is set to +1; otherwise, the power command bit is set to -1. The base station adjusts its transmitter power by 1 dB[1] up or down, depending on the value of the power command bit it receives. The dynamic range in the transmitted power is set to 40 dB. Note once again that this control algorithm is totally based on the individual CIR measurements available at the mobile stations. In addition, we assumed error free and zero delay for the power command bits.

Since the outage probability is defined as the average probability that the received CIR is below the system protection ratio γ_0, we can obtain the outage probability curve by taking the envelop of the CDF curves obtained at different CIR thresholds. For example, the envelop of the curves shown in Figure 3-5 actually becomes the outage probability curve for centralized power control. The same technique is used to obtain the outage probability curve of the distributed power control algorithm. Figure 3-6 shows the outage performance of both the fully centralized and fully distributed power control algorithms.

[1] In our simulations, power control with 1 dB step size results the lowest outage probability compared with the one with 0.5 dB and the one with 2 dB step size.

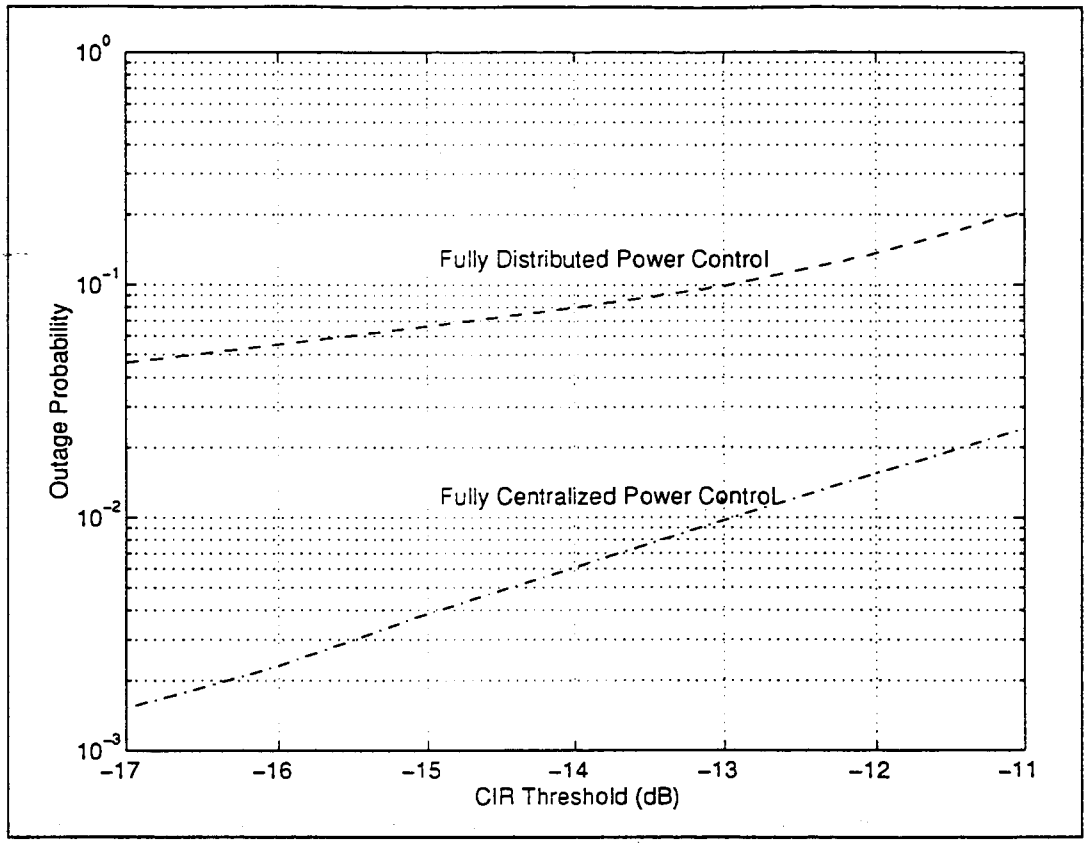

Figure 3-6. Comparison of Outage Probabilities with fully centralized and fully distributed power control schemes

It is obviously that the fully centralized power controlled system outperforms the fully distributed power controlled system. Figure 3-6 shows that centralized power control results in very low outage probabilities which are within the range of 0.16~2%, whereas distributed power control yields much higher outage probabilities in the same range of CIR thresholds. This can be explained from the fact that centralized power control works on full knowledge of channel information, whereas distributed power control does not have any form of information exchange among mobiles or base stations. In addition, distributed power control based on individual received CIR causes complicated interactions among all users' power adjustments as well as fluctuation in their received CIRs [38]. As a result, its outage probability is much higher than its counterpart.

3.4 Conclusions

Based on the numerical evaluations of the fully centralized and fully distributed power control schemes, we conclude that the former is a more effective power control scheme as far as the outage probability is concerned. Furthermore, with full knowledge of the link gain information, the central controller commands the transmitter power in a global scale and yields a fairer collective performance compared with distributed power control.

Aside from the performance, however, such a centralized power control scheme may be too complex to be implemented. It requires a signification measurement effort and an enormous amount of information exchange to obtain all the time varying link gains in the entire system, which may not be possible in practice. On the other hand, a fully distributed power control algorithm does not rely on any form of information exchange. Although its outage performance is not as good as centralized power control, its implementation is much simpler. Therefore, the objective of the latter part of our study will focus on an improved centralized power control algorithm that uses only limited amount of knowledge about the link gain information. Specifically, a regional power control scheme in which neighboring bases exchange information about their own cells may be a good substitution for the hypothetical fully centralized power control scheme.

Another observation for the centralized power control is that at each instant, only a few users have to disable their communication links to let the remaining users achieve γ_0. Those users whose links are removed may experience very low CIR at that instant. However, the total number of users and the fractions of time at which they need to be removed are very small. For example, with the same system model stated before, at a threshold of -14 dB, and with a 10 minute observation interval, the portion of time that 1 user removed is 7.85%; the portion of time that 2 users removed is 0.69%; the portion of time that 3 users removed is 0.06%; and the portion of time that more than 3 users removed is about 0. These small amount of users whose transmission quality are poor are considered handed over to another base station anyway. As the result, their links to the original base are dropped for that instant, but this enables the system CIR, γ^*, to increase so that $\gamma^* \geq \gamma_0$, and maximize the capacity gain.

Chapter 4

An Improved Centralized Power Control Algorithm

As we have already shown in the last chapter that centralized power control outperforms distributed power control in the sense that it minimizes the system outage probability. However, attempting a practical implementation of the fully centralized power control scheme can be difficult. It requires a significant measurement effort plus an enormous amount of information exchange in order to allocate the transmitted power for all users at the central controller. Thus, the second part of our research is to design an improved centralized power control algorithm, which not only closely approximates the performance of the fully centralized power control scheme but also has a feasible implementation complexity. For convenience, we call this improved centralized power control scheme as the reduced complexity-centralized power control scheme or RC-CPC. In the following sections, we will show how the RC-CPC algorithm is able to determine the global power

allocation by using only limited link gain information, distributed computation and user prescreening.

4.1 Dominant Interferers

In a cellular CDMA system, because the same channel is reused in every cell, the total interference at a mobile user to the given downlink signal is comprised of interferences from all cells in the system. If considering all the link qualities between a user and every base station in the system, then the power control process would require a lot of information tracking and exchange. However, in a mobile radio environment, the radio signal decays rapidly with distance. As a result, the dominant interference seen at a user is contributed mostly by the close-in interferers -- the mutual interferers in the same cell and the interferers from the first tier of neighboring cells [5]. With the application of synchronized orthogonal signaling in the downlink for the same-cell users, the intracell interference is assumed null. Thus, the interference experienced by a user is most likely contributed by the first tier of surrounding cells. We suggest that in a downlink power control system, the users keep track of any significant interference signal, in particular, the pilot signals received from the closest neighboring cells, see Figure 4-1. Such multiple cell tracking and pilot measurements are already incorporated in the soft hand-off operation in CDMA systems, and hence it requires no additional system overhead for the power control purpose.

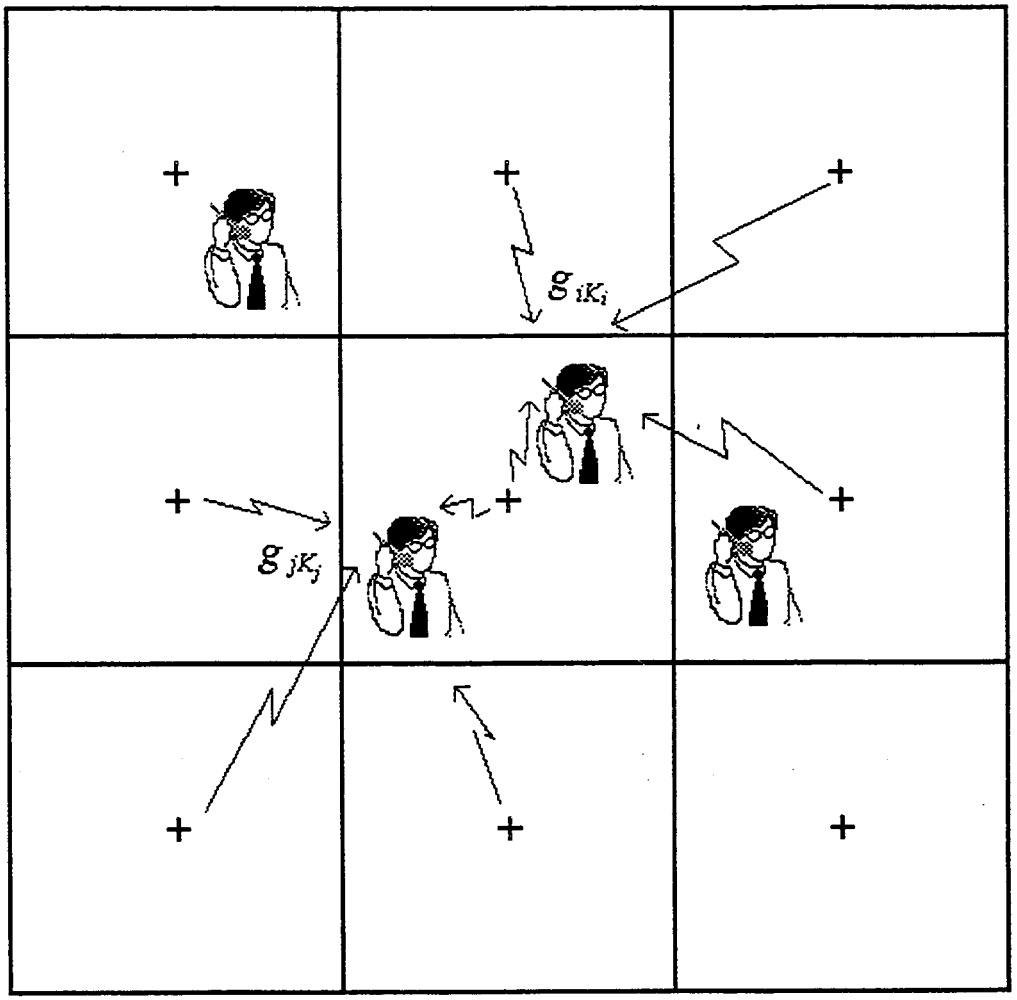

Figure 4-1. Pilots tracking from nearby base stations

Recall in a DS/CDMA cellular system, each cell transmits a cell-specific pilot signal for hand-off, timing reference, and identification purposes. While a mobile is tracking the pilot signal from its home base, it can also search for the pilots from its adjacent cells. To make this simple and practical, all the cell-specific PN sequences are actually generated using the same maximal-length PN code generator but with different time-offsets. Particularly, during the initial set up, each mobile is supplied with a list of cells which are most likely to be the candidates for hand-off and their specific time-offsets

in the pilots. This feature allows a mobile to easily detect the pilot signals, identify the cells and calculate the propagation losses accordingly, i.e., measuring the link gains. In the context of the proposed power control algorithm, a mobile can monitor the signal strength of the pilot signals on the list supplied to it and convey the information on the most dominant pilot signals, i.e., dominant interferers, to the central controller via the mobile's home base stations. This way, only limited link gain information needs to be estimated and exchanged. Note that with this method, the entries in the **H** matrix corresponding to non-dominant interferers are forced to zero.

As explained in chapter 3, due to both slow and fast fading, the propagation losses vary in distance, frequency, and time. For fast power control, we need to update the link gains continuously at a rate that is greater than the maximum fade rate. This may require a great amount of information tracking and exchange, even though only the dominant interferers are considered. To further simplify the link gain measurement and reduce the amount of information exchange in the power control system, we suggest using an AGC circuits with a one-bit-per-link type of adaptation algorithm. The algorithm is described as follows:

- Assume at time n, the true link gain from a base to a mobile is $g(n)$, the mobile estimate of it is $g_m(n)$, and the base estimate of it is $g_b(n)$, where $g(n)$ is a continuous random variable while $g_m(n)$ and $g_b(n)$ are discrete.

- At time $n+1$, the mobile tries to estimate $g(n+1)$ from the received pilot signal and reports it to the base. Assuming $g(n+1)$ is greater than $g_m(n)$, then the mobile will obtain $g_m(n+1)$ by adding a fixed increment to $g_m(n)$, i.e.,

$$g_m(n+1) = g_m(n) + \nabla d \,. \tag{4.1}$$

- At the same time, the mobile sends *one bit* to the base, telling it to adjust $g_b(n)$ upward by the step size ∇d, i.e.,

$$g_b(n+1) = g_b(n) + \nabla d. \tag{4.2}$$

In the absence of channel errors and with a high enough oversampling rate (comparing with the fade rate), we can always make $g_m(n) = g_b(n)$, and both will be within a reasonable margin from the true gain $g(n)$. Note that the above is the same algorithm being used in a fixed step distributed power control system [36-39] to update the transmitted power. It means if each mobile monitors M dominant interferers, the overhead required for link gain measurement in RC-CPC is M times that in a distributed power control system.

In summary, by monitoring the pilot strengths from the dominant interferers and updating them with the above one-bit type adaptation algorithm, the corresponding time-varying link gain entries in the **H** matrix are obtained at the base stations, and subsequently at the central controller. However, it should be pointed out that by only considering the dominant interferers, the resultant γ^* will be slightly higher than that obtained when all interferers are considered. The numerical results of the proposed RC-CPC will be presented in the next chapter.

4.2 Distributed Computation

In the RC-CPC algorithm, once the link gains are reported to the base stations, the next step is to process the link gains at the base stations before passing the necessary

information to the central controller. This distributed processing approach will reduce the amount of information being exchanged to and processed by the central controller.

Recall in a fully centralized power control system, all link gains between every base station and every user are reported to the central controller through the base stations. Thus, the number of link gains gathered at the central controller is $K \times N$, where K is the number of cells, and N is the total number of users. As stated in chapter 2, we index this set of N users in such a way that the first set of U_1 users belong to cell 1, the next set of U_2 users belong to cell 2, and so on. Hence, the transmitted power allocation vector $\mathbf{P}$ and the link gain matrix $\mathbf{H}$ can be partitioned as in equations (2.6) and (2.7). In addition, we assume no intracell interference in the multi-cell, multi-user DS/CDMA system. That means if the i-th and j-th users are within the same cell, then

$$h_{ij} = h_{ji} = 0. \tag{4.3}$$

Also, if the i-th and j-th users are in the same cell while the k-th user is in another cell, then

$$h_{ki} = h_{kj} \ . \tag{4.4}$$

Based on the above observations, equation (2.9) can be rewritten explicitly as

$$\begin{aligned} p_1^1 &= \lambda_{\max}^{-1}[p_1^1 + h_{1,2}\sum_{U_2} p_j^2 + h_{1,3}\sum_{U_3} p_j^3 + \cdots + h_{1,K}\sum_{U_K} p_j^K] \\ &= \lambda_{\max}^{-1}[p_1^1 + \sum_{n=2}^{K} h_{1,n}\sum_{U_n} p_j^n], \\ p_2^1 &= \lambda_{\max}^{-1}[p_2^1 + \sum_{\substack{n=1,\\ n\neq 2}}^{K} h_{2,n}\sum_{U_n} p_j^n], \\ &\cdots \end{aligned}$$

$$p_i^1 = \lambda_{\max}^{-1}[p_i^1 + \sum_{\substack{n=1,\\ n\neq i}}^{K} h_{i,n} \sum_{U_n} p_j^n],$$

$$\sum_{U_1} p_i^1 = \lambda_{\max}^{-1}[\sum_{U_1} p_i^1 + \sum_{i=1,}^{U_1} \sum_{\substack{n=1,\\ n\neq i}}^{K} h_{i,n} \sum_{U_n} p_j^n]. \tag{4.5}$$

where P_j^n is the transmitted power allocation for the j-th user in cell n. Now let us define

$$S_I = \sum_{U_I} p_i^I = \lambda_{\max}^{-1}[S_I + \sum_{\substack{n=1,\\ n\neq I}}^{K} \sum_{i=1}^{U_I} h_{i,n} S_n], \tag{4.6}$$

as the total amount of transmitted power form the I-th base. This means equation (4.5) can be written in matrix form as

$$\lambda_{\max} \mathbf{S} = \mathbf{F}\mathbf{S} \tag{4.7}$$

where $\mathbf{S} = [S_1, S_2, \cdots, S_K]$, is the power allocation for the different base stations, and $\mathbf{F}$ is a matrix where the (k,i)-th element is

$$f_{ki} = \begin{cases} 1, & \text{if } k = i; \\ \sum_{l=1}^{U_k} h_{l,i}, & \text{if } k \neq i. \end{cases} \tag{4.8}$$

The summation term in (4.8) is the sum of the link gains from cell i to all the U_k users in cell k, where $h_{l,i}$, $l=1..N$, are the entries in the i-th column in the full link gain matrix $\mathbf{H}$ (in equation 2.7). With (4.8), each of the K^2 number of submatrices in $\mathbf{H}$ can be collapsed into one simple element in the $\mathbf{F}$ matrix. As a result, the size of the link gain matrix is

reduced from $N \times N$ to just $K \times K$, which is confined by the number of existing cells in the system.

As the **F** matrix becomes the coupling matrix between different cells rather than individual users, each base station only needs to calculate and report to the central controller the K entries of the associated row of the **F** matrix. Upon receiving all these information, the central controller then computes

$$\gamma^* = \frac{1}{\lambda_{\max} - 1},$$

where λ_{max} is the maximum eigenvalue of **F**. The existence a unique λ_{max} is guaranteed by the theory of non-negative matrices from Perron, Frobenius and Wielandt [47]. It should be pointed out that the largest eigenvalue of **F** is identical to that of the link gain matrix **H**, since the row entries in the **F** matrix are linear combinations of the independent row entries in the **H** matrix. Their independent eigenvalues[1] are preserved.

Once the power allocation vector **S** is determined based on the **F** matrix, each base station distributes the transmitted power for individual users in its own cell. To have a balanced CIR, the transmitted power for each user is calculated according to the following:

$$\gamma^* = \frac{p_i^n}{\sum_{j=1,}^{K} h_{ij}^n S_j - S_n}, \tag{4.9}$$

[1] In addition, none of these eigenvalues are equal to one.

where p_i^n is the transmitted power allocated for the i-th user in cell n, and h_{ij}^n is the link gain from the j-th base measured at the i-th user. The denominator in the above equation is the intercell interference seen at the i-th user with power allocation $\mathbf{S}$ [2].

In short, the base stations carry out the distributed computation before and after exchanging the relevant information with the central controller. The central controller determines the global power allocation $\mathbf{S}$ among different cells with a reduced size coupling matrix $\mathbf{F}$, and from $\mathbf{S}$, the base determines the transmitted power for individual user. In this way, the central controller effectively controls the intercell interference level and ensures the system stability with a reduced complexity compared with that in the fully centralized power control scheme.

It should be pointed out, if the $\mathbf{F}$ matrix is collapsed from the original $\mathbf{H}$ matrix with full link gain information, then we will have the same λ_{max} and the same balanced CIR as in the fully centralized power control scheme. The same is true for the power allocation to each user. In other words, there is no additional performance loss in using the distributed computation suggested here. However, in our proposed RC-CPC algorithm, the $\mathbf{H}$ matrix, as described in section 4.1, only reflects on the dominant interferers. Hence, the resultant γ^* will be slightly higher than that obtained with full knowledge of channel information. The performance comparison between the fully centralized power control and the proposed RC-CPC schemes will be presented in the next chapter.

To further simplify the original centralized power control algorithm, we will subsequently reduce the amount of processing at the central controller by applying a distributed user removal procedure in the RC-CPC algorithm.

---

[2] Although the sum is over all the K cells, only the dominant interfering cells enter into the picture in reality.

4.3 Combination of SRA and the User Prescreening Process

Recall that in a centralized power control system, pure CIR balancing without cell or user removal can be disastrous, since all links may drop below the system protection ratio, γ_0 [22]. The same also applies to our RC-CPC algorithm. It requires a user removal mechanism in order to achieve a balanced CIR that is above γ_0. In the following sections, we will first present a modified stepwise removal algorithm (modified SRA) tailored for the RC-CPC. Then we will introduce a user prescreening process which can be used in combination with the modified SRA to further reduce the complexity of our improved centralized power control scheme.

4.3.1 Modified SRA in the DS/CDMA cellular systems

The two existing removal algorithms which have been reviewed in Chapter 2 are the SRA and the SMIRA. Both these algorithms work on full knowledge of the link gain matrix **H** at the central controller. To adopt these removal algorithms into our proposed RC-CPC technique and apply them to the multi-user CDMA cellular systems, we need to modify them first.

As stated in section 4.2, to reduce the amount of information exchange between the bases and the central controller, only the reduced size ($K \times K$) matrix **F** is made available at the central controller, where K is the number of cells each having at least one user ($K \leq N$). Note that the entries in **F** are the summation of link gains in each cell rather

than the individual link gains as in **H**. If SRA or SMIRA is applied (e.g., in the case of $\gamma^* < \gamma_0$) to remove a row and a column in the **F** matrix, then all users in the corresponding cell are removed. Such a "cell removal" process would considerably increase the outage probability in the system, especially when the system is heavily loaded. To avoid removing too many users and to achieve γ_0 at the same time, a base station needs to report some of the dominant link gains h_{ij}^n $(i=1..U_i, (n, j)=1..K)$ to the central controller when such a request is made. The link gains corresponding to individual users in cell n can be added together as row sums like the following:

$$R_i^n = \sum_{j=1}^{K} h_{ij}^n . \tag{4.11}$$

Accordingly, we need to modify the SRA as follows:

Modified Stepwise Removal Algorithm:

Step 1: The central controller determines γ^* corresponding to the matrix **F**. If $\gamma^* \geq \gamma_0$, then use the corresponding eigenvector **S** as the power allocation among all cells and stop; otherwise set $K' = K$ and perform Step 2.

Step 2: Determine cell n, whose row sum Z_n $(n=1..K')$ in **F** is the maximum in all K' cells,

$$Z_n = \sum_{k=1}^{K'} f_{nk} \tag{4.12}$$

then request the n-th base to report the dominant link gains corresponding to the i-th user, whose row sum R_i^n in (4.11) is the maximum among the remaining users in cell n.

Step 3: Upon receiving the i-th user's link gains, the central controller modify the n-th row in **F** matrix by deleting from it the link entries h_{ij}^{n}. Check if K' has to be changed, e.g., if cell n has no "usable" link left, then $K' = K' - 1$. Form the $K' \times K'$ matrix **F'**. Determine γ^{*} corresponding to **F'**. If $\gamma^{*} \geq \gamma_0$, then use the corresponding eigenvector **S** and stop; otherwise, repeat from step 2.

With the above modified SRA procedure, the "unusable" links are removed one by one to reduce the norm of the **F** matrix until the CIRs in all the remaining links are larger than the system protection ratio.

Similarly, the SMIRA can be modified as above by comparing the interferences perceived with the transmitted power vector as in equation (2.14) instead of comparing the row sums. However, the calculation of the interferences **H*P-P** in the SMIRA requires even more information exchange and additional computation complexities in each removal step. Thus, we incorporate the modified SRA into our RC-CPC scheme as a sequential user removal procedure.

Note that the modified SRA is accomplished at the central controller. It requires additional information (M dominant link gains for each removal step) to be sent from a base through the backbone connection. Therefore, it should be used as infrequently as possible. A way to diminish the need for executing this stepwise process is for each base to prescreen the user's link qualities first before passing the necessary information to the central controller. With this in mind, we propose a distributed user prescreening process which can be combined with the SRA to remove the "unusable" links.

4.3.2 User Prescreening Process

In [22], the SRA removes users based upon the rationale of

$$1<\lambda_{max}\leq\|\mathbf{H}\|, \tag{4.12}$$

where the largest eigenvalue λ_{max} has an upper bound, which is the norm of the **H** matrix [47]. By lowering the norm of the **H** matrix, λ_{max} is reduced, and γ^* is increased accordingly as in equation (2.11). Based on this, the user prescreening process is to remove (at individual bases) users whose received pilots from its neighboring cells are too strong compared with the pilot from its home base (normalized to 1). In other words, if a user suffers too much interference, it should be removed from the current cell and handed over to a cell with which it communicates better. In fact, such comparison of the pilot strengths is already required in the hand-off process. As a result, by deleting the link gains that are too large, $\|\mathbf{H}\|$ is reduced. Once the λ_{max} of resultant link gain matrix **H** satisfying the following criterion,

$$\lambda_{max} \leq \lambda_0 = \frac{1+\gamma_0}{\gamma_0}, \tag{4.13}$$

then the maximum achievable CIR, γ^*, will be greater than γ_0 according to equation (2.10).

Before describing the user prescreening procedure, let us define the term

$$\chi = \frac{1+\gamma_0}{\gamma_0}\times\mu = \mu\lambda_0, \quad (\mu > 1) \tag{4.14}$$

as the prescreening threshold. The weighting factor μ should be set properly. If μ is too small, then there is a risk that the prescreening process removes more than the necessary number of links. On the other hand, if μ is too large, some "unusable" links are inappropriately kept and consequently the achievable CIR after prescreening may still not satisfy the requirement. We suggest setting μ according to γ_0 and the average value of the norm of **H**.

The distributed **user prescreening algorithm** is as follows:

Step 1. Given γ_0, set the prescreening threshold χ accordingly with an chosen μ.

Step 2. At each base station, gather the dominant link gain information, which are the nonzero row entries in the **H** matrix. Calculate the row sums R_i^n ($i=1...U_n$ for the n-th cell) and compare each of them with the threshold χ.

Step 3. Remove the links for once whose row sums are greater than the threshold.

The user prescreening process is accomplished at the base station as part of the distributed processing, before the base even computes the corresponding entries in the **F** matrix and exchanges the necessary information with the central controller. This process should be required for hand-off anyway; hence, it does not impose any additional computational burden on the central controller. On the other hand, by prescreening the users first, the stepwise removal process is called upon less frequently, so that the complexity of such centralized power control is reduced.

We proposed in the RC-CPC scheme that the user prescreening process is combined in use with the modified SRA. This is more desirable because as mentioned earlier, we don't have an exact formula to determine μ. and χ. That means it is difficult to perfectly prescreen all users in a distributed fashion. Therefore, we set a bit higher threshold to prescreen user first. Then, at the central controller, the stepwise removal is needed only when there are still "unusable" links to be removed. When the modified SRA

is proceeded, the number of removal steps (i.e., the number of unusable links left after prescreening) is greatly reduced as well.

Similar to the call admission control (CAC) mentioned in chapter 3, here with the user prescreening process and the modified SRA, if a newly arrived user detects excessive link gains from those interfering cells, the assigned base or the central controller may reject this new user because it causes the system's CIR to fall below the system protection ratio. However, this rejected user is allowed to try again later with a random access delay. Note that when soft hand-off is incorporated in the power control system, a new user is assigned to the base station whose pilot signal received at the user is least attenuated. In summary, the "unusable" links should be considered handed over to other cells to improve the system's CIR. The user removal processes, including distributed user prescreening, modified stepwise removal and call admission control (CAC), can all be incorporated with the hand-off operation in the power control system.

4.4 The RC-CPC Algorithm

Finally, we summarize the above discussion with the following RC-CPC algorithm:

Step 1. Each user continually estimates, tracks and reports to the home base the channel qualities between itself and the dominant interferers. A one-bit-per-link type of adaptation algorithm can be used for this purpose. See page 64.

Step 2. Each base station collects the link gain information from users in its own cell. Base on the information received, the corresponding base station prescreens

and removes some of the links if necessary. It then calculates and obtains the row entries in the reduced size link gain matrix **F**. As previously discussed, many entries in **F** equal to zeros because only the link gains from dominant interferers are considered.

Step 3. The central controller collects information from all base stations, removes the "unusable" links if necessary and computes the power allocation vector **S** ($\lambda_{max}\mathbf{S} = \mathbf{FS}$). It then passes **S** to all base stations.

Step 4. Each base station distributes the transmitter power according to the amount of interference experienced by each user in the cell as equation (4.9) shows.

In summary, the RC-CPC proposed here uses the distributed computation and user prescreening process to thoroughly reduce the complexity. In addition, rather than rely on the full knowledge of the link gain information, the new algorithm considers only the limited amount of link gain information from the dominant interfering cells. By doing so, the RC-CPC is not only capable of controlling the transmitter power in a global scale but also practical to be implemented.

Chapter 5

Simulations

In the last chapter, we presented an improved centralized power control algorithm called the RC-CPC (Reduce Complexity-Centralized Power Control) algorithm. To evaluate the outage performance of the power control system, we applied the RC-CPC algorithm to both the fast and the slow power control processes in a multi-cell, multi-user DS/CDMA model. The fast power control tracks the Rayleigh fading gain with an oversampling rate that is at least 10 times faster than the fade rate (i.e., the normalized fade rate $f_D T_p \leq 0.1$); whereas the slow (average) power control only compensates for the propagation losses due to distance and shadowing effect. We then compare the system capacity of the RC-CPC algorithm with those of the fully centralized and fully distributed power control schemes studied in Chapter 3. As defined earlier, the capacity is evaluated as the maximum number of simultaneous users that can be supported in the system without exceeding a given outage probability. Since the DS/CDMA system capacity is limited by the downlink capacity [5,36]; therefore, the numerical evaluations of the power control strategies will focus on the downlink power control performance only.

5.1 Fast Power Control Simulation

The same DS/CDMA cellular system presented in section 3.1 is adopted here, and the following numerical setting are applied in the fast power control process:

- The maximum velocity of the mobile unit is 5 km/hour; and the maximum Doppler frequency, f_D, is 10 Hz (the carrier frequency centered at 2 GHz).
- The travel direction of the mobile user is randomly generated between 0 and 360° in a two dimensional phase.
- Power sampling frequency is 100 Hz, which means the power updating period, T_p, is 0.01 seconds and the normalized fade rate $f_D T_p = 0.1$.
- The power control processing and transmission delay is assumed zero.
- The power adjusting step size is 1 dB in the fixed step distributed power control scheme.
- The propagation model has the path loss exponent $\alpha = 4$.
- The shadow fading is log-normal distributed with a variance of $\sigma = 8$ dB.
- The fast fading gain is generated by a third order recursive filter described in Chapter 3.
- A noise component is assumed in each link with an average SNR of 20 dB at the vertices of cells on the square grid.

The third order recursive filter is considered a good compromise between the simplicity and accuracy requirements in generating the Rayleigh fading process.

In terms of the user traffic model, the user arrival process is modeled by a Poisson arrival process. The call duration is exponentially distributed with an average duration of 3 minutes. The average number of active users in the system is varied depending on the average rate of user arrival and their call duration in each simulation run. The arrived users are uniformly distributed over the entire area. A mobile user travels for the duration of the call and thus may cross many cells.

Assume the system is initially empty. During the transient state, the number of users is gradually increased because of the user arrival process. There are occasions that only a few users are scattering apart in the system. That means the coupling matrix **F** in the RC-CPC algorithm, which considering only the dominant interferers, may contains too many zero entries (i.e., has zero rows and columns). In that case, the matrix **F** can be subdivided into submatrices each representing a group of the mutual interfering cells. For example, if two groups of cells are located far apart with no active users in the cells between them, then the interaction between these two groups is very limited. Their mutual interferences are neglected. We may actually have two submatrices for these two groups of cells and each can be solved independently. In this way, the central controller essentially control the power allocation independently for areas that do not affect each other.

In the simulation, we assumed the user arrival rate and the average call duration are constants. After a period of time, the average number of active users in the system reached a steady state. Within the steady state period, we evaluated the system performance by comparing the outage probabilities of various power control schemes. Let γ denote the CIR at some randomly chosen mobile user. The Cumulative probability Distribution Function (CDF) of γ is defined as

$$F(x) = Prob(\gamma \leq x). \tag{5.1}$$

The outage probability is attained by averaging $F(x=\gamma_0)$ over all system users. First, let us look at a 16-cell system supporting an average number of 100 users during the steady state period. Figure 5-1 shows the resultant outage probabilities of the four different power control techniques: A - Fixed equal transmitted power, B - Fully distributed power control, C - Reduced complexity-centralized power control (RC-CPC), and D - Fully centralized power control.

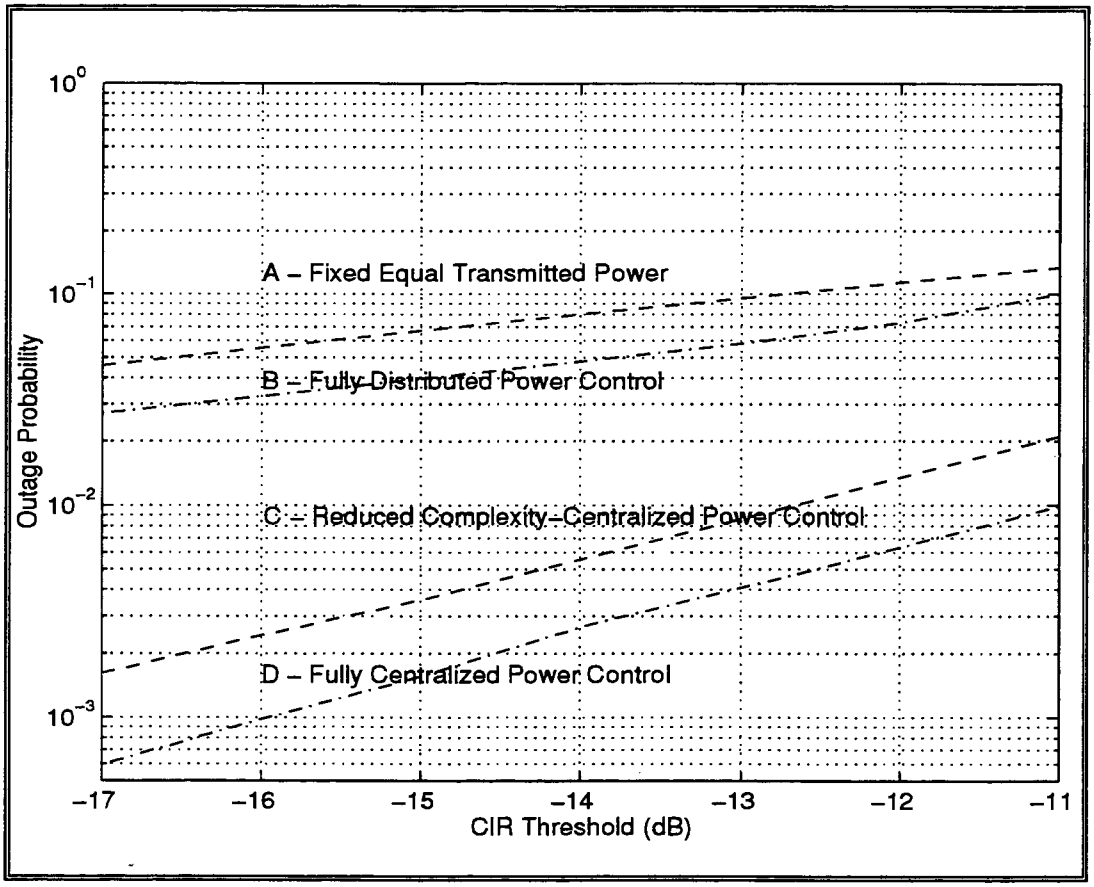

Figure 5-1. Outage Probability Comparison
($f_D T_p$=0.1, SNR=20 dB).

In figure 5-1, the bottom two curves (C and D) are very close to each other within the considered range of thresholds. The difference is very small, between 0.14% and 1% depends on the CIR threshold required. It means that the RC-CPC can approximate the outage performance of the fully centralized power control reasonably well. On the other hand, fully distributed power control results in much higher outage probabilities. As shown in the same figure (figure 5-1), the fixed step fully distributed power control scheme with a power sampling rate equal 10 times the fade rate shows only slightly improvement over the fixed transmitted power scheme. Moreover, as γ_0 increases from -17 to -11 dB, the outage probability increases rapidly from 3% to 10%. This result justifies one of the findings in [39], that is, significant fading can still be observed in the received signal after power control with $f_D T_p$=0.1 and zero loop delay. Thus, we conclude that the RC-CPC achieves better performance than the fully distributed power control scheme ($f_D T_p$ =0.1) in terms of the outage probability.

As we stated at the beginning, the main purpose of power control is to increase the system capacity. To estimate the capacity is to compute the maximum number of users, N, that the system can accommodated subject to the constraint that the resultant outage probability is less than a fixed level. For example, 0.01 is used as the criterion in [36] for the distributed power control simulation with a sampling rate at 800 Hz and a Doppler frequency at 2 Hz ($f_D T_p$=0.0025). In our simulation, we use a much lower sampling rate ($f_D T_p$=0.1), and instead of fixing the outage probability constraint, we fixed the number of users, N, within the observation period in each simulation trail. Then we evaluate the corresponding outage probability by averaging all CIRs measured on each link between a base station and a user. For different power control systems with different set of parameters, we construct various figures that contain multiple outage probability curves each corresponding to a different number of users, *N*. To find out the maximum number

of the users the system can support, we simply locate the required outage level on the plot at the required threshold level γ_0. The advantage of this reverse way of computing the system capacity is that even the outage constraint is varied, e.g., under varied communication quality requirement, we can still find out the corresponding number of users the system can support.

For the fixed transmitted power and the fully distributed power control systems with various CIR thresholds and $f_D T_p$=0.1, the outage probability curves corresponding to different N users are shown in Figure 5-2 and 5-3 respectively.

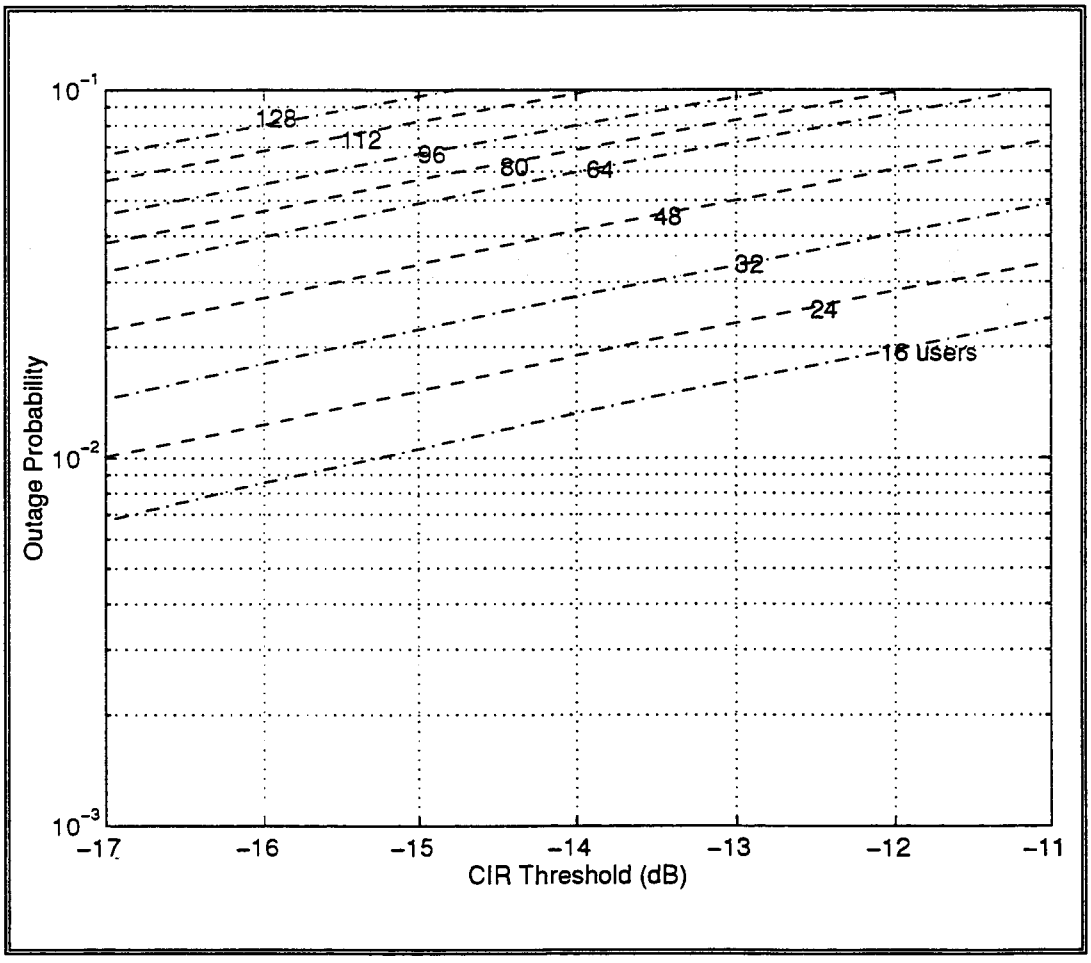

Figure 5-2. Outage Probability Curves for the Fixed Equal Transmitted Power Scheme ($f_D T_p$=0.1, SNR=20 dB, N=16, 24, 32, 48, 64, 80, 96, 112, 128 users in 16 cells).

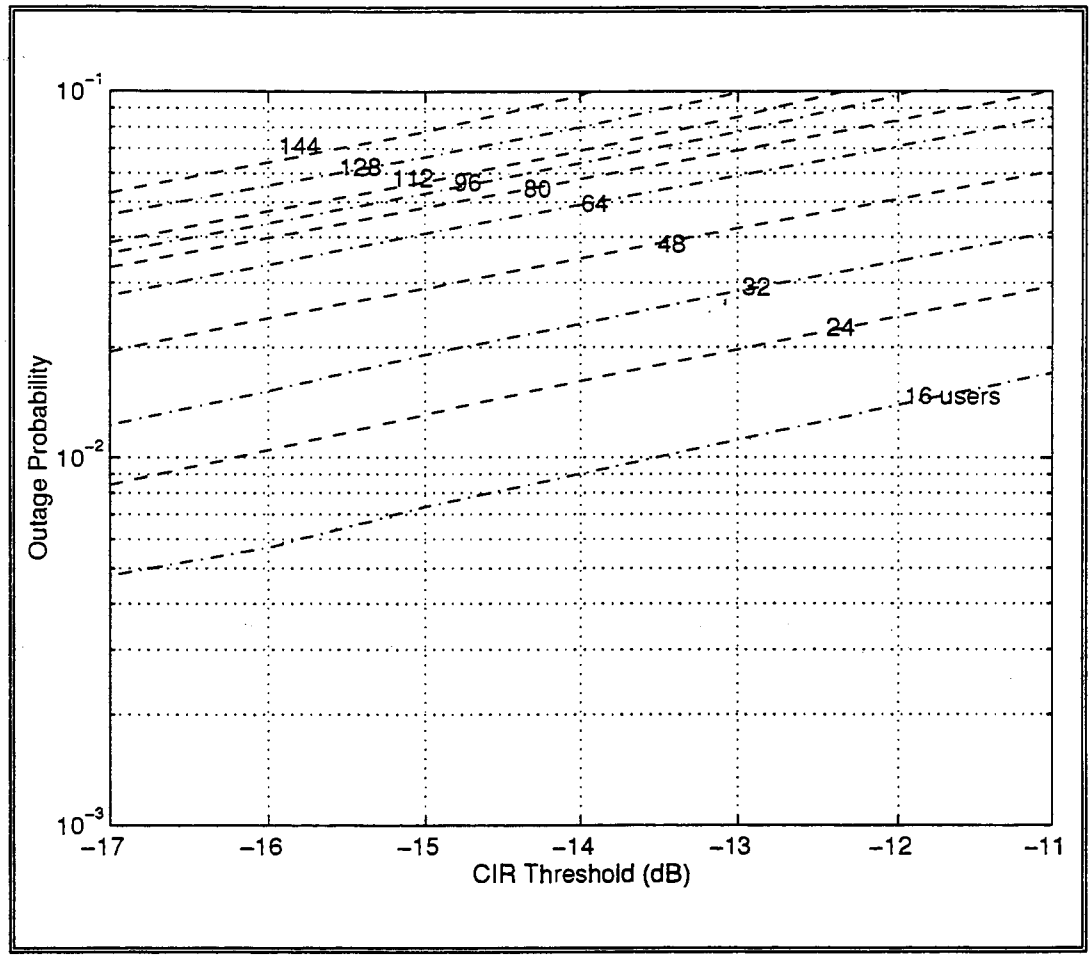

Figure 5-3. Outage Probability Curves for Fixed Step Fully Distributed Power Control ($f_D T_p$=0.1, SNR=20 dB, N=16, 24, 32, 48, 64, 80, 96, 112, 128, 144 users in 16 cells).

In comparing figure 5.2 and 5.3, we can see that the capacity improvement achieved with the fixed step distributed power control over fixed transmitted power is not very significant. If the outage criterion is 0.01 at γ_0 = -16 dB, we have 24 users in the system with distributed power control versus 20 users in the system with fixed equal

transmitted power. This result further justifies what we have found in the previous comparison of the outage probabilities among various power control techniques. The reason is explained in [39] that distributed power control with f_DT_p=0.1 is unable to increase power fast enough to track the rapid channel fades. Consequently, the received signal after power control still contains significant fading. Therefore, for the feedback power control to work effectively against fast fading, the power updating rate must be higher than 10 times the maximum fading rate and the loop delay must be minimized as well. Base on this explanation, we simulate the distributed power control system with f_DT_p=0.02 and examine the improvement of the fixed step distributed power control scheme over the fixed equal transmitted power scheme.

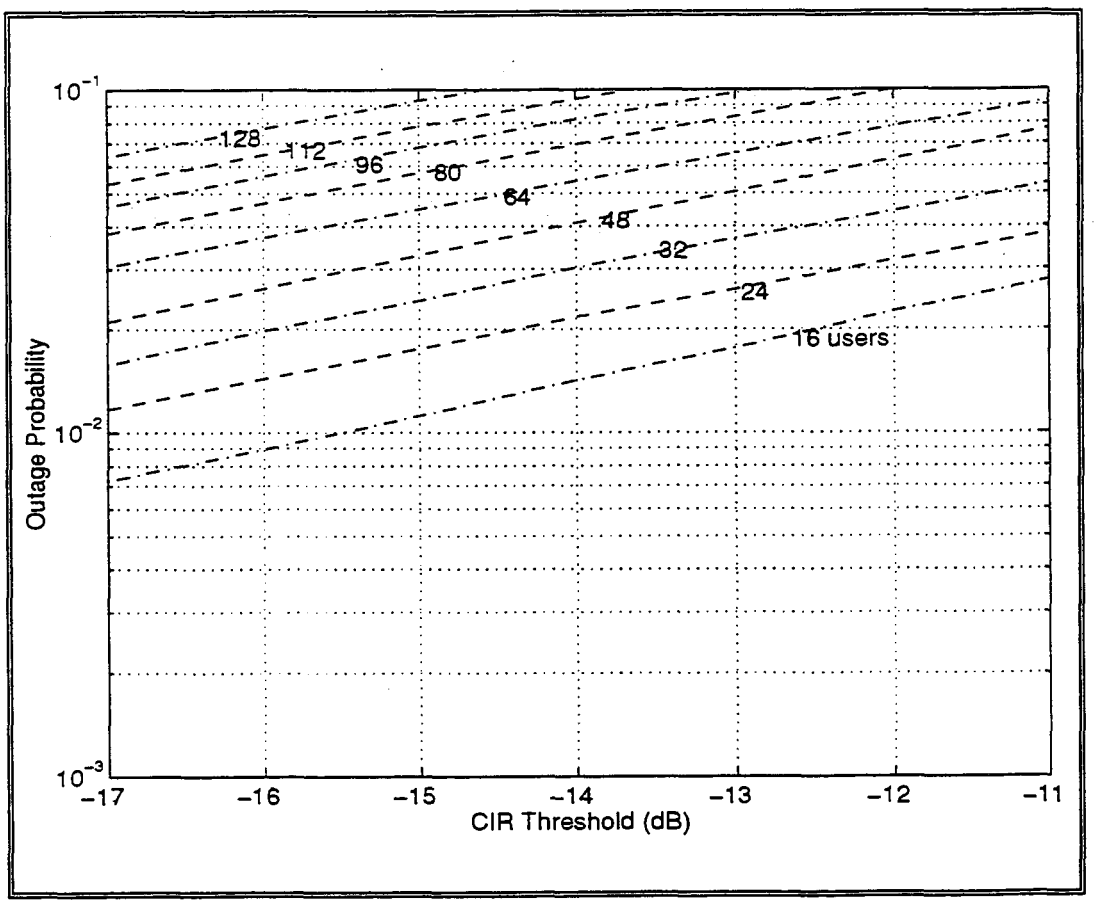

Figure 5-4. Outage Probability Curves for the Fixed Equal Transmitted Power Scheme (f_DTp=0.02, SNR=20 dB, N=16, 24, 32, 48, 64, 80, 96, 112, 128 users in 16 cells).

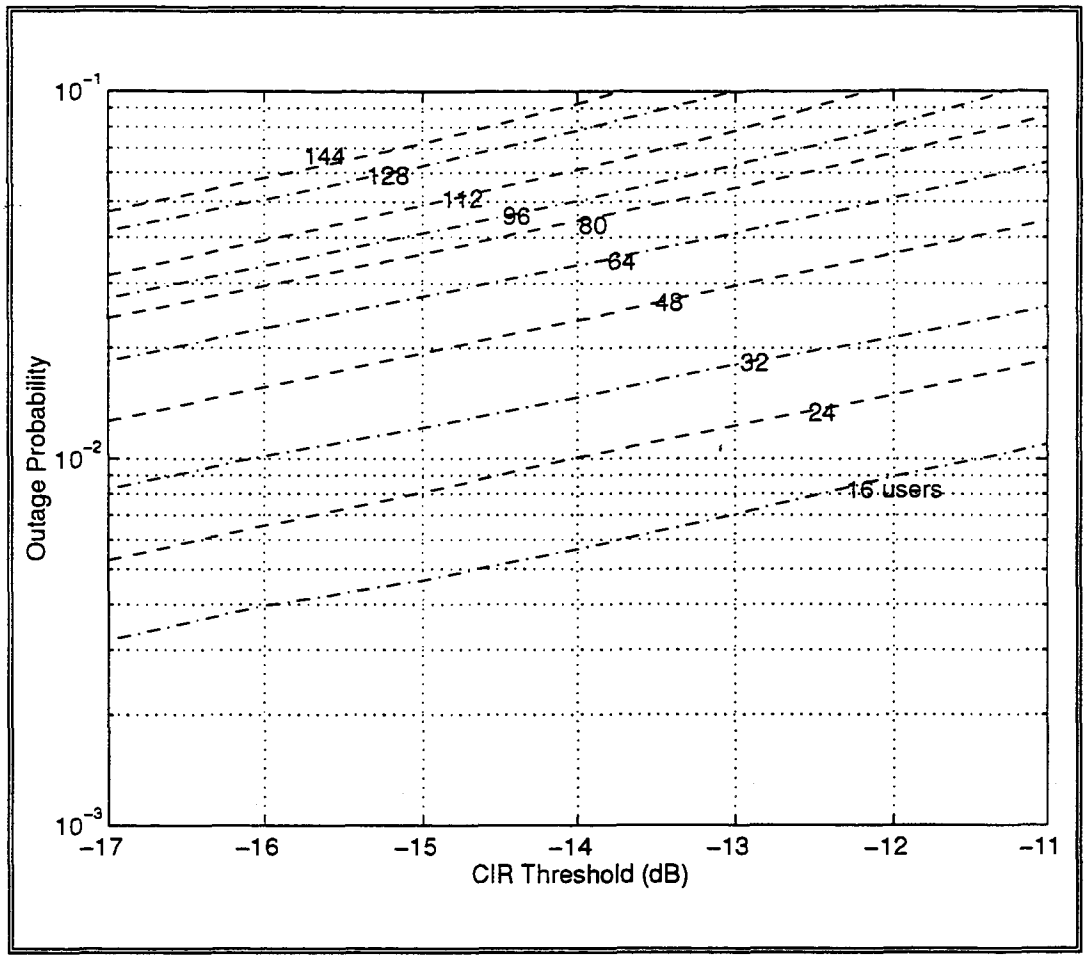

Figure 5-5. Outage Probability Curves for Fixed Step Fully Distributed Power Control (f_DT_p=0.02, SNR=20 dB, N=16, 24, 32, 48, 64, 80, 96, 112, 128, 144 users in 16 cells).

Figure 5-4 and 5-5 show that fixed step distributed power control system with f_DT_p=0.02 obtains higher capacities than the fixed equal transmitted power system (i.e., without power control). As an example, with the same outage criterion equal 0.01 at γ_0=-16 dB, the fixed equal power system can only support 20 users, whereas the fixed step distributed power control system can support 32 users, which is a 60% increment

compared with the capacity of the system without power control. Compared with the previous result at $f_D T_p$ =0.1, the result at $f_D T_p$ =0.02 is obviously improved. Therefore, we concluded that the capacity performance of distributed power control is also depends on the value of normalized fade rate $f_D T_p$.

Other than the $f_D T_p$, we also want to investigate the effect of noise component in the link gain measurement. In the previous four figures, we used SNR=20 dB at the vertices of cells. Figure 5-6 and 5-7 show the results at SNR=0 dB and -20 dB respectively, which means at the vertices, the noise variance is the same as, or 20 dB higher that of the signal power.

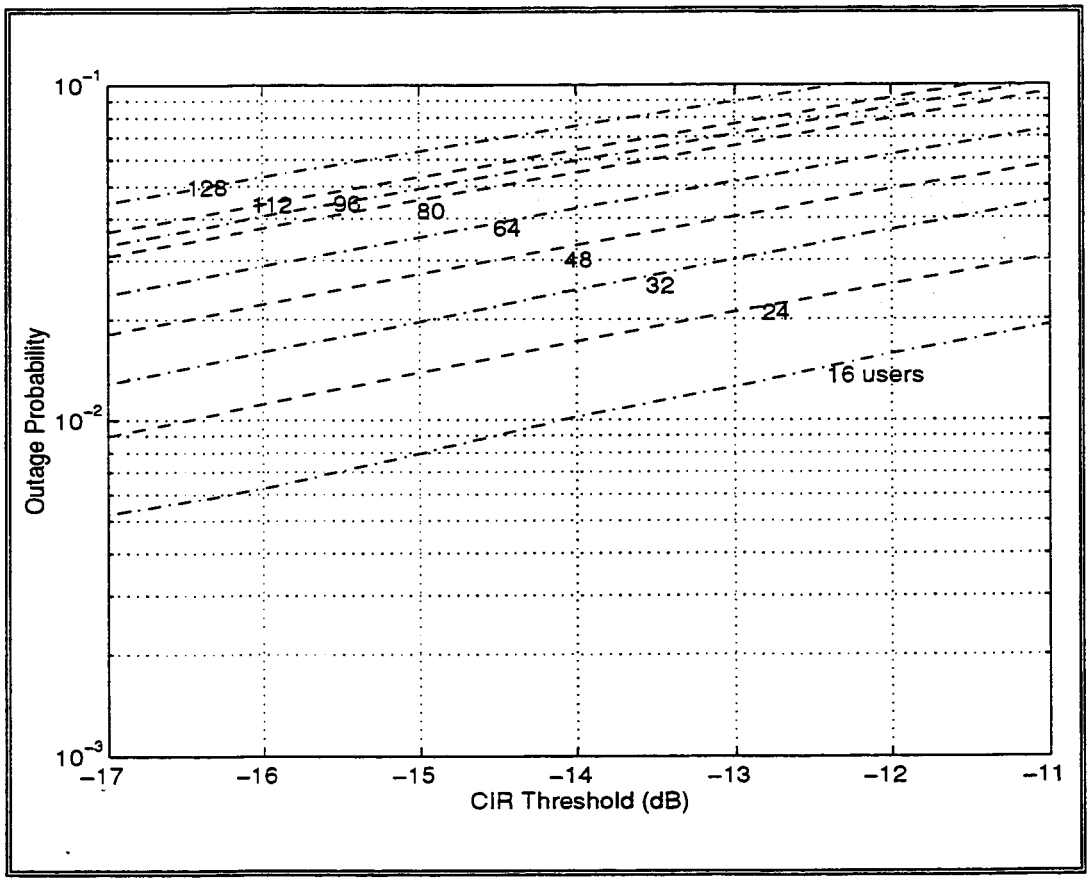

Figure 5-6. Outage Probability Curves for Fixed Step Fully Distributed Power Control ($f_D T_p$=0.1, SNR = 0 dB, N=16, 24, 32, 48, 64, 80, 96, 112 users in 16 cells).

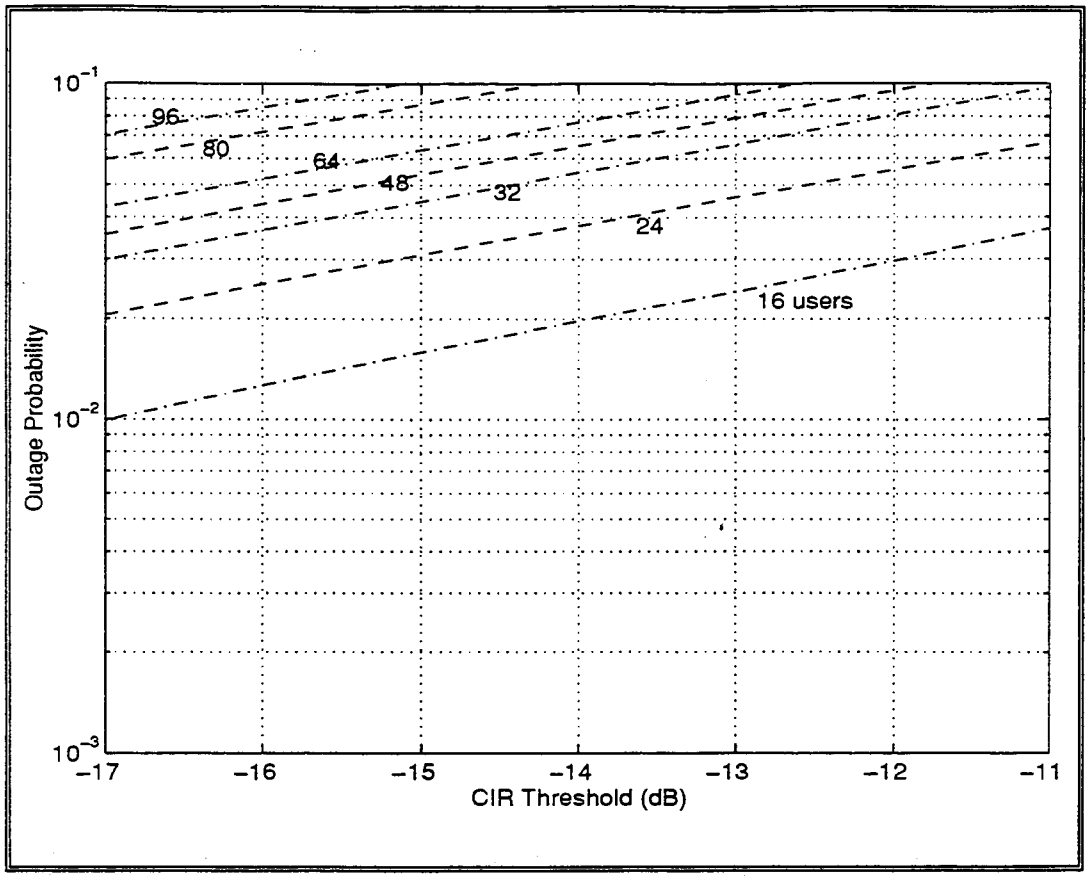

Figure 5-7. Outage Curves for Fixed Step Fully Distributed Power Control (f_DT_p=0.1, SNR = -20 dB, N=16, 24, 32, 48, 64, 80, 96, 112 users in 16 cells).

Comparing the results in Figure 5-3 with the results in Figures 5-6 and 5-7, we can see that with a decreased SNR value, i.e., increased noise level, the capacity reduces accordingly. Given 0.01 as the outage criterion at γ_0= -16 dB, we have N=24 users in the first case with SNR= 20 dB (Figure 5-3). But when the noise level increases and SNR=0 dB at the vertices, the capacity is reduced to a little more than 16 users (Figure 5-6). When the SNR decreases to -20 dB at the vertices, the capacity performance is even worse, for there is less than 1 user per cell in the system (Figure 5-7). The reason is because the white Gaussian noise changes quite fast. As the noise power increases and becomes comparable to the fading signal power, we have a more rapid fading signal after combining the two. However, the fixed step distributed power control scheme at f_DT_p=0.1

is not fast enough to track the deep fades; therefore, it results higher outage probabilities and lower capacities.

As stated in Chapter 3, in the fully distributed power control scheme, the power adjustment is made based on individual CIR measurement. The interaction among the individual power control processes is not monitored or controlled in a global scale as is in the case with fully centralized power control. Some links may experience very high CIRs, while others always suffer from too low CIRs. On the other hand, by temporally disabling a few links that can not achieve γ_0, the centralized power control technique enables the remaining users to achieve CIRs above γ_0. In the following sections, we will show the system capacity achieved by the fast centralized power control scheme and our proposed RC-CPC scheme.

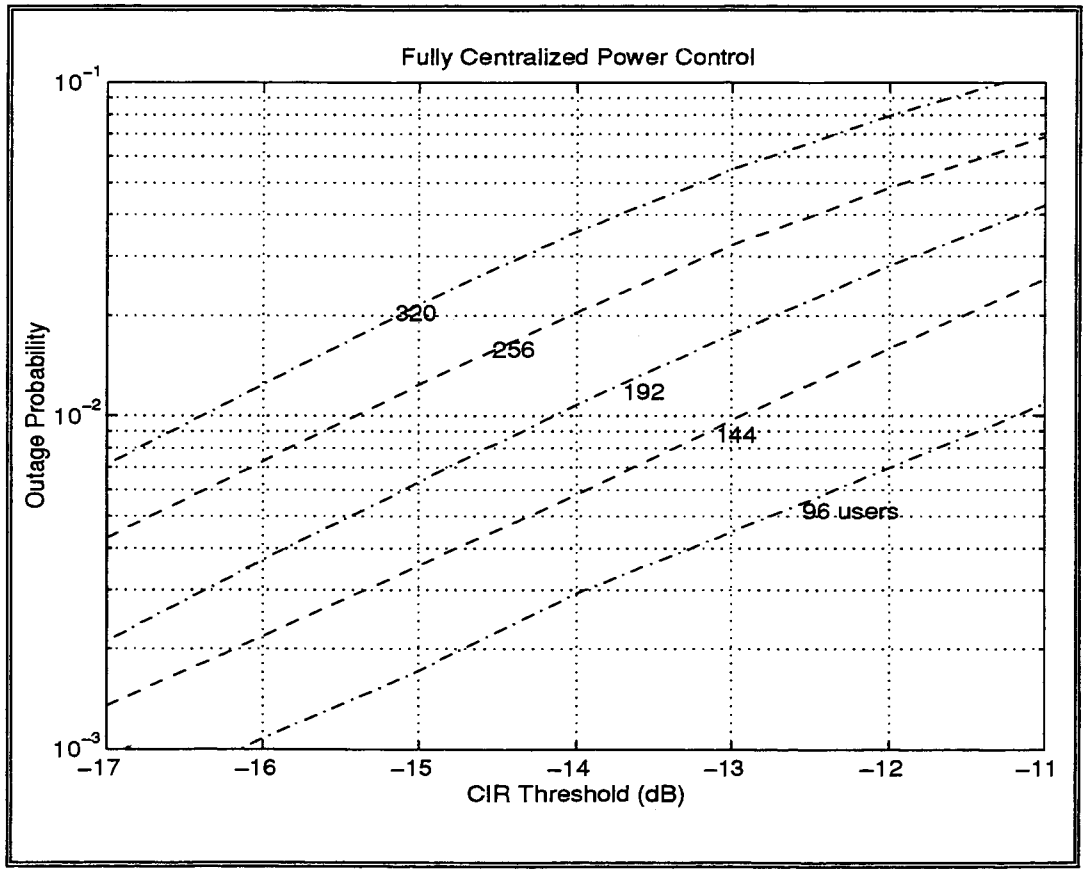

Figure 5-8. Outage Probability Curves for Fully Centralized Power Control (f_DT_p=0.1, SNR=20 dB, N=96, 144, 192, 256, 320 users in 16 cells)

As shown in figure 5-8, the fully centralized power control scheme can achieve a very high capacity. Given an outage probability of 0.01 with γ_0 =-16 dB as the criterion, the capacity is around 300 users in 16 cells, which is more than 10 times of the capacity achieved by the fully distributed power control system. However, as explained before, the centralized control requires a large amount of accurate channel tracking and information exchange which is not suited for practical implementation. Nevertheless, the capacity attained by the fully centralized control scheme provides upper bounds on the performance of transmitter power control algorithms.

Next, we evaluate the capacity of the system with our improved centralized power control scheme, RC-CPC. The curves are shown in Figure 5-9.

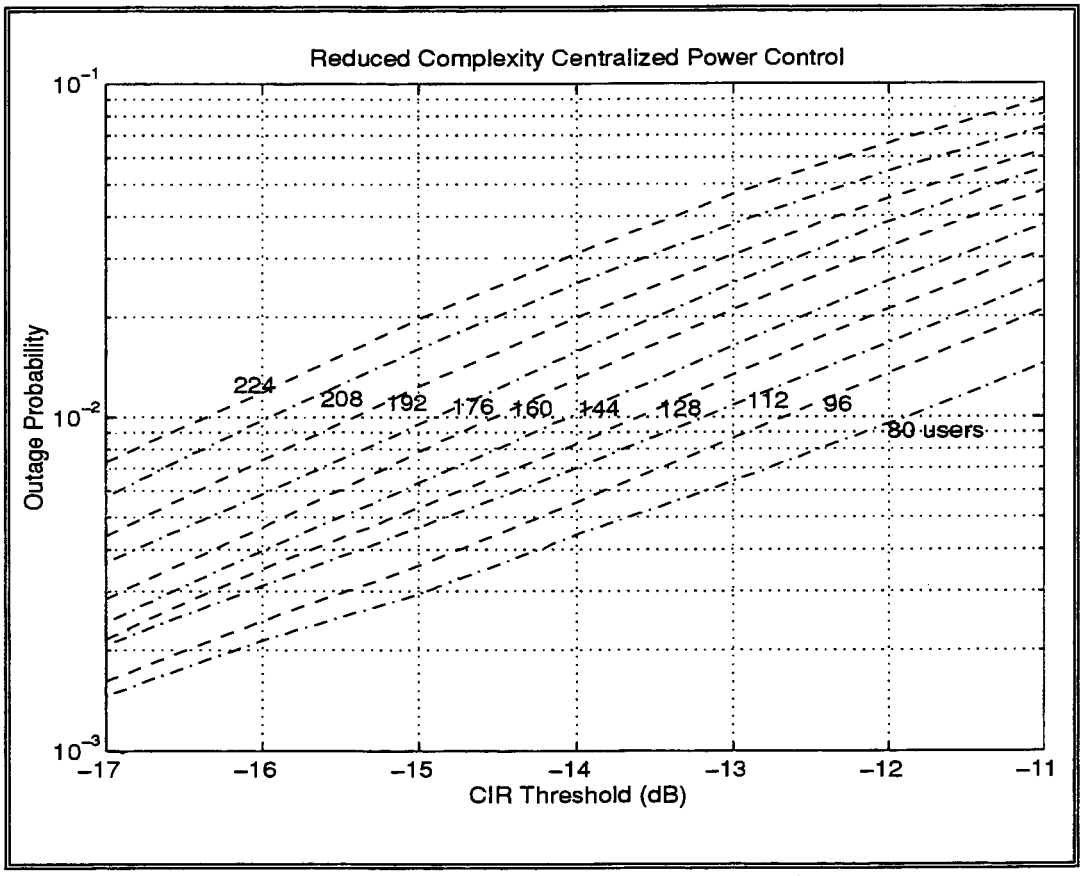

Figure 5-9. Outage Probability Curves for the RC - CPC Scheme ($f_D T_p$=0.1, SNR=20 dB, N=80, 96, 112, 128, 144, 160, 176, 192, 208, 224 users in 16 cells)

Given an outage criterion of 0.01 at γ_0=-16 dB, the capacity is 208 users in 16 cells. Although this figure is not as good as the one we have for the fully centralized power control scheme, it is still much higher when compared to the capacity of the fully distributed power control system (Figure 5-3). Moreover, as we explained in chapter 4, the RC-CPC algorithm is lot more feasible for implementation than the fully centralized power control scheme.

Recall that in the RC-CPC algorithm, to reduce the complexity of the removal procedure, a user prescreening procedure is used in combined with the modified SRA to remove the "unusable" links. In the user prescreening process, the weighting factor, μ needs to be chosen properly to set the threshold χ for $\|\mathbf{H}\|$ (the infinite norm of $\mathbf{H}$) as in equation (4.13). With an average of 100 users in the system, Figure 5-10 shows the outage performance of the prescreening process with different values of μ chosen. As a comparison, the outage performance of the combined removal process (user prescreening and the modified SRA) adopted in the RC-CPC algorithm is also shown in the same figure.

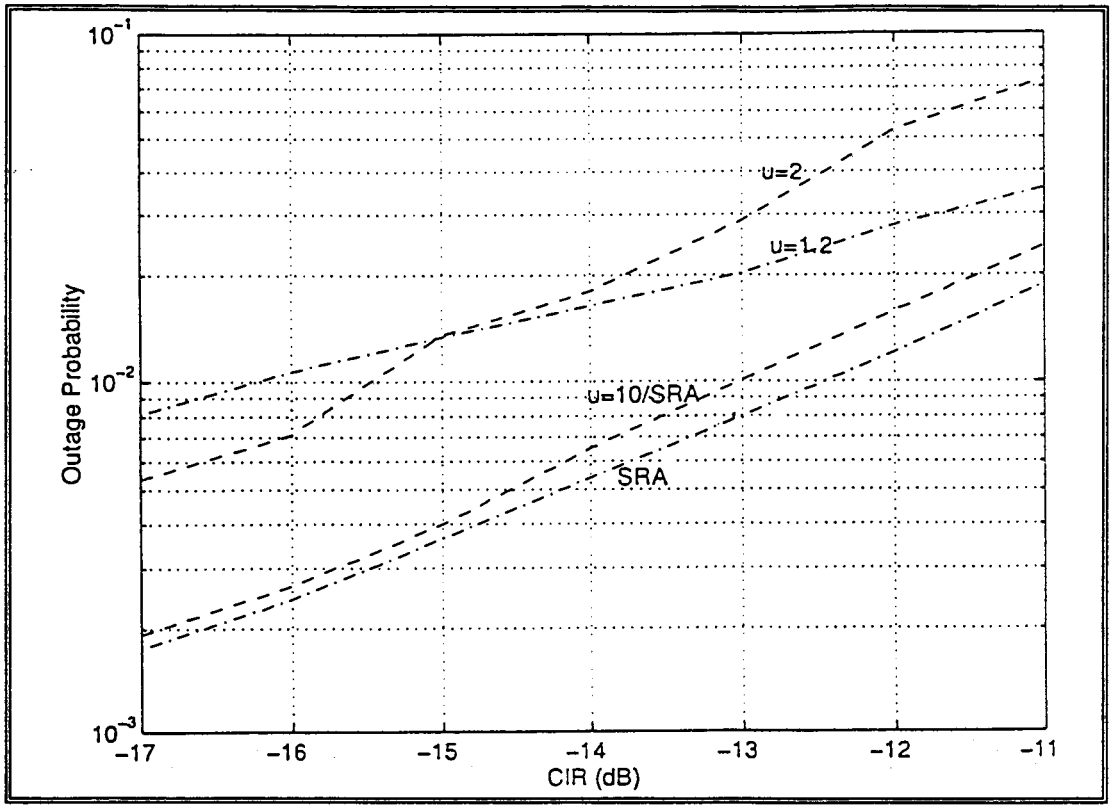

Figure 5-10. Outage Comparison of Different Removal Schemes
($f_D T_p$=0.1, SNR=20 dB, N=100 users)

From the above graph, we can see that the prescreening process itself with a fixed μ over the entire threshold range attains higher outage probabilities than the SRA itself. In fact, finding a proper μ analytically for every threshold required can be difficult. We will suggest it for the future study rather than probe any further here. Nevertheless, as explained in section 4.3, the user prescreening process proceeded at each base station simplifies the centralized removal process, SRA, in a great amount. When this distributed process is combined with the SRA, the resulting outage performance, as shown in Figure 5-10, is comparable to the SRA alone.

To further study the effect of the removal algorithm in RC-CPC, we focus on the statistics of the maximum achievable CIR, which is denoted by γ^* . γ^* was defined earlier as

$$\gamma^* = \frac{1}{\lambda_{\max} - 1}.$$

where λ_{max} is the maximum eigenvalue of the link gain matrix **H** and **F**. Note that **H** and **F** have the same λ_{max} as explained in section 4.1. To compare γ^* before and after the user removal process, we simulate a system with total 100 users in 16 cells. Figure 5-11 shows the Probability Density Function (pdf) of γ^* in the case of (a) without user removal, (b) with removal and γ_0 = -17 dB, (c) with removal and γ_0 =-13 dB. Noticeably, the pdf of γ^* in case (a) spreads out in a wide range from -55 to 0 dB. But with the prescreening/SRA removal process, γ^* is confined in the small range above γ_0. Comparing the pdf of γ^* at different γ_0, the tail of the pdf above γ_0 decays faster as γ_0 increases from -17 to -13 dB. This is because more links are needed to be removed to achieve the higher γ_0. The standard derivation of the pdf is also larger with a higher γ_0. The sharp edge of the pdf at γ_0 shows that the user removal scheme guarantees that the system CIR can be pushed above the threshold so that capacity gain is always attained.

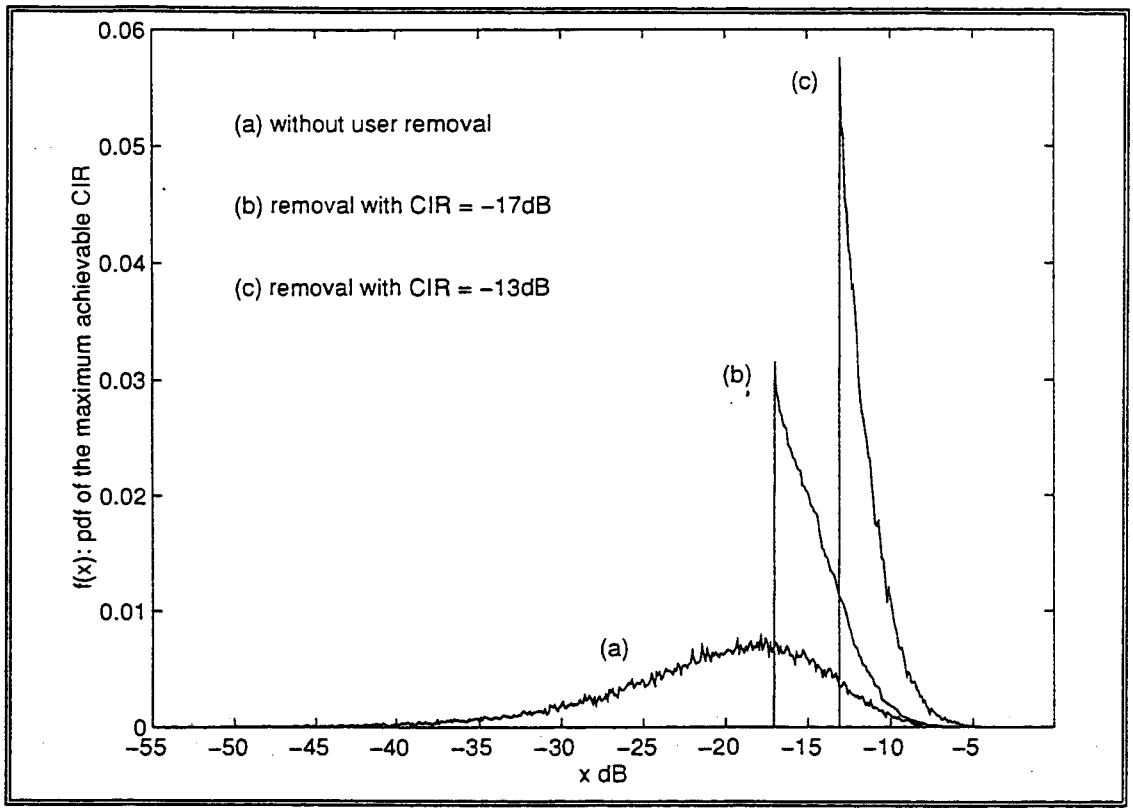

Figure 5-11. Comparison of the pdf of the Maximum Achievable CIR ($f_D T_p$=0.1, SNR=20 dB, N=100 users)

Since we are trying to control the transmitted power in the system, the dynamic range of the transmitter also plays an important role in the implementation of power control systems. Figure 5-12 shows the distribution of the dynamic range (DR) with RC-CPC. There are 96 users in the system, and a CIR threshold equal -16 dB is chosen.

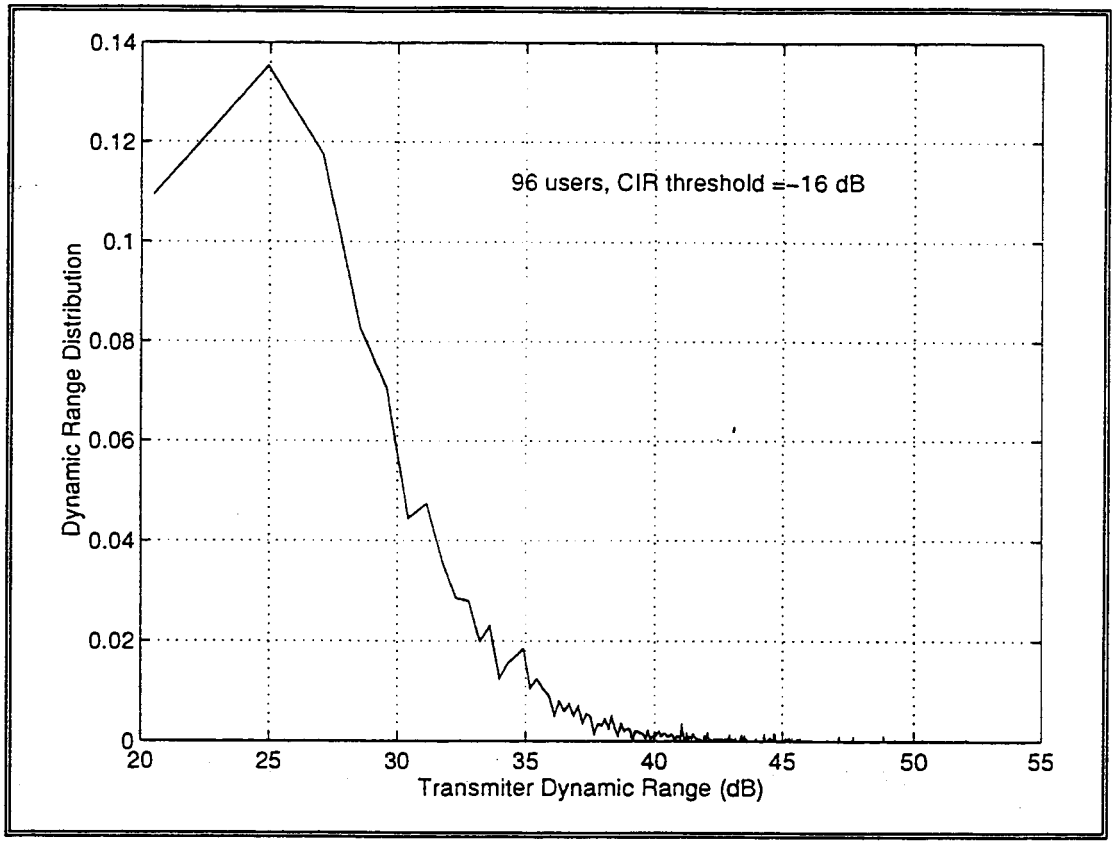

Figure 5-12. Distribution of Dynamic Range for RC-CPC.

From the above figure, we can see that the dynamic range distribution of the system using RC-CPC mainly spreads in the range of 20 to 40 dB. We expect that even if we limit the allowable dynamic range to 50 or 40 dB, the performance should not degrade dramatically. Figure 5-13 and Figure 5-14 show the system performances with RC-CPC under a dynamic range of 50 and 40 dB respectively.

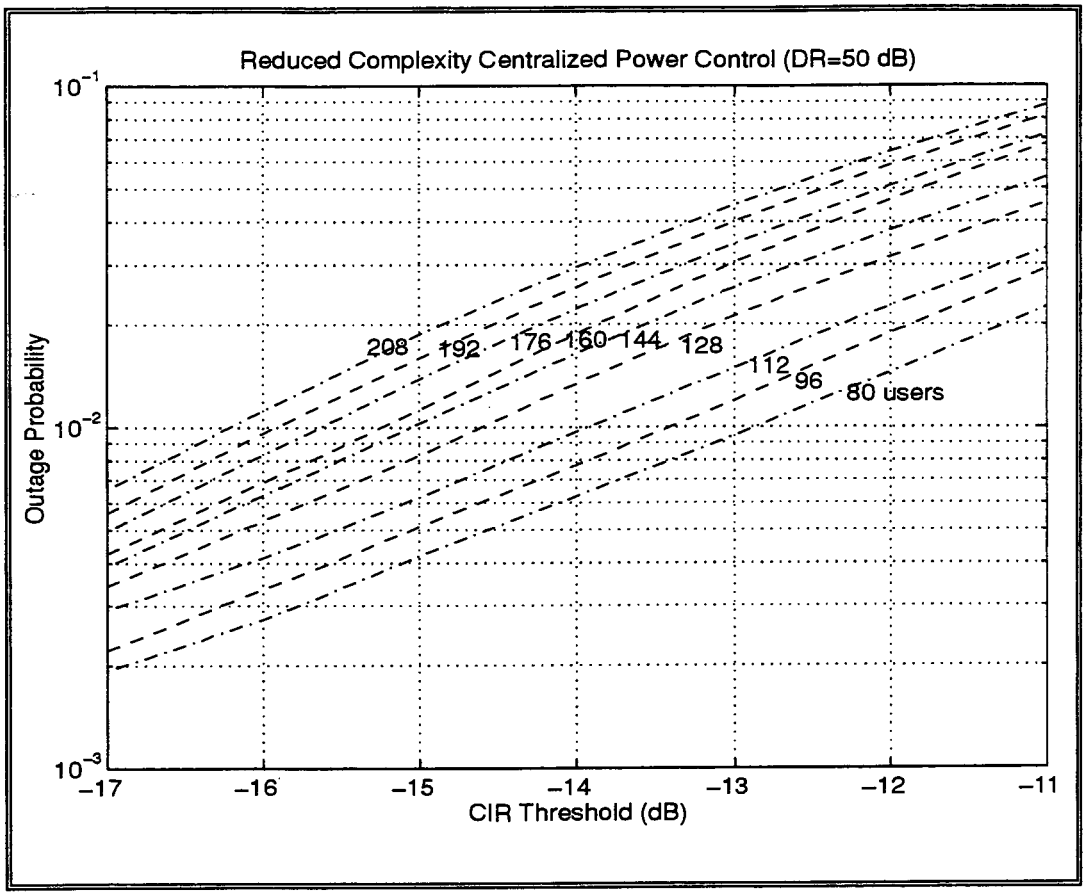

Figure 5-13. Outage Probability Curves for the RC - CPC Scheme ($f_D T_p$=0.1, SNR=20 dB, DR=50 dB, N=80, 96, 112, 128, 144, 160, 176, 192, 208 users in 16 cells).

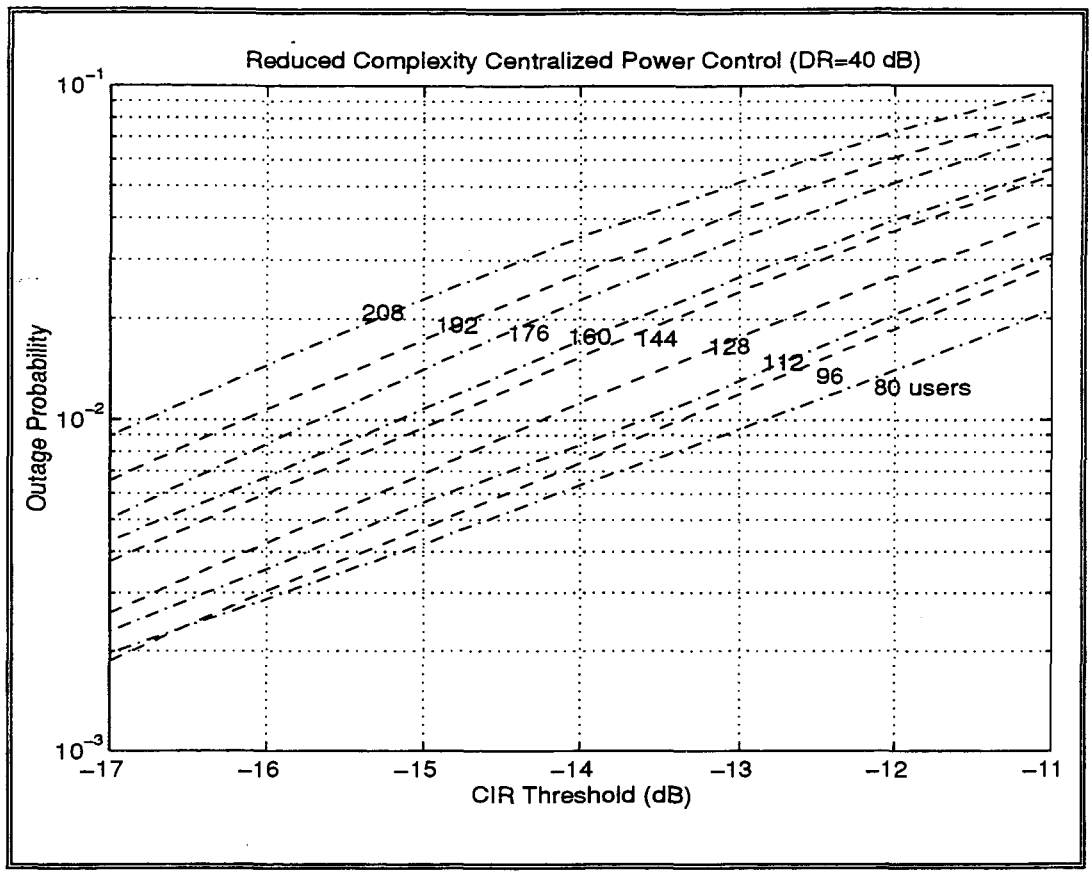

Figure 5-14. Outage Probability Curves for the RC - CPC Scheme (f_DT_p=0.1, SNR=20 dB, DR=40 dB, N=80, 96, 112, 128, 144, 160, 176, 192, 208 users in 16 cells).

As we compared figure 5-9 with figures 5-13 and 5-14, we can see that with a DR=50 dB, the capacity is almost the same as the power control system without any constraint on the dynamic range. The same is true for DR=40 dB. These results confirm what we predict based on the distribution of dynamic range in figure 5-12. There are only a little percentage of users that require power setting exceeding the dynamic range. Those users require too little power compared with the others are the ones that experience very little interference. We may increase these users' power a little to meet the DR requirement, and these individual's CIRs will increase. Even thought the resultant CIRs

for all users will not be the same, i.e., the CIRs are not balanced. But as long as the objective of lowering the outage probability is met, the CIRs need not to be exact the same for all users. As a result, we still have a high capacity performance with RC-CPC under a reasonable dynamic range constraint.

The following is a table that compares the reuse factors of the various fast power control systems we have studied. Given a CIR threshold γ_0 =-16 dB, the ideal single cell can hold 40.8 users according to equation (1.3). Thus within a 16-cell system, the ideal system can support totally 653 users. We calculate the reuse factors by dividing the capacity N of various systems by 653, and we have the approximate reuse factors for the following four systems.

	Fixed equal Transmitted power	Fixed step fully distributed power control	Reduced-Complexity Centralized Power Control (RC-CPC)	Fully centralized power control
Number of Users in 16 cells	16	24	208	300
Reused Factor	0.025	0.04	0.32	0.46

Table 5-1. Comparison of the System Capacities and the Reuse Factors.

We have mentioned that 1/7 or 14.3% is the reuse factor in an FDMA cellular system. Compared with 14.3%, we see that the CDAM system using the proposed RC-CPC algorithm has more than twice the reuse factor as FDMA cellular system. This result

further confirms that our RC-CPC scheme can effectively reduce the co-channel interference and improve the capacity performance of DS/CDMA micro-cellular systems.

5.2 Average Power Control Simulation

We have so far focused on the system performance with the fast power control process. The fast power control process is done at a much higher power sampling rate, e.g., at least 10 times faster the maximum fade rate. This is essential for the system to track and compensate for the moving portables, which may be caught in deep fades. However, such fast information tracking and power adjustment require a higher system complexity compared with slow or average power control. In the following sections, we will take a brief look at the slow power control process with our proposed RC-CPC scheme.

The main purpose of average power control is to maintain an average CIR performance and to minimize the average transmitted power for all users. Consider the average channel condition in which the link gain is modeled with the slow varying propagation loss. The average fading gain is represented by the product of the α-th power of distance and a log-normal component representing the shadowing loss as in equation 3.1. This model applies to both reverse and forward links. As in the case with fast power control, we chose $\alpha = 4$ for the path loss exponent and $\sigma = 8$ dB for the standard deviation of the log-normal fading. One major difference in the slow power control simulation is that the transmitter power is updated only when there is a new user arrives or a user terminates the call.

In order to apply the previous discussed centralized power control techniques to the average power control process, we assume the following: At a mobile user, the n-th average link gain from a base station is measured by

$$\overline{g_n} = \frac{(n-1)\overline{g_{n-1}} + g_n}{n}, \tag{5.1}$$

where g_n is the measured link gain at the n-th sampling instant, and the over bar means the average value. By considering only the propagation losses due to the distance and shadowing effects, the link gain g_n changes very slowly with time [7]. For n >>1, we have the following:

$$\overline{g_{n-1}} \approx g_n. \tag{5.2}$$

With this assumption, the normalized average link gain can be expressed as

$$\overline{h_n} = \overline{\left(\frac{g_n}{g_n'}\right)} = \frac{\overline{g_n}}{\overline{g_n'}}, \tag{5.3}$$

where g_n' is the link gain from the mobile's home base station to the mobile itself measured at the n-th sampling instant. After gathering all the average link gains, we then have the average link gain matrices **H'** and **F'**. By applying the theorem from Perron, Frobenius [47] again and solving the eigenvalues and eigenvectors of the **H'** and **F'** matrices as in Chapter 2 and 4, we have the fully centralized and the RC-CPC average power control schemes respectively.

It can be seen from equation (5.3) that the average coupling matrix **F'** consists of slowly varying link gains. We can allocate the average transmitter power by solving the following matrix equation

$$\lambda'_{max}\mathbf{S}' = \mathbf{F}'\mathbf{S}', \tag{5.5}$$

where $\mathbf{S}'$ is the average power allocation vector to each cells and λ_{max}' is the maximum eigenvalue of the $\mathbf{F}'$ matrix. With the same RC-CPC algorithm described in Chapter 4, we can compare outage performance of the RC-CPC scheme with the fixed transmitted power scheme (no power control at all), the fully centralized and the fully distributed power control schemes using average power control.

To simulate the average power control process, γ_0 is chosen from the range of [-8, 0] dB. Because the link gain model does not consider the fast fading effect, for the same BER performance, (e.g. BER=10^{-3}), the required base-band SIR in the Rayleigh fading channel is 5~10 dB higher than in the AWGN channel [14]. Figure 5-8 shows the outage performance with average power control using A - fixed equal transmitted power B - fully distributed power control, C - RC-CPC, and D - fully centralized power control.

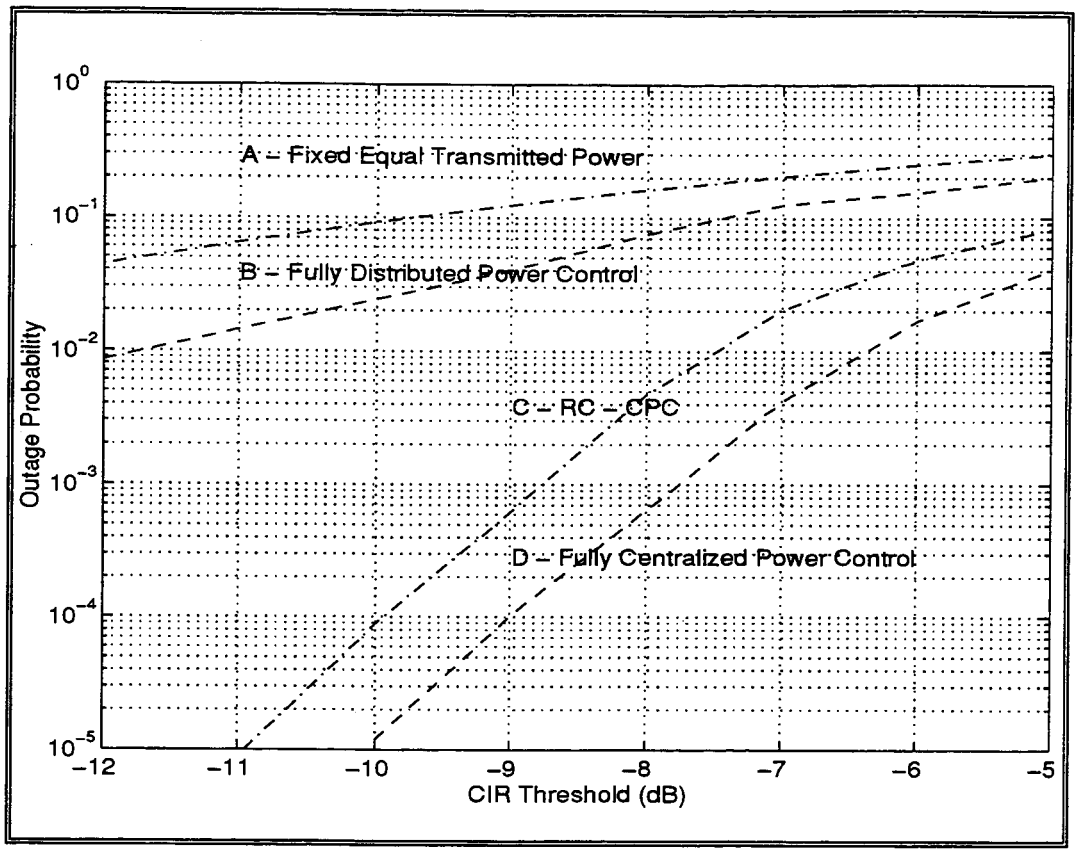

Figure 5-8. Comparison of the Outage Probabilities with Slow Power Control (SNR=20 dB at the vertices of cells)

The simulation result shows that the RC-CPC scheme can achieve outage performance close to the fully centralized power control scheme. Particularly in the lower range of the CIR thresholds, e.g., -12 to -9dB, the outage probability with the fixed transmitted power is only slightly improved by the fully distributed power control scheme, but it is much improved by the RC-CPC scheme. We can conclude that the RC-CPC technique with limit available link gain information and centralized power management can be applied in both the fast and slow power control processes. The result obtained compares favorably with the performance of fully centralized power control technique.

5.3 Summary

All the simulation results show that the improved centralized power control algorithm called the RC-CPC algorithm can approximate the outage performance of the fully centralized power control scheme with only limited link gain information and distributed information processing at the base stations. The RC-CPC scheme also outperforms the fully distributed power control scheme by lowering the outage probability and increasing the downlink capacity in the DS/CDMA system.

Chapter 6

Conclusions and Discussions

6.1 Conclusions

This thesis studied in detail various power control techniques applied in the DS/CDMA microcellular system including the fully centralized power control, fully distributed power control and the improved centralized power control called the RC-CPC (reduced complexity centralized power control) algorithm. The impact of pilot-based link gain measurement, fast varying Rayleigh fading, the interactions among multiple links in a multi-cell, multi-user environment and the effect of variations in the traffic loading are explicitly considered in the system analysis and simulations.

Since the capacity of the DS/CDMA system is considered downlink limited [5,36], our study focuses on downlink power control. In the evaluation of various power control algorithms, we simulated a multi-cell, multi-user DS/CDMA system and measured the instantaneous CIRs at each link between all base stations and all users. The outage

probability performance is investigated under various system protection ratios. Between the fully centralized and the fully distributed power control algorithms, the simulation result shows that the former achieves better performance in the sense that it minimizes the outage probability for a given system protection ratio. However, the centralized power control algorithm requires reliable measurements of all propagation links in the system. Therefore, rather than being suited for practical implementation, the algorithm serves mainly as a tool to derive the upper bound of the performance of transmitter power control algorithms.

Based on the existing centralized power control algorithm, we derived the reduced complexity centralized power control (RC-CPC) algorithm and apply it to both the fast and slow power control processes. One uniqueness of this improved power control scheme is that the pilot signal transmitted in the downlink direction is actually used for downlink centralized power control. Each mobile estimates and updates the path gains from both its home base and nearby bases by tracking and monitoring their pilot signals. It then reports these limited available channel measurements to its home base. The central controller gathers the necessary information from all bases and allocates the transmitter power globally. Another uniqueness of the RC-CPC scheme is that each base station distributed processes the link gain information, including prescreening users and computing associated row entries in the reduced size coupling matrix. Distributed user prescreening is used in combination with the SRA to remove the "unusable" links and achieve the required CIR threshold, γ_0. In addition, the one-bit adaptation algorithm proposed for updating the link gains greatly reduces the amount of data exchanged between the base stations and users. As a result, the RC-CPC algorithm has both the advantages of global power management and implementation practicality. To simulate the power control schemes, it is the first time that the fast Rayleigh fading and the slow shadow fading are both considered in centralized power control. Numerical results show that the RC-CPC achieves comparable outage performance with that of the fully

centralized power control scheme. With the lower outage probability is obtained at the same γ_0, we can see that the RC-CPC scheme can acquire higher capacity than the fully distributed power control scheme.

6.2 Discussions for Future Work

On the downlink power control issue, some suggestions for further work are as follows:

1. Our power control study has assumed that the application of modem technique, perfect channel synchronization and pilot tracking and acquisition are in place. Further work is required to determine the performance in terms of error rate and SIR statistics by incorporating the above techniques in the study.

2. In this study, onmi-directional antenna is assumed for both transmitting and receiving; therefore, only one fading signal energy is captured on each link. The effect of antenna diversity and multipath signal capturing can be considered in future studies.

3. In terms of link gain measurements, the one bit adaptation algorithm has not been tested. The step size for updating link gains needs to be addressed.

4. Our simulation has assumed the error free controlling message, undelayed base selection and hand-off operation, further work is required to access the significance of these factors on the performance of power control.

5. The distributed user prescreening process can be probed further. If the centralized SRA can be completely replaced by a distributed user removal

scheme, the computational complexity of the proposed power control algorithm will be further reduced.

As a final note, the capacity of DS/CDMA cellular systems is dependent upon the accuracy in power control, voice activity gain, antenna gain and other techniques of the physical layer. In order to increase capacity, two main obstacles have to be overcome. First, conventional spread spectrum matched filter receivers are suboptimal in the presence of multiple access interference. Second, they are highly sensitive to the near-far effect [15]. Other than the power control techniques, many researchers are investigating and proposing interference suppression and cancellation techniques that can potentially combat these impediments.

References

[1] P.Jung, P.W.Baier, A.Steil, "Advantages of CDMA and Spread Spectrum Techniques over FDMA and TDMA in Cellular Mobile Radio Applications," *IEEE Transactions on Vehicular Technology*, Vol.42, No.3, August 1993: pp.357-363.

[2] D.L.Schilling, R.L.Pickholtz, and L.B.Milstein,"Spread spectrum goes commercial," *IEEE Spectrum*, August 1990: pp.40-45.

[3] R.L.Pickholtz, L.B.Milstein, and D.L.Schilling, "Spread spectrum for mobile commnications," *IEEE Transactions on Vehicular Technology*, VT-40, May 1991: pp.313-322.

[4] G.R.Cooper, and C.D.McGillem, *Modern Communications and Spread Spectrum*, McGraw-Hill, 1986.

[5] "An Overview of the Application of CDMA to Digital Cellular Systems and Personal Cellular Networks", Qualcom Inc., June 4, 1992.

[6] J.G.Proakis, *Digital Communications*, 2nd ed., McGraw-Hill,1989.

[7] W.C.Y.Lee, *Mobile Communications Design Fundamentals*, 2nd ed., John Wiley and Sons Inc., 1993.

[8] A.J.Viterbi, *CDMA Principles of Spread Spectrum Communication*, Addison-Wesley, 1995.

[9] G.C.Hess, *Land-Mobile Radio System Engineering*, Artech House, 1993.

[10] K.S.Gilhousen, I.W.Jacobs, and *et al.* "On the Capacity of a Cellular CDMA System," *IEEE Transations on Vehicular Technology*, Vol.40, No.2, May 1991: pp.303-311.

[11] J.C.Liberti, and T.S.Rappaport, "Analytical Results for Capacity Improvements in CDMA," *IEEE Transactions on Vehicular Technology*, Vol.43, No.3, August 1994: pp.680-690.

[12] D.Falconer, and F.Ling, "Combined Orthogonal/Convolutional Coding for a Digital Cellular CDMA System", *IEEE Proceedings VTC'92*, 1992: pp.63-66.

[13] N.Sollenberger, and L.F.Chang, "Comparison of Two Interleaving Techniques for CDMA Radio Communication Systems," *IEEE Proceedings VTC'92*, 1992: pp275-278.

[14] S.Ariyavisitakul, and L.F.Chang, "Performance of Convolutional Codes with Interleaving in the Interference Limited Raylaigh Fading Channel", *IEEE Proceedings ICC'91*, 1991: pp.812-816.

[15] R.Kohno, R.Meidan, and L.B.Milstein, "Spread Spectrum Access Methods for Wireless Communications", *IEEE Communications Magazine*, January 1995: pp.58-67.

[16] W.C.Y.Lee, "Overview of cellular CDMA", *IEEE Transactions on Vehicular Technology*, VT-40, No.2, May1991: pp.291-302.

[17] M.Zorzi, "Simplified Forward-Link Power Control Law in Cellular CDMA," *IEEE Transactions on Vehicular Technology*, Vol.43, No.4, November 1994: pp.1088-1093.

[18] O.K.Tonguz, M.M.Wang, "Cellular CDMA Networks Impaired by Rayleigh Fading: System Performance with Power Control," *IEEE Transactions on Vehicular Technology*, Vol.43, No.3, August 1994: pp515-526.

[19] A.J.Viterbi, A.M.Viterbi, and E.Zehavi, "Performance of power controlled wideband terrestrial digital communications," *IEEE Transactions on Communications*, Vol.41, April 1993: pp.559-569.

[20] J.M.Aein, "Power balancing in systems employing frequency reuse," *COMSAT Technology Review*, Vol.3, No.2, Fall 1973: pp.77-299.

[21] H.Alavi and R.W.Nettleton, "Downstream power control for a spread spectrum cellular mobile radio system," *Conference Record - GLOBECOM'82*, Miami,FL, Nov.29-Dec.3,1982.

[22] J.Zander, "Performance of Optimum Transmitter Power Control in Cellular Radio Systems", *IEEE Transactions on Vehicular Technology*, Vol.41, February,1992: pp.57-62.

[23] S.A.Grandhi, R.Vijayan, D.J.Goodman and J.Zander, "Centralized Power Control in Cellular Radio Systems," *IEEE Transactions on Vehicular Technology*, Vol.42, No.4, Nov. 1993: pp.466-468.

[24] J.Zander and M.Frodigh, "Comment on "Performance of optimum tansmitter power control in cellular radio systems"," IEEE Trans. on Vehicular Tech., Vol.43, No.3, August '94, pp.636.

[25] J.C.Lin, T.H.Lee and Y.T.Su, "Power Control Algorithm for Cellular Radio Systems," Electronics Letters, Vol.30, No.3, 1994, pp.195-197.

[26] T.H.Lee, J.C.Lin, Y.T.Su, "Downlink Power Control Algorithms for Cellular Radio Systems", *IEEE Trans. on Vehicular Technology*, Vol.44, February 1995, pp.89-94.

[27] M.Frodigh, J.Zander, "Joint Power Control in Cellular Radio Systems," PIMRC, Spe.'95, Toronto, Canada, pp.41-45.

[28] G.Femenias, F.J.Perez-Briceno, A.Gelonch and I.Furio, "Transmitter Power Control for DS/CDMA Cellular Mobile Radio Networks," PIMRC, Sep.'95, Toronto, Canada, pp.46-50.

[29] S.C.Chen, N.Bambos, G.J.Pottie, "On Distributed Power Control for Radio Networks," *IEEE Proceedings ICC'94*, 1994: pp.1281-1285.

[30] G.J.Foschini, Z.Miljanic, "A Simple Distributed Autonomous Power Control Algorithm and its Convergence," IEEE Trans. on Vehicular Tech., Vol.42, No.4, Nov.'93, pp641-646.

[31] S.A.Grandhi, R.Vijayan, D.J.Goodman, "Distributed Power Control in Cellular Radio Systems", *IEEE Trans. on Communications*, Vol.42, FEB./MAR./APR. 1994, pp.226- 227.

[32] J.Zander, "Distributed Cochannel Interference Control in Cellular Radio Systems", *IEEE Trans. on Vehicular Technology*, Vol.41, August 1992, pp.305-311.

[33] S.A.Grandhi, R.Vijayan, and D.J.Goodman, "A Distributed Algorithm for Power Control in Cellular Radio Systems," Proc. 30th Allerton Conf. Commun., Control and Computing, Monticello, IL, Sept./Oct. 1992.pp.446-452.

[34] S.A.Grandhi, and J.Zander, "Constrained Power Control in Cellular Radio System," Proc. IEEE Veh.Techn.Conf., VTC'94, pp.824-828.

[35] M.Andersin, Z.Rosberg, and J.Zander, "Gradual Removals in Cellular PCS with Constrained Power Control and Noise," *PIMRC'95*, September, 1995: pp.56-60.

[36] A.Jalali, and P.Mermelstein, "Effect of Diversity, Power Control, and Bandwidth on the Capacity of Microcellular CDMA systems," submitted for publications, *IEEE Journal on Selected Areas in Communications.*

[37] S.Ariyavisitakul, and L.F.Chang, "Performance of a CDMA Radio Communications System with Feed-Back Power Control and Multipath Dispersion," *IEEE Proceedings Globecom,'91*, 1991: pp.1017-1021.

[38] S.Ariyavisitakul, "SIR-Based Power Control in a CDMA System," *Globecom'92*, 1992: pp.868-873.

[39] S.Ariyavisitakul, L.F.Chang, "Signal and Interference Statistics of a CDMA System with Feedback Power Control", *IEEE Transactions on Communications*, November 1993: pp.1626-1634.

[40] S.Ariyavisitakul, "Signal and Interference Statistics of a CDMA System with Feedback Power Control - Part II", *IEEE Transactions on Communications*, Vol.42, FEB./MAR./APR.1994: pp.597-605.

[41] P.Mermelstein and A.Jalali, "On the Bandwidth Efficiency of CDMA Systems,"

[42] M.Zorzi and L.B.Milstein, "Optimal Power control in a cellular CDMA mobile radio system," submitted to *IEEE Transactions on Vehicular Technology*, November 1993.

[43] M.M.Wang and O.K.Tonguz, "Forward link Power Control for cellular CDMA networks," *Electronics Letter* Vol.29, June 1993: pp.1195-1197.

[44] R.R.Gejji, "Forward-Link-Power Control in CDMA Cellular Systems," *IEEE Transactions on Vehicular Technology*, Vol.41, No.4, November 1992: pp.532-536.

[45] K.W.Shum, "Fuzzy Distributed Power Control in Cellular Radio Network," *PIMRC'95*, September1995: pp.51-55.

[46] S.C.Gupta and M.A.Mokhtar, "Power Control Considerations for DS/CDMA Personal Communication Systems," *IEEE Transactions on Vehicular Technnology*, Vol.41, No.4, November 1992: pp.479-487.

[47] J.M.Ortega, *Matrix Theory*, Plenum Press, N.Y.,1987.

[48] K.S.Shanmugan, and A.M.Breipohl, *Random Signals: Detection, Estimation and Data Analysis*, John Wiley & Sons, N.Y., 1988.

[49] W.C.Jakes, Jr.,Ed., *Microwave Mobile Communications*, John Wiley & Sons, N.Y., 1974.

[50] E.Biglieri, D.Divsalar, P.J.Mclane, and M.K.Simon, *Introduction to Trellis-Coded Modulation with Applications*, MacMillan, N.Y., 1991.